THE SUPEROXIDE RADICAL IN THE ENVIRONMENT AND ELECTROKINETIC CHARGING IN LIQUID MICRO-JETS

Mark Tattersall, B.A, B.Sc(Hons), Grad. Dip. Ed.

Thesis submitted for the degree of
Doctor of Philosophy

In

The University of Adelaide

(Department of Chemistry)

March 2002

Preface

This thesis is concerned with the application of physico-chemical phenomena to aspects of environmental analysis. The thesis is divided into two sections. The first deals with the measurement of the superoxide radical in natural waters in order to establish the role of the radical in natural water chemistry. The second section is an investigation of the electrokinetic charging behaviour associated with liquid micro-jets in order to understand the unusual charging behaviour reported in the literature with the ultimate goal of determining the viability of using the charging mechanism for *in vacuo* ion generation.

Abstract

The major objective of this research was to develop novel detection techniques for environmental analysis. A reverse flow injection apparatus used chemiluminescent detection to detect and measure the superoxide radical in natural waters. The other area of research was an investigation of the electrical charging effects in liquid micro-jet. Liquid micro-jets may be useable for the direct injection of liquids into the vacuum chamber. The aim was to develop a simple ionization technique for use in a so-called Liquid Beam mass spectrometer.

The research methodology involved the construction of reverse flow injection manifold to measure the superoxide radical. The manifold used the chemiluminescent compound luminol as the basis for the detection of the superoxide radical. The manifold was optimized and calibrated using gamma radiolysis of sodium formate solution to produce standard superoxide radical solutions whose concentration was calculated from the gamma radiation dose rate. The calibrated apparatus was then used to measure the superoxide radical concentration in seawater and fresh water at four sites.

The decay of photochemically generated superoxide radical was studied in UV irradiated water samples taken from the freshwater and seawater sites to provide' background and calibration data. The decay of the photochemically generated superoxide radical was measured and the kinetics were found to be second order with rate constants agreeing with those in the literature for the disproportionation of the superoxide radical. This agreement indicated that the primary role of the superoxide radical in natural water systems is to form hydrogen peroxide via disproportionation.

A liquid micro-jet apparatus was constructed with a view to its development as part of a multi-speciate environmental detection apparatus linking micro-jet liquid injection techniques with mass spectrometry to detect ionic species in natural water. The charging behaviour of liquid micro-jets was examined in order to better understand the unusual charging behaviour of liquid micro jets reported in the literature. This investigation was also intended to examine the feasibility of electrokinetic charging as an ionisation mechanism for the generation of the ions *in vacuo.* The investigation studied the effect of adding various salts to methanol and water micro-jets. The magnitude of the electrokinetic streaming current was found to be a function of flow velocity and solution conductivity. The conductivity dependence was found to be' independent of the chemical species present. Both the flow velocity and conductivity relationships established for methanol and water liquid micro-jets agreed with those reported in the literature for non-polar systems.

Acknowledgements

I would like to acknowledge the invaluable assistance of my supervisors Professor Stephen Lincoln, Dr Gerald Laurence and Dr Mark Buntine. I wish to thank them for their patience and helpful advice throughout the project, and their positive and perceptive comments in writing the thesis.

I would also like to thank my fellow students Kym Hendrickson and Karl Cornelius for their company and help in all matters. I especially would like to thank Karl for his help when using the radiation source. Thank you also to Annabel Wood who provided useful advice in the construction and use of the RFIA apparatus. In addition, I would like to thank the Chemistry department workshop staff for their assistance in constructing the liquid micro-jet apparatus and the RFIA unit.

Declaration

This work contains no material which has been accepted for any other degree or diploma in any university or other tertiary institution nd, to the best of my knowledge and belief, contains no material previously published or written by another person, except where due reference has been made in the text.

I give consent to this copy of my thesis when deposited in the University Library, being available for loan and photocopying.

Mark Tattersall

28/03/02

Abbreviations

DOM	Dissolved Organic Matter
FAB	Fast Atom Bombardment
FIA	Flow Injection Apparatus
LBMS	Liquid Beam Mass Spectrometer
MS	Mass Spectrometry
PMT	Photo-Multiplier Tube
RFIA	Reverse Flow Injection Apparatus
SOD	Superoxide Dismutase

TABLE OF CONTENTS

1.0 Introduction

1.1 The Importance of the Superoxide Radical

The superoxide radical, $O_2^{-\cdot}$ is a product of oxygen reduction. As a radical species it is a highly reactive transient species found in both biological systems, [1] and in the atmosphere [2]. There has been considerable interest in the activity of the superoxide radical in biological systems because of the deleterious effect this radical has on living cells [3]. It is also thought that the superoxide radical exists in natural water systems [4] but there has been no direct evidence to demonstrate either the role or presence of the superoxide radical in such an environment. It is important to understand what contribution the superoxide radical makes to natural water chemistry in order to understand its role in the degradation of organic species. There is a need to confirm its existence, perhaps as a photochemically generated species, and to determine whether the radical is a source of hydrogen peroxide present in many water systems as has been hypothesised [4].

What role, if any, the radical plays in chemical degradation of other species present in natural water systems is clearly dependent on confirmation of its existence and concentration in these systems.

1.1.1 Biological Systems

The production of the superoxide radical in biological systems is a consequence of the use of molecular oxygen by living organisms. The superoxide radical itself has been the focus of much research in biological systems as the radical is thought to be responsible for damage to living cells [3]. This damage may occur through different chemical mechanisms. Either the intrinsic and relatively selective reactivity of the superoxide radical or by the protonation of the superoxide radical to the hydroperoxyl radical (E^{o} +1.45V cf E^{o} +1.73V for the superoxide radical) [3], or through the formation of the very reactive hydroxyl radical through the iron catalysed Haber-Weiss reaction [5].

$$HO_2^{\cdot} + Fe^{3+} \rightarrow O_2 + H^{+} + Fe^{2+}$$

$$Fe^{2+} + H_2O_2 \rightarrow Fe^{3+} + OH^{-} + OH^{\cdot}$$

Because of these possible reactive pathways and its activity, the superoxide radical is viewed as an endogenous toxicant.

The superoxide radical is generated through several pathways in aerobic cellular systems. Enzymatic oxidation, during which some enzymes produce the superoxide radical as part of the oxidation cycle, is a well known source of superoxide radical, and is used to calibrate biological detection techniques for the radical [6].

The effect of the superoxide radical in numerous biological processes has been studied, but these studies examine intra-cellular superoxide rather than extra-cellular and are therefore outside the scope of this study. English et al have studied inflammation

processes in which the superoxide radical is thought to react with plasma, and convert this into a potent neutrophil chemotaxin [7]. This results in the amplification of inflammation response. Evidence of the role of superoxide radical in this process is confirmed by the fact that the addition of a superoxide dismutase will reduce the inflammatory effect produced by the superoxide radicals. The radical has also been studied in order to elucidate its role in the pathogenesis of ischaemic and traumatic brain injury, and neuro-degenerative conditions that are linked to the superoxide radical [3].

The superoxide radical is also thought to play a critical role in plant pathology. Both hydrogen peroxide, and the superoxide radical, have been studied in the context of the oxidative burst in plant defence [8]. The oxidative burst is an accumulation of active oxygen species, in particular, the superoxide radical and hydrogen peroxide in some plant/pathogen systems. These oxygen species behave not only as antimicrobial agents but also act as catalysts to stimulate a more complex immune response to the pathogen. There are however some algal material which have been shown to produce the superoxide radical extracellularly [9] although few organisms appear capable of such chemical activity, and as such there has been little study of the role of extra-cellular superoxide radical.

1.1.2 Environment

The superoxide radical is known to exist in the atmosphere [2] and is also thought to be present in natural water systems. In the upper atmosphere the radical is generated through electron attachment to molecular oxygen.

$$O_2 + e^- \rightarrow O_2^{-\bullet}$$

The existence of this species in the ionosphere has been confirmed by mass spectrometric analysis during rocket flights [2].

Despite the extensive atmospheric and biological research into the superoxide radical, its role in natural water systems is unknown. There is no direct experimental evidence to either confirm the existence of the superoxide radical in natural water systems or its contribution to the chemistry of these systems. However, there is some indirect evidence to suggest that the radical disproportionates to produce hydrogen peroxide and this is its major role. This assumption is based on the evidence that dissolved oxygen content has a direct effect on the rate of production of hydrogen peroxide and the fact that the addition of superoxide dismutase reduces the rate of production of hydrogen peroxide [10]. Conclusive identification and measurement of the superoxide radical have not been available to support this indirect evidence of the role of the superoxide radicals in natural water systems. Such measurements would provide steady state concentration or kinetic data which could support the argument for disproportionation of the superoxide radical to form hydrogen peroxide or even confirm the presence of the radical itself. The lack of direct data means that estimates of superoxide radical concentration are based on estimated rates of formation and the

hypothesis that the upper limit of superoxide radical concentration is 10^{-8} M is unsupported by measurements.

These estimates are based on hypothetical rates of formation and ignore scavenger removal pathways, assuming that the superoxide radical will decay primarily through disproportionation to hydrogen peroxide. Because of a lack of definitive information on the superoxide radical and its fate in natural water systems, this project has been undertaken in order to provide both steady state concentration data for the superoxide radical, and kinetic data for the removal of the radical from natural water systems. This data has contributed to an understanding of the removal pathway of the radical from natural water, and its overall contribution to natural water chemistry.

1.2 Superoxide Detection Methods

There are a number of techniques available for detecting the superoxide radical in solution, such as UV-VIS absorption, scavenger and electrochemical techniques. Each of these techniques have advantages but also have inherent limitations, and therefore their suitability is determined by the required detection limits, equipment portability, and their specificity for the superoxide radical. These techniques are discussed in the context of their suitability for the detection of the superoxide radical in natural water.

1.2.1 UV-VIS Absorption

UV-VIS absorption is one of the most direct methods used to study the superoxide radical [11]. The molar absorptivity of the superoxide radical of 2234 M^{-1} cm^{-1} at 246 nm was used to follow the disproportionation behaviour of the radical and the rate constant for this process to be determined from pH 0-13 [11]. This is a direct technique and one of the easiest ways to monitor the superoxide radical steady state concentrations. However, the low estimate of the steady state concentration of the superoxide radical in natural water (10^{-8} M) is beyond the micromolar detection limits of the technique. For absorption to be above 0.001 (which is the typical detection limits for a UV-VIS absorption photometer) would require a cell path length of 50cm for 10^{-8} M superoxide concentration. In terms of a practical apparatus for in-situ measurements this is not practical, and interference from more concentrated species absorbing in the same wavelength region would prevent useful measurements.

1.2.2 Electrochemical Techniques

Another method for the detection of the superoxide radical is an electrochemical technique. Scheller and Bier [12] have used the response of a permeable Teflon covered platinum electrode to measure superoxide radical concentration. The superoxide radical source was a hypoxanthine-xanthine oxidase system. The platinum electrode worked as a detector by converting superoxide radical to hydrogen peroxide and measuring the variation in current with time at the electrode. In order to prevent a background signal from endogenous hydrogen peroxide, Teflon membranes with a low permeability to hydrogen peroxide were used.

The electrode was found to have a linear response to hydrogen peroxide inside the Teflon membrane at micromolar concentrations. However, the micromolar detection limit for hydrogen peroxide and hence superoxide radical is two orders of magnitude above the anticipated concentration of the superoxide radical in natural water which prevents the use of an electrochemical technique for the detection of the superoxide radical in natural water.

1.2.3 Scavenger Techniques

Cytochrome c (CTC), Nitro Blue Tetrazolium (NBT) and Tetranitromethane are three compounds that have been used to measure the superoxide radical [11]. These compounds react with the superoxide radical to form products with intense optical absorbance. The problem with using these compounds as scavenger molecules is that they are not specific for the superoxide radical and therefore restricts their use.

Although these scavenger compounds will react with the superoxide radical, they will also react with many other radical species e.g. CTC reacts with hydrated electrons, ethoxy and carbon dioxide radicals. In addition, the detection limit for scavengers used such, as CTC is at most 10^{-7} M which is an order of magnitude higher than the expected steady state concentration for the superoxide radical in the environment. CTC may also be inhibited by reaction with other molecules, and in view of these problems, a more suitable technique is needed with greater specificity for the superoxide radical.

1.2.4 Chemiluminescent Detection Methods

The technique of chemiluminesence has seen widespread application in environmental and biological systems [13]. In biological systems it is the most commonly used technique for measuring the superoxide radical, using the reaction of the radical with luminol or lucinegin, and observing the chemiluminescent intensity produced by the oxidation of these species as a measure of superoxide radical concentration [14]. In environmental situations luminol oxidation has been used to detect picomolar concentrations of various transition metals including cobalt [15], manganese [16], iron and copper [17]. For chemiluminescence to be a direct measure of the superoxide radical, the intensity of light emitted when the chemiluminescent compound is oxidised should be proportional to the superoxide radical concentration.

1.3 Chemiluminescent Detection of the Superoxide Radical

The two key factors in selecting a detection technique for the superoxide radical in natural water are the required detection limit and the specificity of the technique. In all the techniques described previously there are possible interferences. Ideally, the detection technique should be able to detect the superoxide radical at nanomolar concentrations without any interference from any other species present in natural water. In reality it is not possible to have such an ideal technique. However, the low steady state concentration of the superoxide radical means that the only technique available is chemiluminesence in conjunction with a rapid analysis technique such as stopped-flow or continuous flow analysis. The latter has been used to measure

hydrogen peroxide in natural water at concentration levels similar to the anticipated concentration of superoxide in the environment. This indicates that the technique would be suitable for the detection of the superoxide radical providing a suitable chemiluminescent chemical with sufficient specificity for the superoxide radical can be found.

1.4 Luminol or Lucinegin

Both Luminol and Lucinegin have been used frequently for the detection of the superoxide radical in biological systems, and it is generally assumed that both these compounds react with the superoxide radical, leading to the production of photons which are detected to measure the superoxide radical concentration. Research indicates that although both react with the superoxide radical to produce luminescent excited states, the underlying chemistry of both molecules is very different. Their use is determined by their suitability in detecting the superoxide radical in natural water. Luminol displays greater specificity for reaction with the superoxide radical, because the chemiluminescent reaction involves the superoxide radical an integral part of the oxidation process to produce light, unlike lucinegin [13].

1.4.1 Luminol

Luminol, 3-aminophthalhydrazide, is a widely used chemiluminescent compound in chemiluminescent studies. Luminol can be oxidised by a number of compounds such as ferricyanide, perchlorate, persulfate ions as well as hydrogen peroxide and the superoxide radical. One of the reasons why these ions oxidise luminol is that one electron oxidation of luminol by these species yields a luminol radical which can

reduce oxygen to the superoxide radical or react with the superoxide radical itself. The integral role of the superoxide radical in the oxidation mechanism of luminol, and the fact that it is capable of oxidising luminol, has led to the widespread use of luminol in chemiluminescent techniques to detect the superoxide radical. An important factor in the luminol oxidation reaction is that it is base catalysed, and the luminol must exist as an anion to undergo oxidation. In fact, at neutral pH, no chemiluminescent activity can be seen and this activity only becomes evident at higher pH (typically pH 9-10), and in this project the luminol solution pH was 10.25. The base catalysed nature of the chemiluminesence reaction means that luminol is not a good chemiluminescent agent in biological systems at biological pH. However, in inorganic systems the pH of the solution can be raised as high as pH 11. The only restriction is that at very high pH some insoluble precipitates such as $Mg(OH)_2$ and $Ca(OH)_2$ and $CaCO_3$ can form when the luminol solution is mixed with sea water.

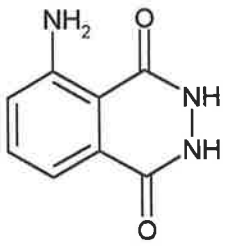

Figure 1.1 Luminol Structure

1.4.2 Lucinegin

The chemistry of lucinegin involves the reaction of the superoxide radical with a radical form of the luminescent compound. However, unlike luminol, the radical reactive form is generated by univalent reduction which can then react with the superoxide radical. There is no evidence however to suggest that the superoxide radical alone is capable of reducing lucinegin. Consequently, this molecule is not a reliable indicator of the superoxide radical concentration because the radical itself is not sufficient to cause chemiluminesence, and is not recommended as an indicator of the superoxide radical [13].

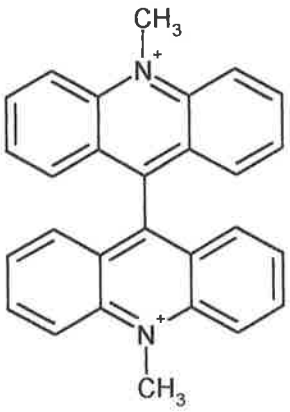

Figure 1.2 Lucinegin Structure

1.4.3 Chemiluminesence Mechanism- Luminol Oxidation

The need for the presence of the superoxide radical for the oxidation of luminol for oxidation has been demonstrated by the reaction of luminol with xanthine oxidase.

The enzymatic cycle involving xanthine oxidase is known to produce the superoxide radical and the overall reaction is.

$$\text{Enzyme-}H_2 + 2O_2 \rightarrow \text{Enzyme} + 2H^+ + 2O_2^{-\cdot}$$

$$\text{Enzyme-}H_2 + O_2 \rightarrow \text{Enzyme} + H_2O_2$$

In the presence of molecular oxygen the reduced enzyme can lose these electrons via two pathways, a univalent reduction leading to the formation of the superoxide radical or a divalent reduction leading to the formation of hydrogen peroxide. The predominance for one pathway over the other can be controlled by pH variation.

The role of the radical in the xanthine-oxidase catalysed chemiluminesence of luminol was revealed by the inhibitory effect of superoxide dismutase. Superoxide dismutase strongly inhibits the chemiluminesence of luminol whether the chemiluminesence is elicited by xanthine oxidase plus xanthine [18] or by other oxidants such as hydrogen peroxide, ferricyanide persulfate or hypochlorite [19, 20]. The inhibitory nature of superoxide dismutase which catalyses the dismutation of the superoxide radical only, is clear evidence for the role of the superoxide radical in the chemiluminescent mechanism. The explanation for the inhibitory nature of SOD is that univalent oxidation of luminol yields a luminol radical that can both reduce O_2 to $O_2^{-\cdot}$, and can also react with $O_2^{-\cdot}$, yielding an unstable endoperoxide whose decomposition leads to the electronically excited aminopthalate. The reactions of this process lead to the production of chemiluminesence, as seen in Figure 1.3.

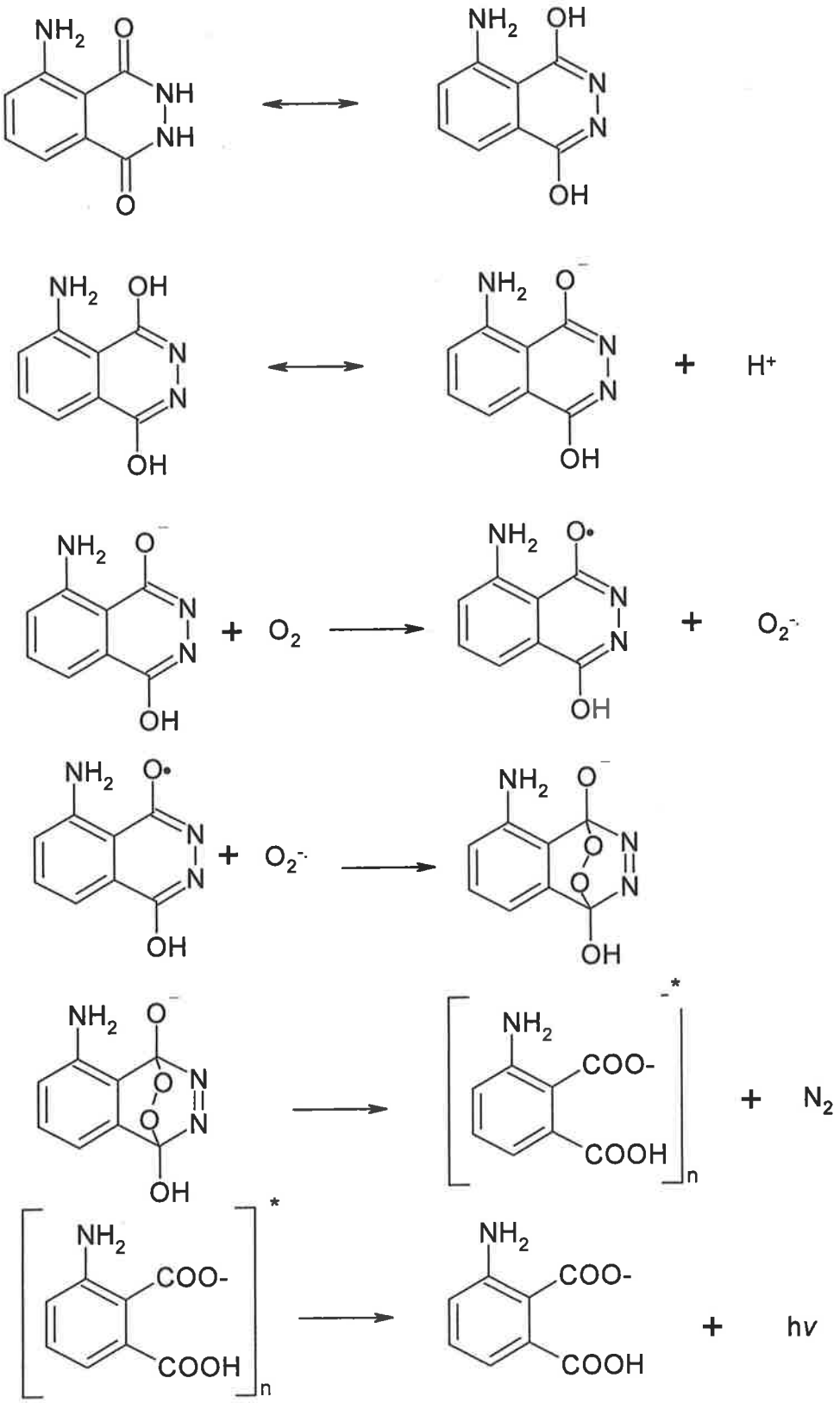

Figure 1.3 Reaction scheme for the oxidation of luminol [13]

The pH dependent chemiluminescence of luminol on oxidation and its ability to generate superoxide radicals means that it is not well suited to detection of the superoxide radical in living cells. In natural water many problems associated with the use of luminol in biological systems can be overcome. The pH of a luminol solution can be maintained at a high pH (10-11) and is only limited by the possibility of the precipitation of metal hydroxide species found in natural water, especially sea water. Precipitation of these species could interfere with the detection apparatus by scattering and reducing the transmission of light or in the case of a continuous flow apparatus, blocking the apparatus. Luminol can both generate and detect the superoxide radical, which may lead to confusing results. In the case of water analysis it is possible to obtain a blank solution free from photochemically generated superoxide radical by removing the sample from sunlight. This blank solution can be used to calibrate the background chemiluminesence that may arise from the self-production of the superoxide radical by luminol, as the blank will have the same oxygen concentration as the sample analysed in the stream. The difference between the two solutions is then used as the measure of photochemically generated superoxide radical.

1.5 Detection Apparatus

A chemiluminescent detection system requires measurement of the light intensity during the chemiluminesence reaction to provide a readily interpretable measure of the superoxide radical concentration. Both stopped flow or continuous flow methods. could be used to measure the superoxide radical. However, stopped flow has the disadvantage of being a batch type analyser where the flow is stopped for a period and

then the apparatus must be emptied and refilled whereas continuous flow techniques are more convenient because the reagents will flow continuously without the need to refill the apparatus. This yields a higher sampling rate and is a less labour intensive technique. Continuous flow techniques have already been used to detect numerous species using chemiluminesence, including trace amounts of transition metals and hydrogen peroxide. The speed of analysis of this technique with sampling rates for hydrogen peroxide of 120 samples per hour [21] and the reproducibility of FIA made this system a suitable system. Plans of existing systems constructed to detect hydrogen peroxide using luminol as a chemiluminescent detection compound needed only minor modification in terms of the detection unit to measure the superoxide radical. The major design focus was the optimisation of the chemistry for the detection of the superoxide radical.

1.6 Calibration

In any analytical technique it is essential to develop a suitable calibration technique. The transient nature of superoxide radical, which decays through disproportionation, creates difficulties in providing standard solutions of the radical for calibration purposes. The calibration system must be able to produce a steady state superoxide radical concentration for the chemiluminescent system. The two most suitable techniques for the calibrated production of the superoxide radical are enzymatic generation and gamma radiolysis.

1.6.1 Enzymatic Generation

A number of enzymes such as xanthine oxidase, aldehyde oxidase, dihydro-orotic dehydrogenase and a number of flavin dehydrogenases all produce superoxide radicals during their catalytic cycles. The most studied of these catalytic cycles is the action of milk xanthine oxidase on a xanthine substrate. The reaction mechanism of this cycle is well understood as it was one of the earliest catalytic cycles identified [22].

In the case of the reduction of Cytochrome c by milk xanthine oxidase the presence of oxygen is required. When xanthine oxidase acts on its substrate in the presence of oxygen it univalently reduces oxygen to the hydroperoxyl radical which deprotonates at biological pH to the superoxide radical.

$$EH_2 + O_2 \rightarrow EH^{\cdot} + HO_2^{\cdot}$$

$$HO_2^{\cdot} \rightarrow H^+ + O_2^-$$

The univalently reduced enzyme can then produce a second hydroperoxyl radical by reaction with molecular oxygen or the hydroperoxyl radicals can dismutate

$$HO_2^{\cdot} + HO_2^{\cdot} \rightarrow H_2O_2 + O_2$$

or, in the presence of ferri-cytochrome c the hydroperoxyl radical could reduce the ferri-cytochrome c.

$$HO_2^{\cdot} + \text{Cytochrome } c^{+++} \rightarrow O_2 + H^+ + \text{Cytochrome } c^{++}$$

In the absence of cytochrome c the steady state concentration of the hydroperoxyl or superoxide radical will depend on its rate of formation and disappearance.

In the standard laboratory technique for superoxide radical generation by enzyme action the preferred substrates are xanthine and acetaldehyde. These substrates are oxidised to uric acid and acetic acid respectively [23]. In the enzymatic pathway there are two reaction pathways for the reduction of xanthine oxidase. A one-electron oxidation leads to the production of the superoxide radical (Reaction 1) and a two-electron oxidation leads to the formation of hydrogen peroxide (Reaction 2).

$$\text{Enzyme-}H_2 + 2O_2 \rightarrow \text{Enzyme} + 2H^+ + 2O_2^{-\cdot} \quad \text{Reaction 1}$$

$$\text{Enzyme-}H_2 + O_2 \rightarrow \text{Enzyme} + H_2O_2 \quad \text{Reaction 2}$$

The yield of the superoxide radical in this system expressed as a function of xanthine oxidised varies between 20 and 100% depending on pH, oxygenation and the turnover rate of the radical. Raising the pH and oxygen concentration or lowering the turnover rate will favour reaction 1. Although this technique is a useful source of superoxide radical, caution must be exercised in its use as small amounts of metal impurities in such enzyme systems can lead to Fenton type reactions and hence misinterpretation of observed results e.g.

$$Fe^{2+} + H_2O_2 \rightarrow Fe^{3+} + {}^{\cdot}OH + OH^-$$

In addition, the presence of some metallic impurities will catalyse the disproportionation of the HO_2/O_2^- causing a rapid build up of hydrogen peroxide which can interfere with chemiluminescent detection techniques.

1.6.2 Gamma Radiolysis

Two techniques have been used to produce the superoxide radical through gamma radiolysis. These techniques involve the irradiation of hydrogen peroxide solutions or sodium formate solutions [11].

The irradiation of hydrogen peroxide solution is one of the oldest techniques for the generation of the superoxide radical. After the initial production of the primary radicals from the radiolysis of water, both e^-_{aq} and H are converted into OH radicals by reaction with hydrogen peroxide

Primary Radical Formation $H_2O \longrightarrow\!\!\!\!\wedge\!\!\wedge\!\!\rightarrow H,\ e^-_{aq},\ OH,\ H_2,\ H_2O_2,\ H_3O^+$

$$e^-_{aq} + H_2O_2 \rightarrow OH + OH^-$$

$$H + H_2O_2 \rightarrow OH + H_2O$$

The OH radicals then react with hydrogen peroxide to yield HO_2

$$OH + H_2O_2 \rightarrow H_2O + HO_2$$

$$HO_2 \leftrightarrow H^+ + O_2^-$$

The major problem with the use of this system with a chemiluminescent molecule for superoxide radical detection is the fact that hydrogen peroxide is capable of oxidising luminol as well as the superoxide radical. This makes it impossible to distinguish whether the signal arising from the oxidation of luminol is due to hydrogen peroxide or the superoxide radical.

The gamma radiolysis of sodium formate solutions is particularly useful because it does not involve the presence of large amounts of hydrogen peroxide in the solution.

In oxygenated formate solution the following reactions occur on radiolysis of water

$$e^-_{aq} + O_2 \rightarrow O_2^{\cdot-} \quad \text{Reaction 3}$$

$$e^-_{aq} + H^+ \rightarrow H \quad \text{Reaction 4}$$

$$H + O_2 \rightarrow HO_2$$

$$HCO_2^- + OH \rightarrow CO_2^{\cdot-} + H_2O$$

$$HCO_2^- + H \rightarrow CO_2^{\cdot-} + H_2$$

$$CO_2^{\cdot-} + O_2 \rightarrow CO_2 + O_2^{\cdot-}$$

Reaction 4 occurs in air saturated solutions only if the pH<4, otherwise all will be Reaction 3

The only pathway for hydrogen peroxide formation is the reaction between two hydroxyl radicals.

$$OH + OH \rightarrow H_2O_2$$

and at sufficiently high sodium formate concentrations only the initial radiolytically generated hydrogen peroxide (G =0.78) will be present.

The formate system has been used for kinetic measurement of the disproportionation reaction of the superoxide radical because the quantitative conversion of the primary radicals to HO_2/ $O_2^{\cdot-}$ occurs at near diffusion controlled rates independent of pH. Some alcohols may be substituted (ethanol, methanol, 2-propanol) for formate. In this project a sodium formate solution was used because an alcoholic aqueous solution does not accurately reflect the composition of natural water and would introduce unnecessary complications to the measurement of the superoxide radical in water. The

major advantage of the formate system is that it contains less hydrogen peroxide than the amount present due to the radiolysis of hydrogen peroxide solution. This will result in less interference with the detection of the superoxide radical than using a hydrogen peroxide solution.

Dosimetry can be used to calculate the source dose rate and hence the rate of production of the superoxide radical [24]. Knowing the forward production rate of the superoxide radical, and the rate of decay of the radical through disproportionation, the time to reach a steady state superoxide radical concentration, and the steady state concentration can be accurately calculated. The calculations of source dose rate and the rate of production of the superoxide radical can be found in detail in chapter four.

References

1. Pryor W.A, *The formation of free radicals and the consequences of their reactions in vivo.* Photochemistry and Photobiology, 1978. **28**: p. 787.
2. Anderson D.E, Henderson C.F., *Ionospheric Species.* J. geophys. Res, 1971. **76**: p. 6666.
3. Lees G.J, *Contributory mechanisms in the causation of neurodegenerative disorders.* Neuroscience, 1993. **54**: p. 287.
4. Zafiriou O.C, Zepp R.G, Zika R.G, *Photochemistry of Natural Waters.* Environ. Sci & Tech., 1984. **18**(12): p. 358A.

5. Haber F, Weiss J., *Uber die Katalyse des Hydroperoxides.* Naturwissenschaft, 1932. **20**: p. 948.

6. Land E.J, Swallow A.J., *One electron reactions in biochemical syatems as studied by phase radiolysis.* Biochem. Biophys. Acta, 1971. **234**: p. 36.

7. English D.K., Petrone W.F, Wong K., *Free radicals and inflammation: superoxide dependent activation of a neutrophil chemotactic factor in plasma.* Proc. Natl. Acad. Sci. USA, 1980. **77**: p. 1159.

8. Low P.S, Low M.J., *The oxidative burst in plant defense: Function and signal transduction.* Physiol. Plant, 1996. **96**: p. 533.

9. Tanaka K.M, Shimada M., *Generation of superoxide anion radical by the marine phytoplankton organism, Chattonella antiqua.* J. Plankton Res., 1994. **16**(2): p. 161.

10. Cooper W.J., Zika R.G., Petasne R.G., Plane J.M.C, *Photochemical Formation of H_2O_2 in natural waters exposed to sunlight.* Environ. Sci. & Technol., 1988. **22**(10).

11. Bielski B.H.J, Cabelli.D.E, Arudi R.L, Ross AB, *Reactivity of HO_2/O_2^- radicals in aqueous solution.* J. Phys. Chem Ref. Data, 1985. **14**(4): p. 1041.

12. Bier F.F., Scheller F., Min Ik Song., *A method to detect superoxide radicals using Teflon membrane and superoxide dismutase.* Bioelectrochem. Bioenerg., 1995. **38**: p. 419.

13. Faulkner K, Fridovich.I., *Luminol and lucinegin as detectors for O_2^-.* Free Rad. Bio. Med, 1993. **15**: p. 447.

14. Dzialoszynski T.J., Linklater K, *A new technique for enhaning luminol luminescent detection of free radicals and reactive oxygen species.* Biochemistry and Molecular Biology International, 1994. **33**: p. 1179.

15. Johnson K.S.,Sakamoto-Arnold C.M., *Determination of picomolar levels of cobalt in sea water by Flow Injection Analysis with Chemiluminesence Detection.* Anal. Chem, 1987. **59**: p. 1789-1794.

16. Chapin T.P., Johnson K.S., *Rapid determination of manganese in sea water by flow-injection analysis with chemiluminescence detection.* Anal. Chim. Acta., 1991. **249**: p. 469.

17. Coale K.H, Johnson K.S, Sakamoto-Arnold C.M., Stout P.M., *Determination of copper in sea water using a flow-injection method with chemiluminesence detection.* Anal. Chim. Acta., 1992. **266**: p. 345.

18. Henry J.P, Michelson A.M, *Studies in bioluminesence.VIII. Chemically induced luminesence of Pholas Dactylus luciferin.* Biochimie, 1973. **55**: p. 75.

19. Fridovitch I, Hodgson.E., *The role of $O_2^{-\cdot}$ in the chemiluminesence of luminol.* Photochem. Photobiol., 1973. **18**: p. 451.

20. Fridovitch I, Miller.E.K., *A demonstration that O_2^- is a crucial intermediate in the high quantum yield luminesence of luminol.* J. Free. Rad. Biol. Med, 1986. **2**: p. 451.

21. Price D, Worsfold P.J, Fauzi R., Mantoura C., *Determination of Hydrogen Peroxide in sea water by flow injection analysis with chemiluminesence detection.* Analytica Chimica Acta., 1994. **298**(2): p. 121.

22. Fridovitch I, Miller E.K., *The reduction of cytochrome c by milk xanthine oxidase.* J. Biol. Chem., 1968. **243**: p. 5753.

23. Fridovitch I., *Quantitative Aspects of the production of the superoxide radical by milk xanthine oxidase.* J.Biol. Chem, 1970. **245**: p. 4053.

24. Allen A.O ,Van Nostrand D., *Radiation Chemistry of water and aqueous solutions.* 1989: p. 20

2.0 Experimental

2.1 Materials

2.1.1 Reagent Preparation

The chemiluminescent compound luminol was obtained as its sodium salt. A stock solution of luminol was 0.001 M in 0.01 M sodium carbonate. This stock solution was diluted to $2x10^{-4}$ M for use as the reagent in a 0.15 M sodium carbonate solution. The stock luminol was refrigerated while the luminol reagent solution was oxygenated for 10 minutes prior to use.

The superoxide anion is generated through gamma radiolysis of sodium formate solution. This was prepared by dissolving AR grade sodium formate in Milli-Q water to produce the 0.01 M sodium formate solution which was used in the gamma radiolysis experiments. For calibration purposes in various natural waters, the superoxide radical was generated using the same technique but the natural water sample was used to dissolve the sodium formate rather than Milli-Q water.

Hydrogen peroxide (A.R grade) was standardised by titration with potassium permanganate. All hydrogen peroxide solutions were refrigerated or used immediately after preparation to avoid decay of hydrogen peroxide. The decay of hydrogen peroxide is also affected by exposure to light and the solutions were stored in the dark.

The rate of decay is about 10^{-14} M/hr but increases to 10^{-9} M/hr when exposed to sunlight.

The water used in all experiments was deionised and purified by a Milli-Q RX plant. In order to remove trace amounts of hydrogen peroxide and organic contaminants (which could interfere with the measurement of the superoxide radical,) the water was redistilled from a solution of acidified potassium dichromate.

Stock solutions of first row transition metal ions were prepared by dissolving the A.R sulfate salts of the metals in Milli-Q water.

All gases (oxygen and nitrogen) used were instrument grade.

2.2 Reverse Flow Injection Analysis

2.2.1 Introduction

The apparatus required for the detection of superoxide was designed to provide a high level of sensitivity, and discrimination, for the measurement of the superoxide radical in natural water. The detection technique uses light emitted by the oxidation of the chemiluminescent compound luminol as a measure of the superoxide radical concentration. The emitted light is detected by a photomultiplier tube and reaction cell, which are combined with a Reverse Flow Injection manifold for sample injection. Both

the manifold and detector were designed to enable the detection unit for the superoxide radical to be used in the field.

2.2.2Apparatus

The apparatus for the detection of the superoxide radical consists of two major components-

1. a detection unit
2. a delivery manifold.

The detection unit design is determined by the speed at which luminol oxidises in the presence of the superoxide radical and the reaction rate of this oxidisation determines the rate of light emission. The design of the detection system had to take into account the chemiluminesence behaviour of luminol in the presence of the superoxide radical. In order to measure the light emitted by this reaction a photomultiplier tube was used as the detector because of the ability of this detector to measure the low intensity of the emitted light. In the detection unit the photomultiplier tube was combined with a flow cell design which maximised the observed light intensity from the reaction between luminol and superoxide. The design of this flow cell is described in detail in section 2.3.1.

The manifold has two functions, to provide a transport system, and an injection port, to allow the detection regent to mix with the sample. The manifold also incorporates the detection cell. The manifold is a conventional flow injection manifold, i.e. the system has four components- a pump to transport reagents; an injection system to mix

the reagents with a sample; a reaction zone for the reaction to occur between the sample and reagent streams; and a detector.

The key components of the apparatus are illustrated in figure 2.1. The flow of reagents is controlled by a peristaltic pump. The Rheodyne valve is used to inject the luminol into the deionised water carrier stream. This valve is controlled remotely by an electric motor for use in the gamma radiation cell. It should be noted that the deionised water stream does not play a role in the chemistry of the reaction between superoxide radical and luminol anion, rather it simply acts as a carrier for the injected luminol solution.

The photomultiplier tube converts the light intensity produced by the oxidation of luminol to a voltage signal. The voltage output from the apparatus was collected in digital format to enable results to be analysed using existing data processing software. These programs were designed using the Windows based Labview graphical programming language.

An essential feature of the apparatus design was the combination of the components in the Flow Injection manifold. There are two possible manifold combinations - Flow Injection or Reverse Flow Injection. In a Flow Injection manifold the sample is injected into a reagent stream for detection purposes whereas in an RFI manifold the reagent is injected into the sample stream. The use of Reverse Flow Injection is possible when large amounts of sample are available as is the case for in-situ natural water analysis and the limiting factor is the amount of detection reagent (luminol)

present. In a Reverse Flow Injection system the luminol stream can be recycled permitting more samples to be analysed per site than would be the case if a Flow Injection manifold were used. In the Reverse Flow Injection manifold used in this study luminol reagent consumption was 0.45ml/min compared with 1.1ml/min in a Flow Injection manifold.

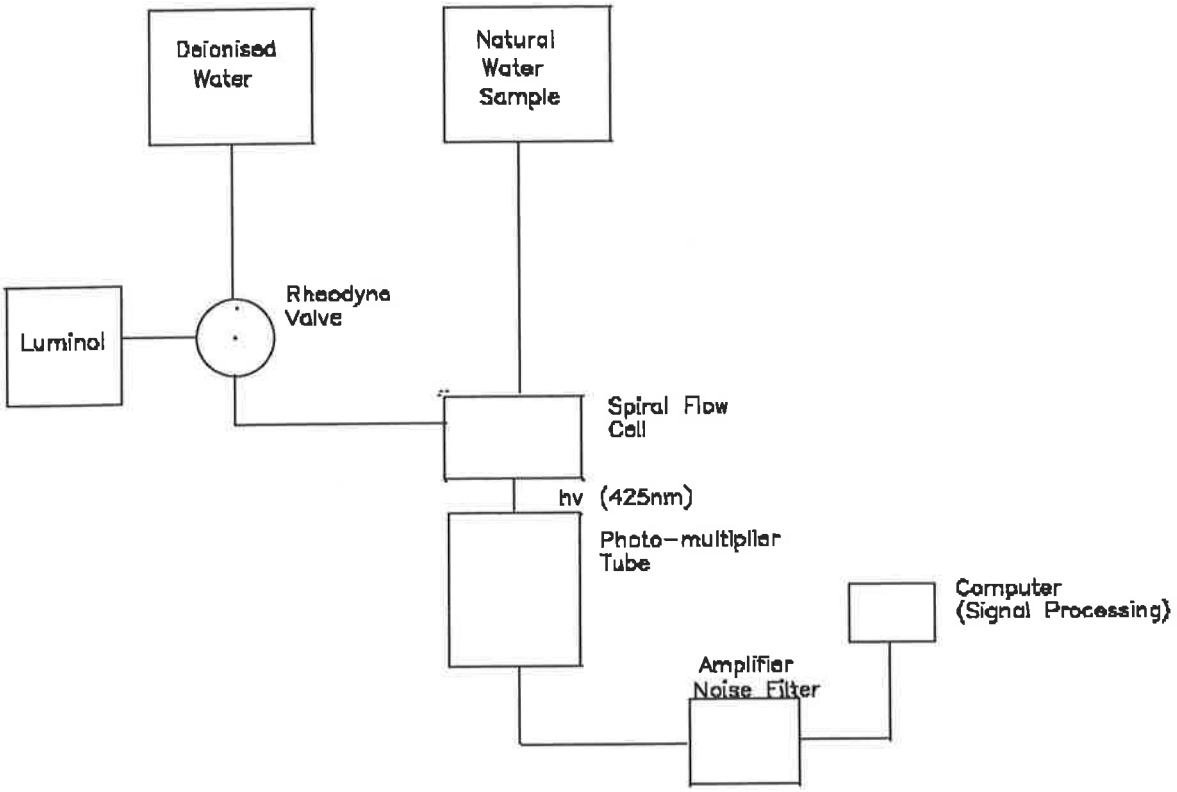

Figure 2.1 Flow Injection Analysis - Apparatus Design

2.2.3 Reagent Delivery System

A number of propulsion systems are available for use in Reverse Flow Injection manifolds. These include a sinusoidal flow pump, a gas-pressure reservoir or a peristaltic pump. All these pump designs are feasible for use in Reverse Flow Injection manifolds because they are compact and portable. In addition the pump design must be

such that the wetted parts are inert at high pH in order to prevent the formation of transition metal ions especially Fe(II) and Cu(II). A major problem in the detection of the superoxide radical is the possibility of the introduction of transition metal ion impurities into the reagent stream. Transition metal ions, in particular Cu(II) catalyse the removal of the superoxide anion from solution. In addition a large number of first row transition metal ions (Co(II), Mn(II), Cu(II), Fe(II)) catalyse the oxidation of luminol by hydrogen peroxide which could interfere with the detection of the superoxide radical. These ions could be produced by the corrosion of the metallic surfaces at the high pH(10.5) used for some reagents.

A peristaltic pump where the reagents are only in contact with inert tubing minimises these effects. A Gilson Minipuls peristaltic pump met the above requirements and had the advantage of being computer controlled while capable of delivering a wide range of flow rates. The flow rate of the reagents could be varied by changing the pump speed or the diameter of the Tygon transmission tubing. The pump speed varied from 0.1 to 48rpm and the tubing diameter varied from 0.02 inches i.d to 0.06 inches i.d so that flow rates from 0.1 μl to 50 ml per minute could be achieved. The peristaltic pump tubing selected for this project was Tygon tubing. This material is a flexible polymer chemically resistant to high pH, which was essential given that the pH of the reagent streams varied from 6.5 to 11.5.

2.2.4 Flow Cell

The flow cell design for chemiluminescent detection in a Reverse Flow Injection manifold is determined by the kinetics of the reaction that produces the chemiluminesence. The overall oxidation of luminol proceeds via the formation of the luminol radical by the oxidation step and the oxidation of the luminol radical by the superoxide anion ($k = 1.4 \times 10^9$ L Mol^{-1} s^{-1}) produces the chemiluminesence. When luminol and the superoxide radical are mixed the speed of the reaction results in light being emitted on a millisecond time scale. It is therefore essential that mixing must be followed immediately by detection in order to maximise the sensitivity of the apparatus.

The standard flow cell design for chemiluminescent detection systems is well documented by Brugera [1]. The flow cell consists of a flow coil that is placed against a photomultiplier tube window to allow the maximum amount of light intensity from the chemiluminesence produced in the cell to be detected. The flow cell design is illustrated in figure 2.2.

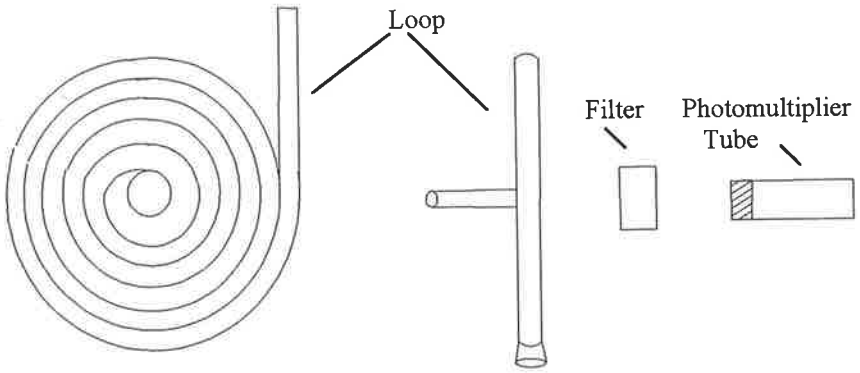

Figure 2.2 Flow Cell Design for use in FI-CL Manifolds [2]

Although the basic design of a spiral flow cell for detection in a chemiluminescent Flow Injection / Reverse Flow Injection manifold is standard, there are a number of practical considerations which must be considered when incorporating the flow cell in the Reverse Flow Injection manifold. The two most important factors identified by Brugera are the distance between the point of mixing and the detector, and the volume of the spiral flow cell. The distance between the injection port and detection coil must be as short as possible in order to maximise the detected intensity of the light produced by the oxidation of luminol. In the flow cell used in this project, the mixing T - detector distance was minimised by placing the mixing T immediately before the spiral flow cell entrance.

The second factor identified by Brugera as affecting the apparatus sensitivity is the volume (or length) of the spiral flow cell. The flow cell must be of sufficient volume to maximise the emitted light intensity to be detected by the photo-multiplier tube. The reaction should be observed in the flow cell over the time in which most of the light

intensity is emitted. If the flow cell is too small compared with the residence time of the reacting luminol/superoxide mixture, only a small amount of the emitted light - intensity that occurs will be observed, and this will lower the sensitivity of the apparatus. Alternatively if the cell volume is too large, the sample and reagent concentrations will undergo considerable dispersion, leading to less effective mixing of the sample and reagent streams in the cell. The less effective mixing will decrease and delay the light intensity produced in the cell.

The sensitivity of the detection unit is determined to a large extent by the volume of the flow cell, which in the case of spiral flow cells is the length of the coil. The length of the spiral flow cell should be such that the oxidation of luminol by the superoxide anion achieves near completion in the spiral flow cell in order to maximise the emitted light intensity detected by the photomultiplier tube.

In order to determine the required length of the flow cell, the light intensity vs time relationship for the oxidation of luminol must be determined. This relationship is determined by observing the decay of emitted light intensity when luminol solution is mixed with the superoxide radical. The intensity vs time plot of the oxidation of luminol is shown in Figure 2.3.

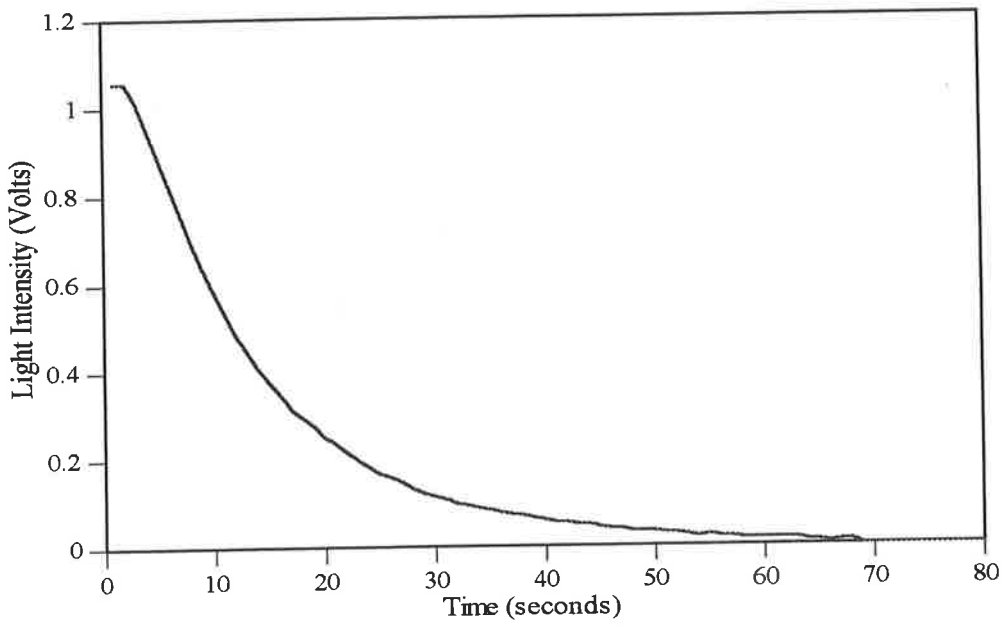

Figure 2.3 Light Intensity as a function of time for oxidation of luminol in the presence of the superoxide radical

Figure 2.3 indicates that 90% of the emitted intensity from the oxidation of luminol in the presence of the superoxide occurs within 30 seconds after mixing. This means that the residence time of the luminol solution in the flow cell need not be more than 30 seconds to record almost the entire emitted intensity of the reaction. The residence time should be considered in the context not only of observing the emitted light intensity, but also the time taken to analyse a sample. As the residence time in the spiral flow cell increases, the sampling rate falls due to increased sample dispersion, leading to peak broadening and increased time for the maximum intensity to be observed. Therefore, the residence time must be sufficient to observe most of the emitted light intensity but at the same time provide a realistic sampling flow rate.

Another factor to consider in deciding the flow cell volume is the effect of flow cell volume on sampling rate. The relationship between sampling rate (samples per minute) and base line-to-baseline time (Δt) for the signal is given by

$$\text{sampling rate per minute} = \frac{60}{\Delta t}$$

The relationship between baseline to baseline time and hence the sampling rate and a number of flow parameters such as cell length, flow rate, and molecular diffusion coefficient have been determined by Vanderslice [3].

Vanderslice describes a flow system in which there is no chemical reaction and the characteristics are determined entirely by the flow dynamics of the system. However, Vanderslice provides an indication of the relationship between flow cell volume and sampling rate for systems with a chemical reaction occurring. In the spiral flow cell design a number of parameters are fixed- the flow rate and tubing radius are optimised before other considerations such as reagent concentration. The cell volume or length is therefore the critical parameter to be optimised.

The cell length is related to the baseline-to-baseline time by the relationship

$$\Delta t \propto L^{0.64}$$

Increasing the length of the flow cell increases the baseline to baseline time and consequently reduces the sampling rate. Therefore, a decision on the flow cell length must be based on the trade-off between the time needed to observe the light

intensity emitted by the oxidation of luminol, the chemical reaction time and flow rate, and the effect of increasing cell length on the sampling rate of the apparatus. Figure 2.3 provides the necessary information to make a decision on the residence time. Given that 90% of the light intensity occurs in the first 30 seconds residence times beyond 30 seconds were not considered. Three residence times were examined 30,15 and 10 seconds. The effect of residence time on sampling rate is shown in Table 2.1.

Table 2.1 The effect of residence time on light intensity and sampling rate

Residence Time(Seconds)	Percentage of Maximum Intensity Observed	Sampling Rate
10	50%	150%
15	70%	136%
30	90%	100%

Based on the information in Table 2.1 it was decided to base the flow cell volume and length was based on the residence time of 15 seconds.

The flow cell length and volume were calculated based on a residence time of 15 seconds and an optimised sample and reagent flow rate of 1.0 ml/min.

The cell volume is ΠR^2L where R is the tubing radius, and L is flow cell length.

The flow cell length is given by volumetric flow rate = $\frac{A \times L}{\Delta t}$

where volumetric flow rate = 2 x q where q is the reagent and sample flow rates,

Δt = residence time in spiral flow cell

Therefore

$$2 \times q = \frac{A \times L}{\Delta t}$$

$$2 \times 1.0 = \frac{\Pi R^2 L}{15}$$

$$30.0 = \Pi \times (0.38)^2 L$$

L= 66 cm

In the completed detection unit, the cell volume was found to be 0.317ml

which means the final length in the flow cell is

$$L = \frac{0.317}{\Pi \times (0.38)^2} = 69 \text{ cm}$$

In the detection unit of this apparatus, the spiral flow cell consisted of 69 cm of transparent Tygon tube coiled in a spiral arrangement in front of the photomultiplier tube. The Tygon tubing was in physical contact with the photomultiplier tube window in order to maximise the detection of the light intensity generated by the oxidation of luminol. The Tygon tubing was coiled into a machined brass block. This is a conventional arrangement for light detection using chemiluminesence, where the coiled tubing provides the most efficient design for the detection of the light generated by the oxidation of luminol.

2.2.5 Detection

The detection of the superoxide anion is dependent on the measurement of the emitted light intensity produced by the oxidation of luminol by the superoxide radical. Therefore, it is essential that a detector be used which can measure the light intensity generated by the oxidation of luminol. The detector must also be capable of responding to changes in light intensity as the reaction progresses, this capability is important as the maximum light intensity is generated within milliseconds of the luminol and superoxide mixing.

The photo multiplier tube used in this apparatus to detect the emitted light intensity arising from the oxidation of luminol is an end-window EMI 9558QB photo-multiplier tube. An end window photo-multiplier allows the spiral flow cell to be placed in physical contact with the detection window in order to maximise the incident light intensity on the window.

The photo-multiplier tube converts the incident light intensity from the oxidation of the luminol into a voltage signal. Before this signal can be used it is necessary to process the signal to increase the signal to noise ratio. In order to reduce the noise component of the signal, the raw voltage signal is passed through an operational amplifier with a time constant of 5 seconds and a gain of 100. The maximum amplification is reduced to a usable level by connecting the output voltage to the input voltage (negative feedback). The amplifier included a switched gain of 1,10 and 100. The large

background noise signal in the output from the amplifier when high voltages were applied to the PMT, made it difficult to distinguish the signal from the oxidation of luminol from the background noise. In order to increase the signal to noise ratio additional circuitry integrated the noise over times between 0.25 and 5 seconds. The integration of the noise reduces background fluctuations and increases the signal to noise ratio of the apparatus and hence improves the sensitivity of the equipment. The electronic circuitry is shown in Figure 2.4.

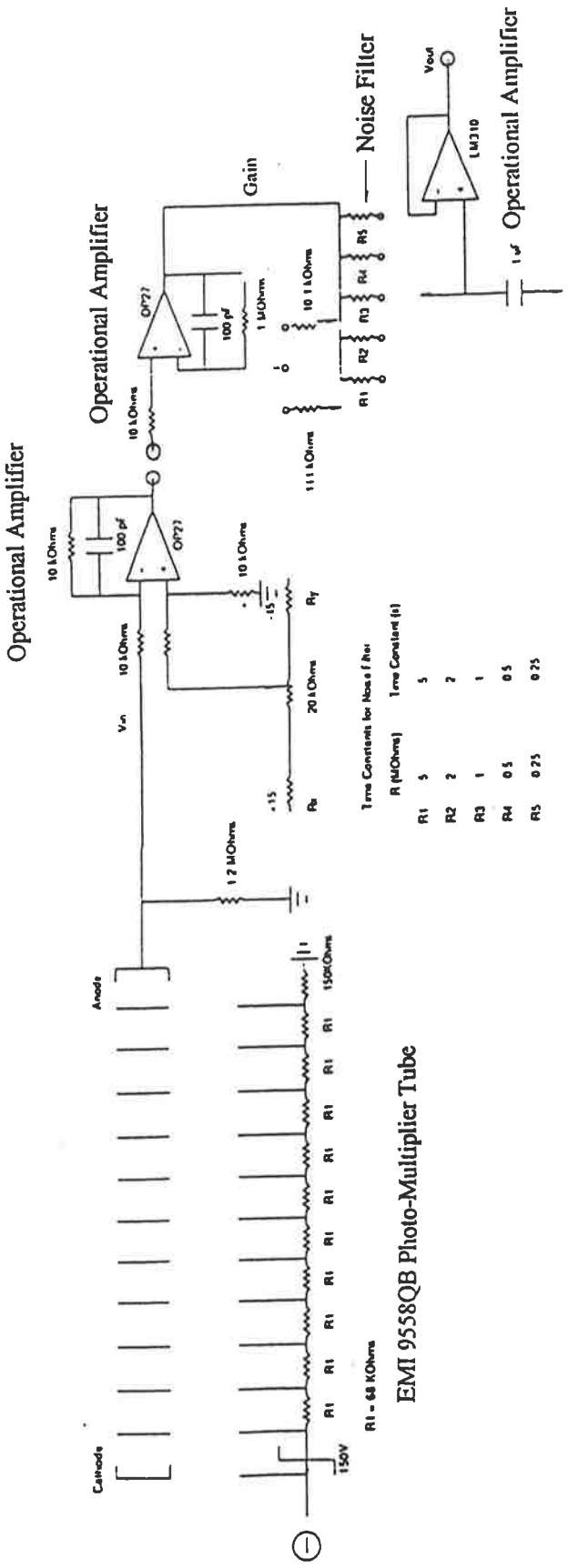

Figure 2.4 Electronic Circuitry for PMT, its Amplifier and Noise Filter

2.2.6 Detection Unit design

The spiral flow cell design in conjunction with an end window PMT is a conventional arrangement for the detection of chemiluminescent systems. The unit has a PMT and associated electronics housed inside a box painted matt black in the interior to reduce the amount of reflected light. The box has a hole large enough to permit the window of the PMT to be coupled with the spiral flow cell that was bolted to the exterior of the box.

During field trials, it was found that sunlight leaking into the housing caused a much larger signal than the signal arising from the oxidation of luminol. In order to reduce the background signal due to sunlight extensive light proofing of the detection unit was necessary. The brass block containing the spiral was screwed onto the box containing the PMT tube, using a layer of black rubber to provide a light seal. In addition, the rim of the box was covered with compressible foam to reduce light entering the unit between the lid and the box body. This light proofing was found to be satisfactory for use indoors, under both fluorescent and natural lighting. However, the measures were not sufficient to eliminate the interference effects in direct sunlight. In order to permit outdoor use, a number of light proofing modifications were introduced. These included painting the inlet tubing and T piece black, as well as covering the spiral cell holder with a metal light shroud that was bolted onto the box. Inlet and outlet holes were drilled in the metal shroud to allow Tygon tubing to be passed through the plate. The use of this metal light shroud prevented much of the

sunlight entering the enclosure and causing the rise in background signal that previously occurred when the unit was used in full sunlight conditions.

2.2.7 Data Collection

The maximum intensity of light striking the PMT window during the oxidation of luminol is a measure of the superoxide concentration. The incident light intensity is converted to a voltage signal by the photomultiplier tube, and after amplification recorded using a Science Workshop® analogue to digital conversion unit connected to a personal computer. This analog-to-digital unit operates in conjunction with Windows based software to allow the voltage signal from the detection unit to be recorded in digital format. The digitised voltage output is accessible in spreadsheet format and a number of data processing functions can be introduced to process the raw data stream.

2.3 Gamma Steady State Irradiation

Steady state gamma radiolysis of sodium formate solution is the technique used in this project to generate standard concentrations of the superoxide radical. All steady state irradiation were performed using the Co60 gamma ray source in the Department of Chemistry, University of Adelaide.

The Co60 decay produces two gamma rays with energies of 1.17 and 1.33MeV. The relatively short half-life of cobalt 60- 5.27 years meant that the source required regular calibration.

Around the radiation well several positions were marked onto which flasks could be placed at varying distances from the source in order to provide a different dose to each sample. The cobalt 60 source was calibrated using a Fricke dosimeter. This dosimeter solution was prepared using the method described in the literature [4].

2.4 UV-VIS Irradiation

A Rayonet photochemical reactor was used for the UV irradiation of water samples. The samples were placed in Pyrex flasks in the centre of the photochemical reactor. The light emitted from the lamps surrounding the flasks was 304 nm. During and after irradiation samples were pumped from the flasks using Tygon tubing and into the Reverse Flow Injection manifold described previously.

2.5 Natural Water Samples

The detection unit for this project was designed for in-situ detection of the superoxide radical, and consequently, samples were analysed on-site. However, samples needed collected from each site for calibration purposes. Seawater is of a reasonably uniform chemical composition and was sampled from two areas in the Port River Estuary. One of these sites was the Royal Adelaide Yacht Squadron Maintenance berth and the other a more regularly flushed and hence a less

contaminated area of the Port River Estuary. These sites were sampled in order to establish whether the presence of heavy metal or other pollutants would result in the inhibition of the chemiluminescent activity of luminol in the presence of superoxide. Fresh water samples were collected from the Mt Lofty Botanical Gardens Main Lake and Spring Dam. The table below gives the sample name and location for water sampled in this project.

Table 2.2 Sampling Locations

Sample Name	Location
BG1(Fresh water)	Main Lake Mt Lofty Botanic Gardens
SD1(Fresh Water)	Spring Dam Mt Lofty Botanic Garden
RYS1 (Sea Water)	Royal Adelaide Yacht Squadron Maintenance Berth
PR1 (Sea Water)	Port River Estuary

2.5.1 Natural Water Sample Collection

Sample collection and storage is extremely important as it can affect results through the introduction of foreign chemicals from the sample vessel or destruction of biological organisms present in the natural water. This is particularly relevant in the case of hydrogen peroxide where biological organisms are a source of hydrogen peroxide. All natural water samples used for calibration purposes were collected in light-proof HDPE bottles and refrigerated within 30 minutes of collection.

References

1.Bruguera J.L, Tomas A.K, *Spiral Flow Cell design.* Anal Proc., 1979. **16**(3): p. 263.

2.Brugera J.L, Tomas .A.K, *Flow Cell Design for Chemiluminescent Systems.* Anal. Chim. Acta, 1980. **114**: p. 209.

3.Vanderslice J.T, Rosenfield A.G, Higgs D.J, *Numerical Solutions for FIA.* Talanta, 1981. **28**: p. 11.

4. Choppin G.R, *Nuclear Chemistry: Theory and Application.* 1969, Washington: Pergamon Press. p. 328.

3. Optimisation

3.1 Introduction

The nanomolar detection limits anticipated for the analysis of the superoxide radical in natural waters require an optimisation procedure to ensure that such concentrations can be measured. This procedure focuses on two critical areas. The first is the identification of the key chemical factors affecting the oxidation of luminol by the superoxide radical, and the second is the determination of the physical parameters which affect the measurement of light produced from the oxidation of luminol in the presence of the superoxide radical.

Before any practical work could take place it was necessary to determine how to interpret the light generated by the oxidation of luminol as a measure of the superoxide concentration i.e whether the maximum intensity of the light signal arising from the oxidation of luminol, or the integrated light intensity during the residence time of the luminol/superoxide radical streams in the flow cell was a measure of the superoxide concentration. Throughout this project the peak height, which represents the maximum emitted light intensity observed in the flow cell is used as a measure of the superoxide radical concentration. The reasons for this decision are discussed in detail in Section 3.1.1.

3.1.1 Chemiluminescent Measurement of Superoxide Radical Concentration

In the system used for the analysis of superoxide, the concentration of the superoxide radical is based on the light intensity emitted by the oxidation of luminol which is measured by the voltage signal from a photo-multiplier tube.

The use of light intensity gives rise to two possible measures of the superoxide radical concentration. These are the maximum signal intensity (peak height) or the time integrated light intensity- (peak area). There is considerable debate over which of the measures to adopt as a measure of analyte concentrations. The controversy over peak height versus area as a measure of concentration has its origins in the misconception that continuous flow techniques are similar to chromatographic techniques such as HPLC. In chromatography peak area has been traditionally used in determining the system response. The peak area is used because of the irreproducibility of the physical and surface properties of adsorption and/or size exclusion, and because the area is related to the total number of moles of the component passing through the detector. This irreproducibility makes the use of peak area necessary because the analyte concentration is assumed to be proportional to the peak area. If peak height is to be used as a measure of analyte concentration then the system must have a highly reproducible time response which chromatographic techniques cannot always provide.

In flow injection techniques, including reverse flow injection, the surface and adsorption effects important in chromatography do not apply and the reproducible time response of flow injection means that peak height becomes a reproducible

measure of analyte concentration. Therefore, both peak area and peak height can be used as measures of analyte concentration. Some researchers prefer to use peak height (intensity) and also incorporate information from the intensity versus time gradient. However, this is not possible in the case of chemiluminescent detection, because the entire reaction (light emitted by the oxidation of luminol) is integrated with respect to the residence time in the spiral flow cell so that no gradient information can be obtained.

Johnson [1], and Price [2] have used peak height as a measure of concentration of chemical species in natural water. Price used a similar chemical system to the superoxide/luminol system where the cobalt catalysed oxidation of luminol was used to determine hydrogen peroxide concentration. Price was able to obtain linear calibration curves for concentrations of hydrogen peroxide as low as 10^{-8} M (see Figure 3.1). Johnson, using differing chemical reactions, was able to obtain a linear peak height response to analyte concentration. These experiments suggest that peak height could be used successfully as a measure of superoxide radical concentration.

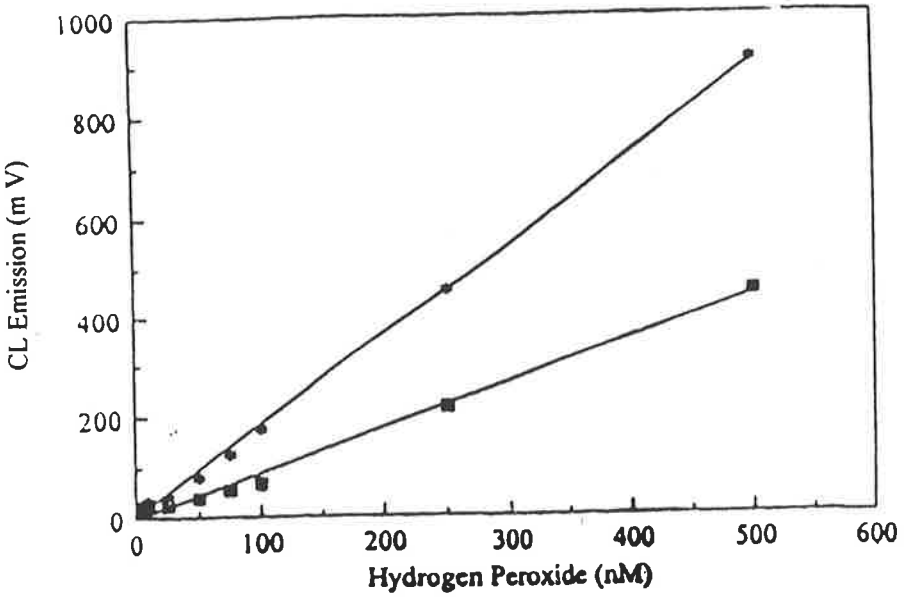

Figure 3.1 Chemiluminescent signal for hydrogen peroxide in estuary (■) and sea water (•)

Adapted from [1]

3.2 Manifold Selection

In order to determine the most appropriate flow manifold for measuring the superoxide radical, the signal response of two manifolds (flow injection and reverse flow injection) to a standard superoxide radical solution was measured for a $3x10^{-8}$ M superoxide radical solution. The radical concentration was measured using the two experimental configurations under otherwise identical experimental conditions for flow rate, reagent concentration and pH. Figure 3.2 illustrates the reverse flow injection configuration in which the reagent and a basic luminol solution are injected into the continuously flowing sample stream. The same equipment is used for a flow injection manifold but the sample and reagent reservoirs are reversed. This experimental configuration injects the sample into a continuous flowing reagent (luminol) stream.

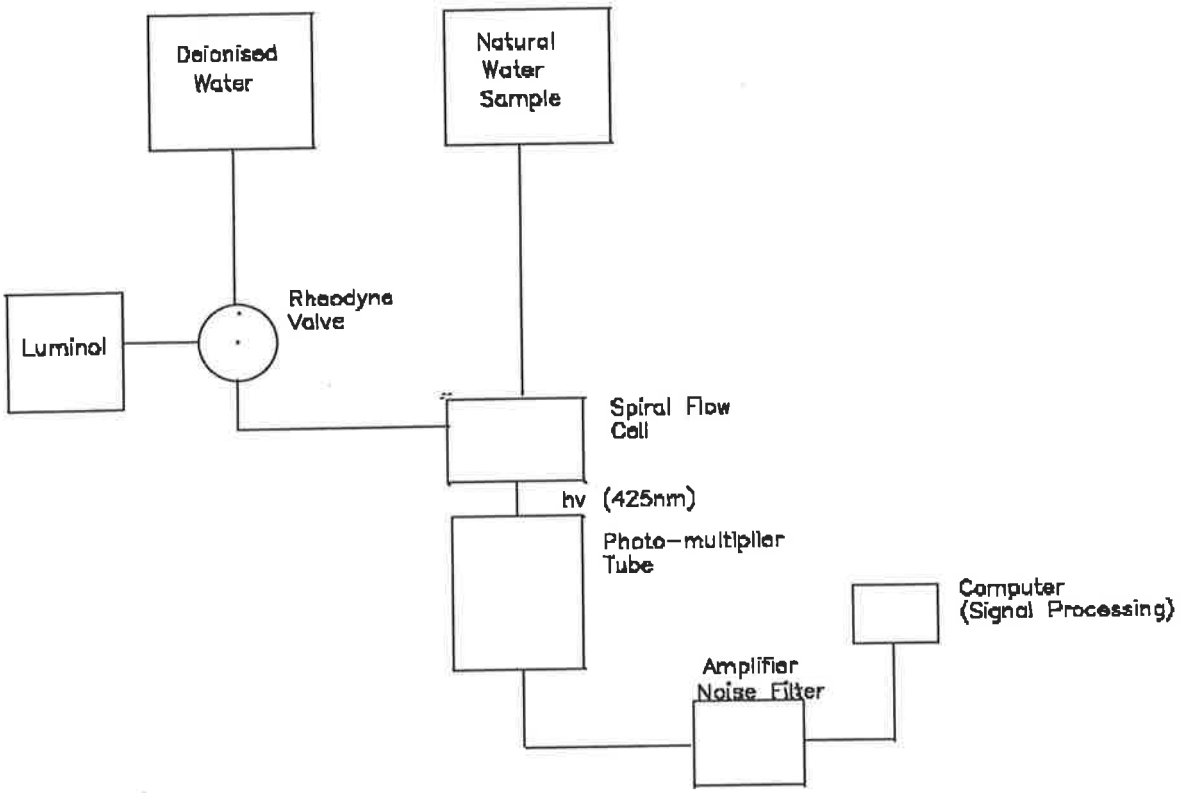

Figure 3.2 Reverse Flow Injection Analysis Experimental Set-up

Note: Luminol is injected into sample stream prior to entry into spiral flow cell

In the conventional flow injection configuration where the sample is injected into the luminol reagent stream, the system response is a characteristic intensity versus time profile (see Figure 3.3). Under these conditions the traditional flow injection analysis profile can be seen, with a trailing edge which is typical of an FIA system in which there is minimal radial diffusion of luminol under laminar flow conditions. This means that the initial concentration profile of injected luminol will remain constant so that the

reaction with superoxide will occur over a shorter time frame with respect to residence time in the spiral coil [3].

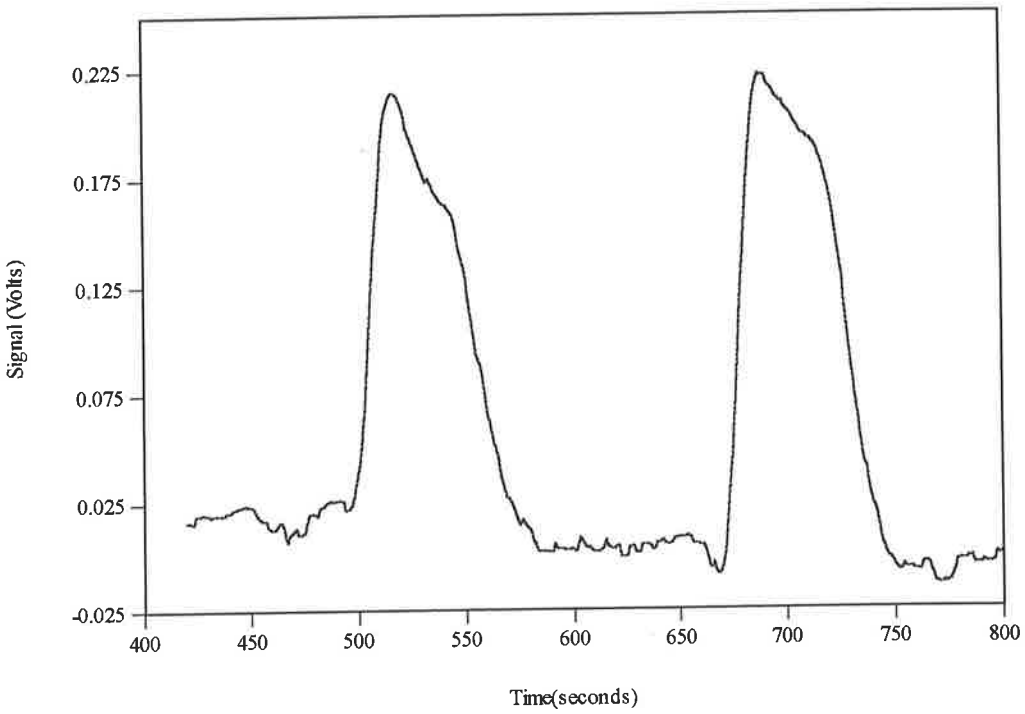

Figure 3.3 Injection Profiles for FIA arrangement

In the Reverse Flow Injection configuration the luminol was injected into the sample stream. Under these conditions, the intensity versus time profile changes to a near Gaussian profile (Figure 3.4) which lacks the trailing edge seen in Figure 3.3. The difference in peak shape arises from the different concentration distributions of the luminol reagent. In the FIA arrangement the trailing edge is characteristic of a laminar flow dominated concentration profile whereas the Gaussian shape found in RFIA arises from the combination of a laminar flow and radial diffusion. The radial diffusion in RFIA means that the reagent concentration in the spiral flow cell is constant over

the residence time of luminol in the cell. However, in FIA, the absence of radial diffusion means that the luminol concentration is greater as it enters the spiral flow cell but decreases during its residence in the spiral flow cell.

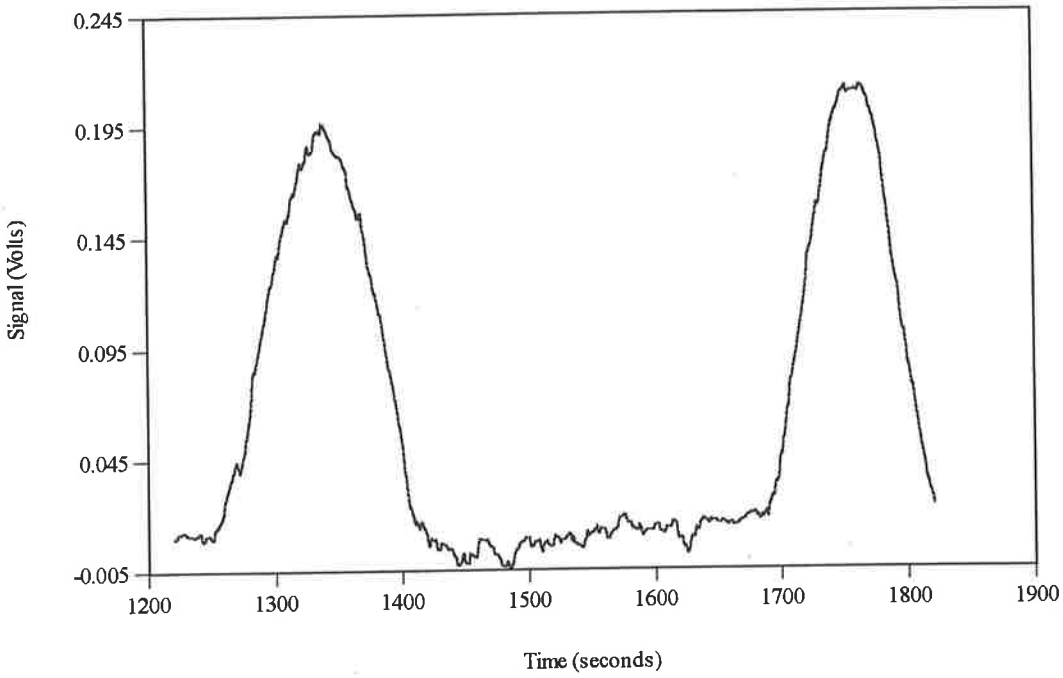

Figure 3.4 Injection Profiles for RFIA arrangement

The peak height response for the flow injection manifold is 10% larger than that obtained from the reverse flow injection manifold. For such a small difference the comparative benefits of the systems were assessed in order to make a decision on which experimental arrangement should be used.

The selection of the manifold can therefore be based on considerations such as the level of reagent consumption and cost of reagent rather than sensitivity. The major benefit of RFIA compared to FIA is that only the injected luminol is consumed which reduces the luminol reagent consumption enabling longer time in the field.

3.3 RFIA Optimisation

Both chemical and physical parameters were considered in optimising the apparatus. The chemical factors are linked to maximising the emission of light from the oxidisation of luminol by the superoxide radical. The physical parameters are responsible for maximising the electronic signal produced as a measure of the light emitted by the oxidation of luminol.

The chemical parameters identified as critical factors in the oxidation of luminol and which required optimisation were:

1. Reagent concentrations
2. Reagent pHs
3. Effect of oxygenation of luminol solution on signal size

The physical parameters that are directly controllable and are part of the experimental apparatus, which were optimised, are listed below.

1. Injection loop sizes
2. Flow rates
3. Photo-multiplier tube dynode-cathode voltages.

The cell size was fixed in this apparatus by design constraints so that instead of optimising flow cell size the reagent flow rates were optimised.

3.4 Chemical Parameters

3.4.1Reagent Concentrations

Luminol

The optimisation of luminol concentration is an important factor because it is not simply a matter of maximising its concentration. The concentration of luminol must be high enough to ensure that all the superoxide radicals present will react with luminol but low enough to avoid the self-quenching effect which occurs at high luminol concentrations [4].

The best estimate of the superoxide radical concentration in natural water is 10^{-8} M [5], therefore the luminol concentration must be at least micromolar to ensure a 100 fold excess. Luminol self-quenching occurs only at or above millimolar luminol concentrations. Furthermore luminol has a linear correlation between light yield, and analyte concentration (oxidant) for luminol concentrations below $1x10^{-3}$ M. Based on these considerations the luminol concentration used throughout this project was 10^{-5} M

Cobalt(II)

In the measurement of hydrogen peroxide, cobalt(II) was used as a catalyst for the oxidation of luminol. The concentration of the cobalt(II) ion must be optimised because with both hydrogen peroxide and superoxide radical present at low cobalt(II) concentrations the oxidation of luminol by hydrog en peroxide is slow compared with that of the superoxide radical, while at higher cobalt(II) concentrations the oxidation via hydrogen peroxide is complete and consequently the superoxide radical cannot be

detected.. The optimised cobalt(II) ion concentration used for the detection of hydrogen peroxide was determined by trial to be $5x10^{-6}$ M.

3.4.2 pH of Reagents

The pH of reagent streams is an important parameter because pH has a direct influence on the chemiluminesence activity of the luminol and the stability of the superoxide radical [6]. In the reverse flow injection manifold used for the detection of the superoxide radical both the luminol reagent stream and the sample stream containing superoxide radical pH required optimisation.

The oxidation of luminol is base catalysed and therefore the pH of this stream is an important consideration. Figure 3.5 clearly shows that increasing the pH above neutral pH results in a significant increase in the chemiluminescent efficiency of luminol in the presence of the superoxide radical

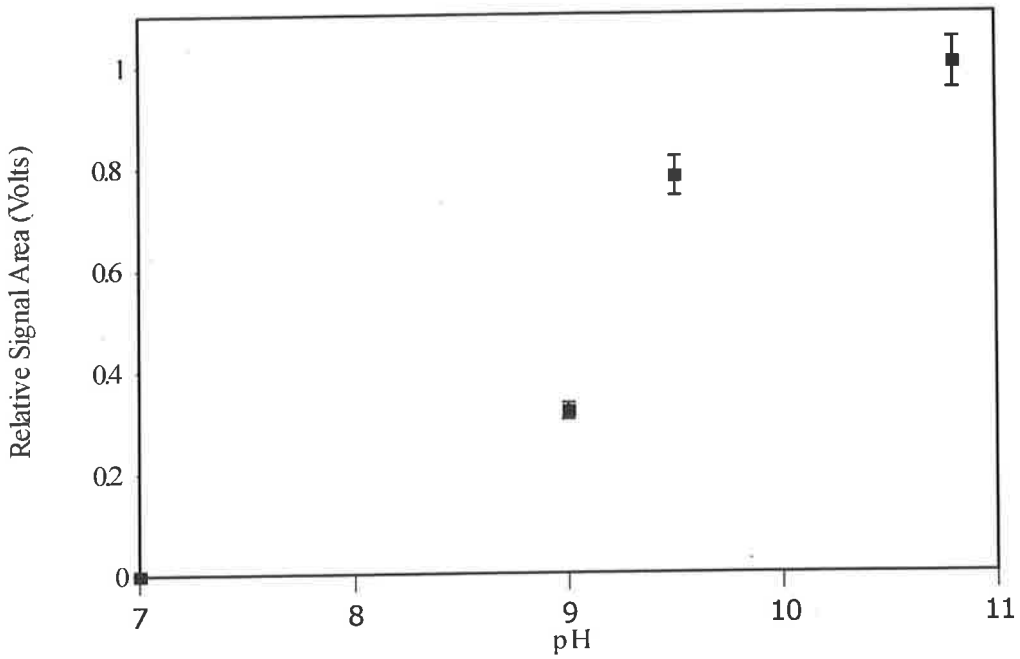

Figure 3.5 pH dependent response of luminol when oxidised in the presence of the superoxide radical

During the optimisation of the luminol solution pH it was found that light was emitted when the blank and luminol solutions were mixed. This small background signal appears when solutions such as a sodium formate solution or even ultra-pure water are mixed with the luminol reagent. The signal is most likely due to hydrogen peroxide present in the ultra-pure water, which has been reported in previous research using luminol in FIA systems [2]. The signal from these "blank" solutions is considerably less than the signal arising from oxidation of luminol by the superoxide radical. This signal was indistinguishable from background noise at low pH but was evident at very high pH. The background signal in the unirradiated solution may also be a consequence of univalent oxidation of luminol in the presence of dissolved oxygen. This reaction involves the production of small amounts of the superoxide radical by the luminol radical in the presence of molecular oxygen. This reaction does

not pose a problem in terms of interference with the oxidation of luminol by superoxide generated either through gamma radiolysis or photochemically, because the signal arising from the oxidation of luminol by superoxide radicals from these sources is significantly larger than the background signal. It is 3 times greater than that of the lowest superoxide concentration generated. The optimum pH of the luminol solution occurs when this background signal is not seen but the signal arising from the oxidation of luminol by the superoxide radical is still clearly distinguishable from the baseline.

After the optimisation of the luminol stream pH it was necessary to consider the sample stream containing the superoxide radical. The disproportionation rate constant for superoxide is pH dependent (see Figure 3.6). This means that the sample stream pH affects the concentration of the superoxide radical because its stability increases with pH. Although the data from Bielski indicates that increasing the pH of the sample stream to 13 would maximise the stability of the superoxide radical there are a number of steady state issues related to the calibration of the apparatus and peculiar to gamma radiolysis which require the sample stream pH to be optimised. These are discussed in detail in Section 3.4.2.

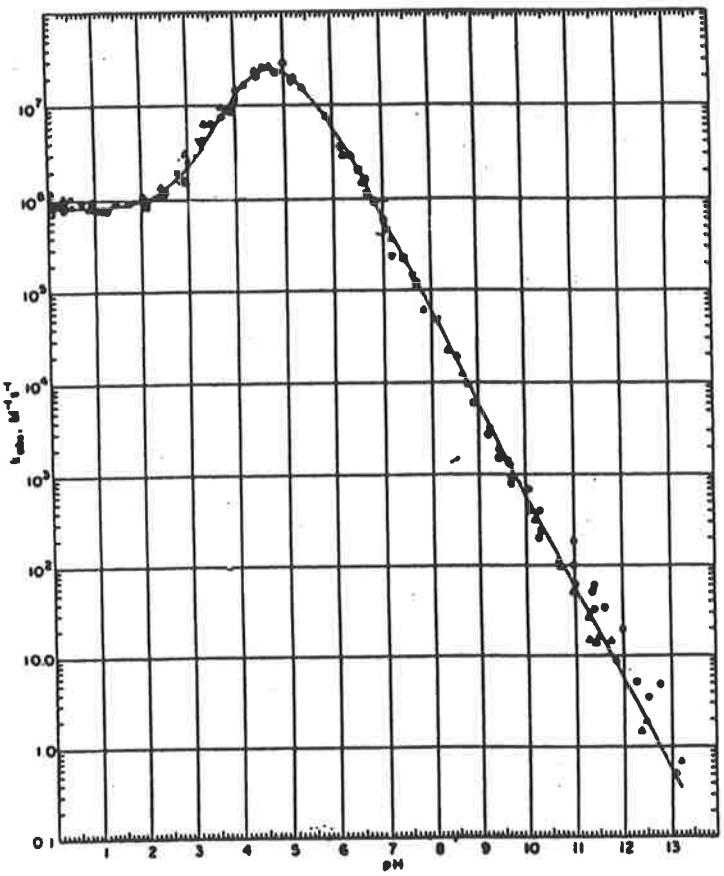

Figure 3.6 Data from Bielski for the second order rate Constant for the Decay of Superoxide Radical [6]

3.4.3 Steady State Time Consideration for Radiolytically generated Superoxide Radical

Given that the pH of the water examined in this study varies between 7.6-8.2 it was important to maximise the concentration of the superoxide radical reaching the spiral flow cell in order to improve the instrument's detection limits. There are two possible methods of maximising the superoxide radical concentration. One method involves raising the solution pH to increase the stability of the superoxide radical and enabling a greater proportion of the superoxide radical in the sample to reach the flow cell.

However, increasing the pH of the superoxide solution results in a significant increase in the time required for the radiolytically generated superoxide radical to achieve steady state concentration. The relationship between pH and time to achieve a steady state is shown in Figure 3.7. The longer time required to achieve steady state superoxide concentrations using gamma radiolysis also increases the amount of hydrogen peroxide present in solution. This increase in hydrogen peroxide concentration poses a problem in calibrating the FIA apparatus because of the difficulty in determining whether the oxidation of luminol arises from the superoxide radical or from hydrogen peroxide which although slow in the absence of a transition metal ion catalyst, can become an issue at concentrations in excess of 3.5×10^{-7} M.

Therefore, the amount of hydrogen peroxide produced is one of the factors which will dictate the maximum exposure time that can be used for gamma radiolysis and hence the formate solution pH. This is due to the need for a steady state concentration of superoxide radical to be generated, and the time to reach this concentration increases with pH as is shown in Figure 3.7.

The gamma radiolysis rate of production of hydrogen peroxide is 0.74moles J^{-1} compared with 6.29 moles J^{-1} of superoxide radical. In the case of hydrogen peroxide there is no loss through disproportionation as is the case for the superoxide radical and the hydrogen peroxide will accumulate in the solution. Under gamma radiolysis

Rate of formation = dose (J L^{-1} s^{-1}) x moles of H_2O_2 produced per Joule of energy (moles J^{-1})

Dose= 0.00023 J L^{-1} s^{-1} from Fricke Dosimetry

G_{H2O2} = 0.72 molecules per 100eV= 7.45 x 10^{-8} moles J^{-1}

Rate of production of H_2O_2 =7.45 x 10^{-8} moles J^{-1} x 0.00023 J L^{-1} s^{-1}

=1.72 x10^{-11} M s^{-1}

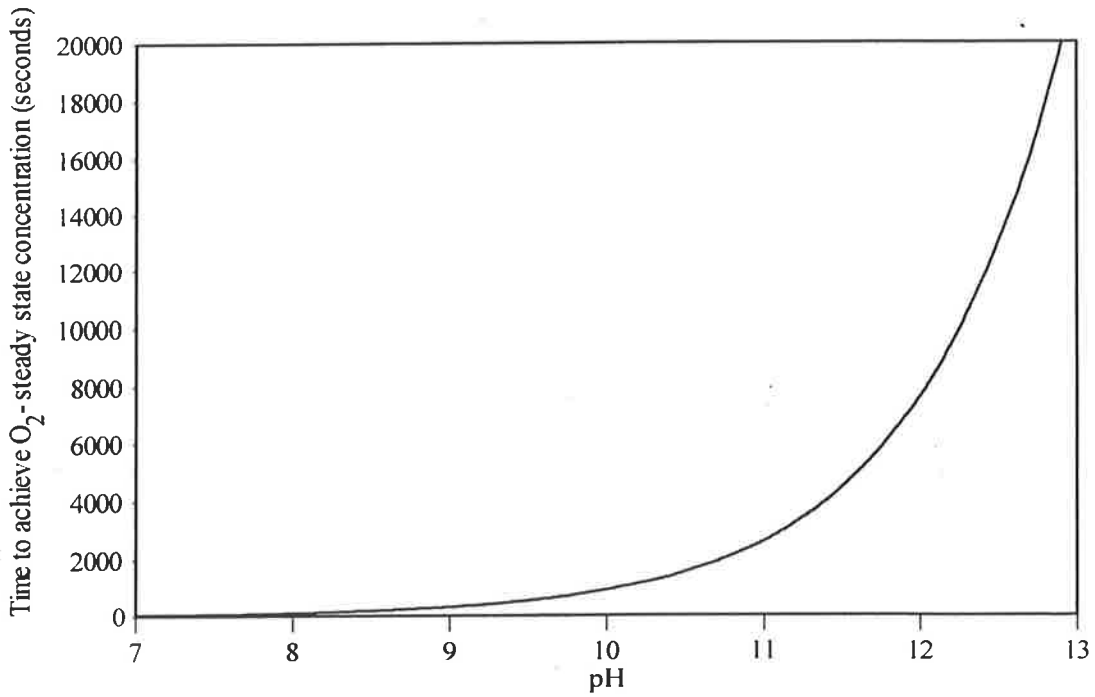

Figure 3.7 Time for the superoxide radical to achieve steady state with varying pH

The time required for the hydrogen peroxide concentration to achieve the threshold concentration (3.5 x 10^{-7} M) for interference with measurement of superoxide radical is 5 1/2 hours.

On this time scale at any pH the superoxide radical will achieve steady state concentration before interference by hydrogen peroxide. However, a significant increase in pH above pH 9 could lead to the precipitation of metal hydroxide species in natural sea water samples, and possible blockage of the spiral flow cell.

A problem with modifying the formate solution pH is that the modification of the pH of the solution containing the superoxide radical has a direct effect on the optimised activity of the luminol solution. The pH of the luminol solution was optimised, assuming a neutral pH for the superoxide stream. This assumption is based on the fact that a high pH sample stream, e.g. pH 12, produced an extremely high background signal when the sample stream reacted with the optimised luminol solution of pH 11. It was therefore decided to maintain the pH of superoxide stream as neutral pH, which after oxygen gas was bubbled through, had a similar pH to that of the seawater and fresh water samples.

To maximise the superoxide radical concentration if a modified solution pH is not used to stabilise the superoxide radical, it is necessary to reduce the time taken for the irradiated sample containing the superoxide radical to reach the flow cell. This minimises the loss of superoxide and lowers detection limits. In order to reduce the time for the irradiated sample to reach the flow cell the physical distance between the sample solution and the flow cell is reduced and, the sample flow rate maximised. Given the simplicity of this approach compared with the pH modification method it

was decided that the pH of the sample stream would not be modified as part of the optimisation procedure.

3.4.4 Superoxide Standard Solutions

The simplest way to change steady state superoxide radical concentrations produced by gamma radiolysis is to modify the pH of the irradiated solution. This changes the rate constant for the disproportionation of the superoxide radical to hydrogen peroxide. The rate constant for the disproportionation decreases with increasing pH; therefore to increase the steady state concentration of the superoxide radical the pH of the irradiated solution must be increased. However, as discussed in section 3.3.2 the modification of pH in order to increase the stability of the superoxide radical has been rejected. The simplest method of varying the steady state concentration is to vary the dose rate each solution receives. This is possible because the dose received by each solution is a function of the distance between the source and irradiated sodium formate solution. This method avoids modification of pH and simply requires the dose rate to be calculated for each position. This technique was used for the calibration work because it also allowed the identical solution to be used in each flask under the same chemical conditions.

3.4.5 Effect of Oxygenation on Luminol Activity

Although molecular oxygen alone is not sufficient in protic systems to oxidise luminol (oxidation by O_2 occurs in aprotic solvents such as DMSO) it has long been

known that luminol is oxidised by oxygen-containing peroxo-species, such as hydrogen peroxide and the superoxide radical [4]. Of particular interest to this research was whether the pre-oxygenation of a luminol solution would increase its chemical activity in the presence of the superoxide radical, because of the role oxygen is known to play in the oxidation process in aprotic solvents. In order to test this hypothesis, oxygenated and non-oxygenated luminol solutions were prepared and tested to determine whether the oxygenation of luminol had a positive effect on the signal arising from the oxidation of luminol by the superoxide radical. An example of oxygenated (a) and non-oxygenated (b) single traces are shown in Figure 3.8.

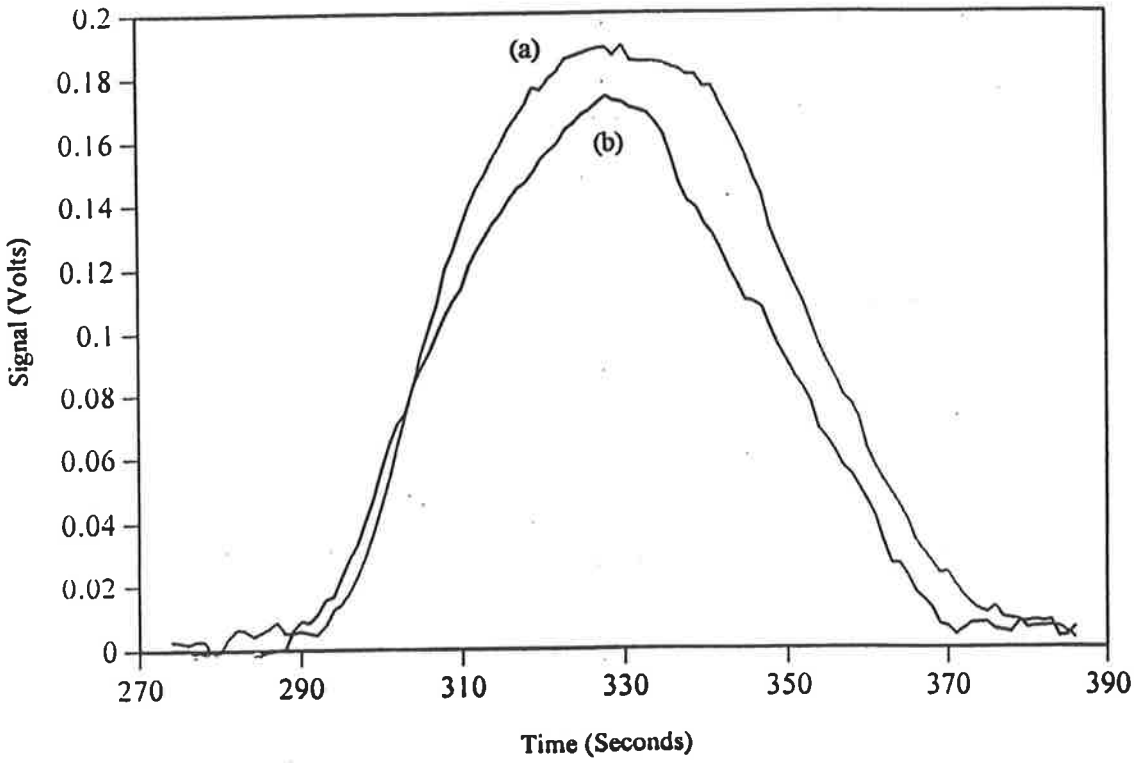

Figure 3.8 The response of oxygenated (a) non-oxygenated (b) luminol solution to a standard solution of superoxide radical.

The results indicate an increase in signal height of 9% when the luminol solution was oxygenated. This small increase in signal is a response to the role molecular oxygen plays in the oxidation mechanism of luminol [7]. Given the increase in signal height when the luminol solution was pre-oxygenated it was decided as part of the experimental protocol to incorporate the pre-oxygenation of the luminol solution with oxygen gas immediately prior to use. Consequently, it was not necessary to make corrections for waters of different oxygen concentrations.

3.5 Physical Parameters

3.5.1 Injection loop Size

The injection loop in the RFIA-CL apparatus contains the chemiluminescent reagent luminol. The size of the injection loop is an important parameter to optimise because the size of the loop has a direct effect on both the sample throughput and the signal size.

Three loop sizes were examined in conjunction with the RFIA-CL apparatus. The details of the loop configuration are outlined in Chapter 2 Section 2.2. The volumes of the injection loops investigated were 0.5ml ,1ml and 5ml, i.e. 1.5, 3 and 15 times the size of the spiral flow cell [0.317ml].

Changing the loop volume has two effects. Firstly, the time for the injection slug to pass through the spiral flow cell change dramatically with loop size. Secondly, the loop size changes the signal-time profile and the position of maximum intensity. The effects of changing loop size on both signal area and injection time (the time for the

luminol to pass through the detector) were investigated. A standard superoxide solution was used to determine the effect of changing loop size on the signal response and injection time. The results are shown in Table 3.1.

Table 3.1

Loop Size	Relative Peak Height	Injection Time (seconds)
0.5ml	0.78	85
1ml	1	110
5ml	0.93	250

The figures in Table 3.1 demonstrate that the loop size has an effect on the sampling rate. It was found that for a 5 ml luminol injection the relative peak size is 15% larger than that of an injected volume 1 ml, but the injection time increases by a factor of 3. The doubling of the injected luminol volume from 0.5 ml to 1 ml leads to a 28% increase in signal height but only a 30% increase in injection time in the flow cell. This increase in injection time is an important factor to consider given that it is necessary to have a number of injections of every sample in order to determine the reproducibility of sample results.

It was observed that varying the loop size changed the concentration contours in the spiral flow cell, giving rise to the different peak shapes and intensities. For both the 5ml and 1ml peaks, the concentration profile arises from a combination of laminar and radial diffusion. The results from the 0.5ml loop are solely due to laminar flow

conditions in the flow cell. The effect of these changes in flow conditions and consequently reagent reactions alter the profile of the intensity versus time response but also the position of maximum intensity. This consideration is important because in the case of the 0.5ml loop, a substantial amount of the luminol and superoxide react before entering the flow cell. This reaction lowers the emitted light intensity. Under these circumstances, despite the fast response time for the sample to be analysed, the lower intensity meant that it was preferable to retain the 5ml or 1ml injection loops. In practice, it was found that the time taken for the luminol/superoxide chemiluminescing mixture to pass through the detector cell was too long to be of practical benefit when using a 5ml loop compared with the 1ml loop. The effect of varying the size of the injection loop is shown in Figure 3.9,which shows that the response of the apparatus to superoxide is dependent on the loop size.

The 1ml loop size has the advantage that it overcomes the problem of delays between injection and detection of the light signal which was a feature of the 5ml loop. In the case of the 5ml loop, the time for a sample to pass through the loop is long, and slows down the throughput of the sample dramatically, compared with the smaller loops. It is possible to have a sample through put of 50 samples per hour with a 1 or 0.5ml loop but this drops to 20 samples per hour for the larger loop size at the same flow rate. The larger loop also uses more of the luminol reagent stream than the smaller loops without producing a larger signal height than the 1ml injection loop. In view of these advantages it was decided to use the 1ml loop.

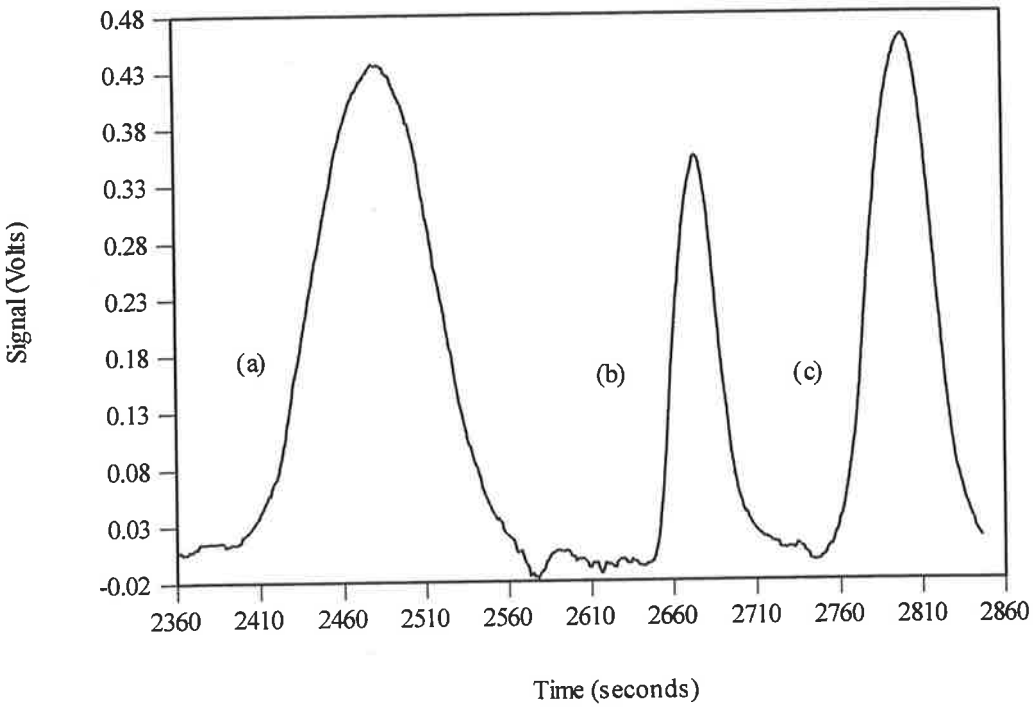

Figure 3.9 Injection Profiles for 5ml(a), 0.5ml (b) and 1ml loops(c)

3.5.2 Reagent Flow Rates

The flow rate of the reagents is an important factor in the optimisation procedure because the flow rate controls the extent of reagent mixing; the residence time of the luminol/superoxide stream in the detection cell and the speed of transfer of short lived radicals from the source to the detection cell. The effect of reagent flow rates was examined for two types of analyte species found in natural water which have different lifetimes- the short-lived superoxide radical, and the longer lived hydrogen peroxide.

In the case of the superoxide radical, flow rates used must take into consideration the rate of decomposition of the radical, which is second order in the superoxide radical concentration in the absence of reactive substrates. As a consequence, the superoxide radical concentration decreases with time on removal from the gamma source in the

case of radiolytically generated superoxide radicals, and this has also been found to be the case for UV photochemically generated superoxide radicals(see 5.3). Therefore, in designing the detection system for the superoxide radical the time taken for the sample stream to mix with, and react with the luminol stream needed to be considered.

The sample stream must be pumped as quickly as possible to the T-piece for mixing with luminol in order to ensure that the concentration of superoxide present in the measured solution was close to that in the sample. However, increasing the flow rate changes the position of the maximum intensity with respect to the flow cell, and this can lead to a decrease in the signal. (The maximum intensity can occur outside the flow cell). Therefore, it was necessary to investigate to what extent these effects would occur under experimental conditions. A series of experiments were conducted in which a standard solution of superoxide radical was pumped at various flow rates.

The results can be seen in Figure 3.10 which indicates that the signal increases with pump speed. For the superoxide radical generated by gamma radiolysis it is apparent that this is a non-linear relationship which arises from the time dependence of the superoxide radical concentration on removal from its source. There is no evidence of a shift in the position of the maximum intensity during the reaction at different flow rates, but it was observed that the optimal flow rate is the fastest available which reflects the dominance of the superoxide kinetics in determining the flow rate.

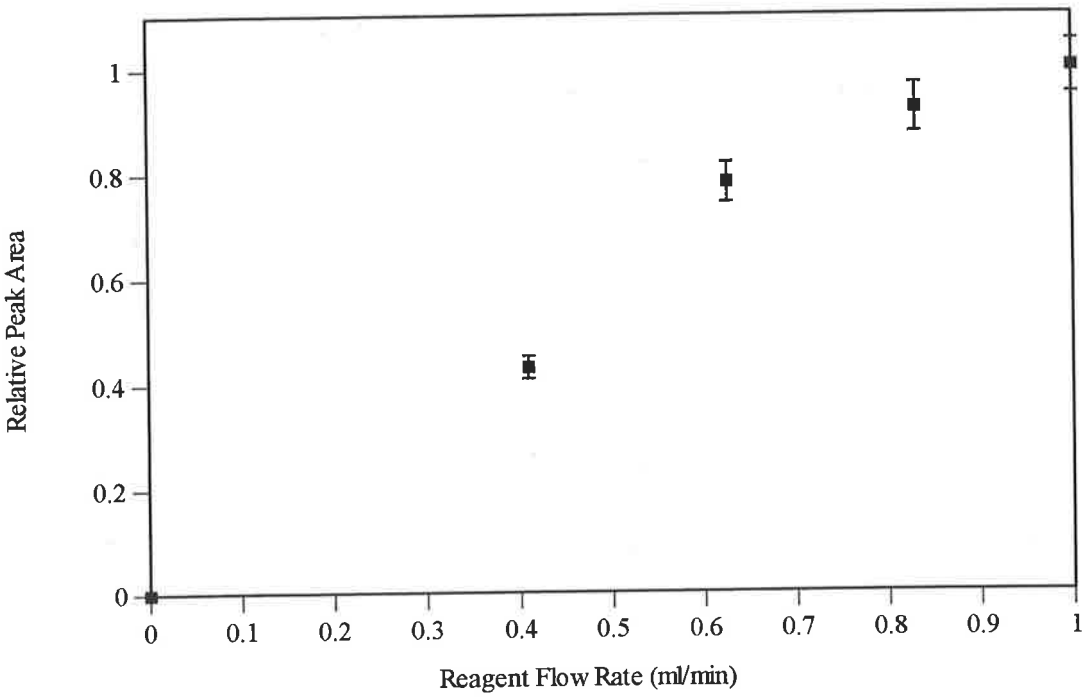

Figure 3.10 The Effect of Pump Flow Rate on Signal Area for gamma radiolytically generated superoxide radicals.

The second chemical reaction examined is the cobalt catalysed oxidation of luminol by hydrogen peroxide where the reaction is slow in the absence of a catalyst. This experiment was conducted in order to provide a comparison between the transient superoxide radical and the more stable hydrogen peroxide. The results are shown in Figure 3.11.

The graph indicates the stable nature of the hydrogen peroxide compared to the superoxide radical. This property is represented in the linear response of the signal and flow rate. This linear relationship suggests that the decay in superoxide concentration with time is a far more important factor in signal size than the residence time for the superoxide/luminol mixture in the spiral flow cell.

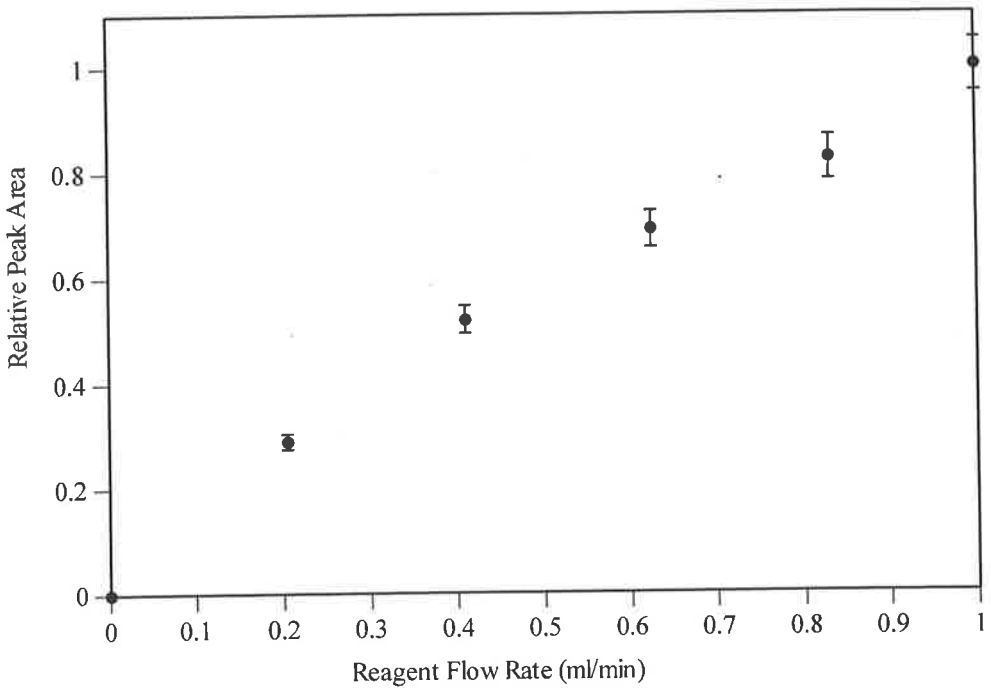

Figure 3.11 The effect of Pump Flow Rate on Signal Area for Hydrogen Peroxide

3.5.3 Photo-multiplier tube voltage

The voltage across the dynode and cathode photomultiplier tube determines the gain of the photomultiplier tube, and therefore the higher the voltage the larger the signal. But the signal/noise ratio is the limiting consideration which governs the use of higher applied voltages. Increasing the dynode-cathode voltage is only useful if the signal/noise ration increases with voltage output.

In order to determine the effect of the applied voltage on the peak height a solution of superoxide was generated, using steady state irradiation. The peak height of this solution was then measured at different applied voltages to the photomultiplier tube.

The upper limit tested was -1150V because at higher voltages there were fluctuations in the baseline which arose through small variations in the mains power and these fluctuations in the high voltage generated too much noise.

The effect of changing the voltage can be seen below in Figure 3.12.

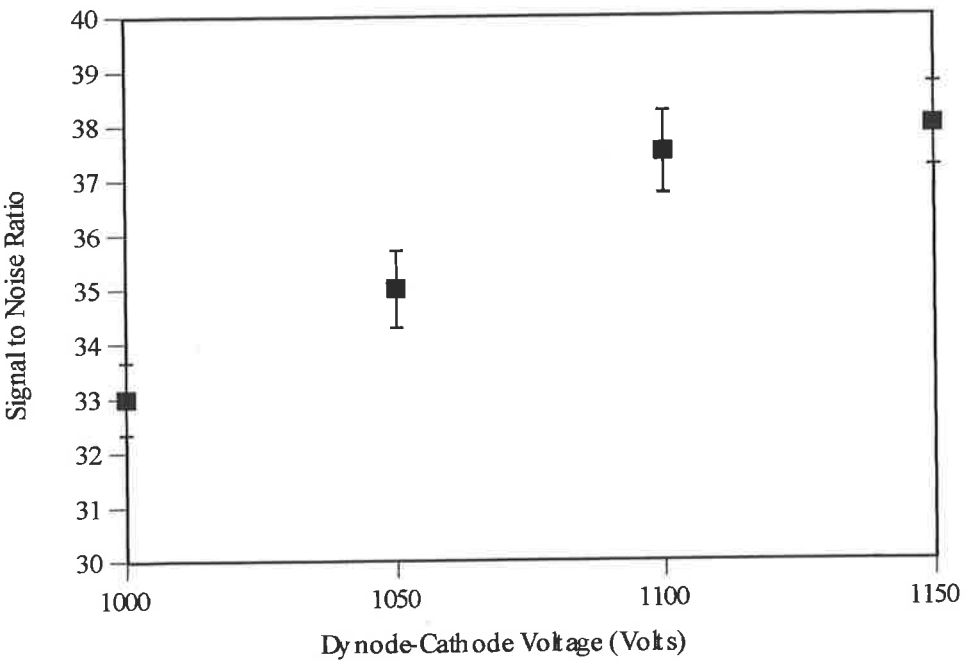

Figure 3.12 Plot of Applied Voltage to Photomultiplier tube Vs Signal/Noise Ratio

It can be observed that the optimal signal/noise ratio occurs at the maximum possible operational voltage of 1150V. Figure 3.12 shows the effect of the voltage on the signal to noise ratio. The lower limit of the voltage applied was 1000V, while the upper limit used was 1150V. The S/N ratio increases with higher voltages. However, at the upper limits of dynode-cathode voltage, 1150V there is not a significant

difference in the signal/noise ratio of 38 compared to the signal/noise ratio for 1100V (37.5).

3.6 Optimised Operating Parameters

The following is a list of the optimised operating parameters for the Reverse Flow Injection Apparatus described in Chapter 2 Section 2.3.

Parameter	Optimised Condition/Value
Loop Size	1 ml
PMT operating Voltage	-1100 V
pH of reagent streams	Luminol 10.5-11.5 (oxygenated) deionised water 6.5-7.1 sample 7.9-8.2
Flow Rate	1ml/min

3.6.1 Specialised Operating Conditions

The size of the signal from the oxidation of luminol varied according to the chemical contents of the water samples examined, and hence some modifications to those conditions listed above were necessary. In the case of hydrogen peroxide measurements, the operating voltage was 1000V. For sea water measurements at the maintenance berth of the yacht squadron an increased luminol pH of 12 and voltage of 1100V applied to the photomultiplier tube due to the poor response to the radical present- 25% of the signal seen for unpolluted marine water.

References

1. Johnson K.S, Sakamoto-Arnold .C, *Determination of Picomolar levels of Cobalt in sea water by Flow Injection Analysis with Chemiluminesence Detection.* Anal. Chem., 1987. **59**: p. 1789.

2. Price D, Worsfold P., Fauzi R, Mantoura C, *Determination of Hydrogen Peroxide in sea water by flow injection analysis with chemiluminesence detection.* Analytica Chimica Acta., 1994. **298**(2): p. 121.

3. Analysts, S.C.o., *Flow Injection Analysis- a practical guide*. 1991, London: HMSO.

4. Gunderman K.D, *Chemiluminesence in Organic Chemistry*. J.Phys. Chem. 1986: Springer Verlag. p78.

5. Zafiriou O.C, Zepp R.G, Zika R.G, *Photochemistry of Natural Waters.* Environ. Sci & Tech., 1984. **18**(12): p. 358A.

6. Bielski B.H.J,Danielli C, Arudi R.L, Ross A.B, *Reactivity of HO_2/O_2^- radicals in aqueous solution.* J. Phys. Chem Ref. Data, 1985. **14**(4): p. 1041.

7. Faulkner K, Fridovich.I., *Luminol and lucinegin as detectors for O_2^-* Free Rad. Bio. Med, 1993. **15**: p. 447.

4.0 Calibration

4.1 Calibration Techniques

The *in situ* superoxide radical concentration in this project is measured using a RFIA manifold in combination with chemiluminescence. This involves determining the manifold response to standard solutions of the superoxide radical. Two suitable techniques have been described in the literature - radical- enzyme reactions or gamma radiolysis of formate or hydrogen peroxide solutions.

The gamma radiolysis of sodium formate is a convenient method to generate a known steady state concentration of the superoxide radical. The superoxide radical concentration is related to the gamma radiation dose which can be measured using a Fricke dosimeter.

4.2 Determination of Superoxide Steady State Concentration

In order to calibrate the RFIA manifold, known steady state superoxide concentrations were generated in the sample stream flowing into the manifold. Different superoxide concentrations were produced by changing the distance between the gamma source and the irradiated solutions which changed the initial superoxide radical concentration in the reaction vessel. These distances ranged from 20 cm to 1.2 m. This variation in distance resulted in sample doses ranging from 1.96 to 0.16 krad/hour. A standard sodium formate solution was used which ensured that all irradiated formate solutions had the same pH and chemical composition. The relationship between the gamma

radiation dose and the steady state concentration of the superoxide radical is illustrated in the procedure outlined below.

1. Establish the dose rate using Fricke Dosimetry (as shown in Section 4.3)

2. Determine the rate of superoxide formation can be calculated using the G value for superoxide.

$$e^-_{aq} + O_2 \rightarrow O_2^- \quad (1)$$

$$e^-_{aq} + H^+ \rightarrow H \quad (2)$$

$$H + O_2 \rightarrow HO_2$$

$$HCO_2^- + OH \rightarrow CO_2^- + H_2O$$

$$HCO_2^- + H \rightarrow CO_2^- + H_2$$

$$CO_2^- + O_2 \rightarrow CO_2^- + O_2^-$$

$$G_{O_2^-} = G_e + G_H + G_{OH}$$

$$= 0.55 + 2.7 + 2.8 = 6.05$$

$$G_{O_2^-} = 6.05 \text{molecules per } 100eV$$

Therefore $R_{formation} = G_{O_2^-} \times$ Dose Rate

3. Determine Superoxide Concentration under Steady State Conditions (oxygenated solution with a formate concentration>0.001M)

$$\frac{d[O_2^-]}{dt} = R_{formation} \text{ s- } R_{decay} = R_{formation} - k[O_2^-]^2 = 0$$

Therefore $[O_2^-]^2 = \frac{R_{formation}}{k}$

where k is the pH dependent rate constant for the decay of superoxide radical [2]

The final concentration, which is detected at the manifold, must take into account the decay of the radical due to the time taken for the irradiated solution to leave the beaker and reach the manifold. The concentration at the manifold is given by

$$\frac{1}{A} - \frac{1}{Ao} = kt$$

where Ao is the initial superoxide radical concentration and A is its concentration at time t (the time taken for the sample to reach the manifold after leaving the irradiated beaker), and k is the rate constant for the disproportionation of the superoxide radical to hydrogen peroxide.

4.3 Dosimetry

In a gamma irradiated solution of ferrous ammonium sulfate in 0.4 M sulfuric acid, the ferrous ion (Fe^{2+}) is oxidised to the ferric (Fe^{3+}) ion and the amount of Fe^{3+} produced is determined spectrophotometrically by measuring the absorption of $Fe(SO_4)^+$ species at 304 nm.

The concentration of ferric ions is given by

$$\text{Absorption } (Fe^{3+} 304nm) = \varepsilon\ (Fe^{3+} \text{ at } 304nm) x\ l x [Fe^{3+}]$$

The dose rate is related to the Ferric ion concentration using

$$\text{Dose (Gray)} = \frac{10*[\ Fe^{3+}\ ](mM)}{G(\ X)*p*1.024}$$

where G(X) = G Value of Fe^{3+} (=15.5 for Fricke dosimetry) p = density of the solution

4.4 Matrix Effects

In other than lab conditions it is possible that various reactions of the superoxide radical could interfere in its detection. In the case of pure water it is possible to generate a calibration curve (see Figure 4.1) for the superoxide radical because the chemistry for the production of the superoxide radical using the gamma radiolysis of sodium formate solutions is known. In natural waters there are a large number of matrix effects such as pH, the amount of dissolved organic matter present and the transition metal ion content. The large number of variables in natural waters raises the question as to whether the gamma radiolysis of natural water samples containing sodium formate actually produces the superoxide radical. The primary path for the generation of the superoxide radical is through the reaction of the hydroxyl radical with the formate ion

$$HCO_2^- + OH \rightarrow CO_2^- + H_2O \quad k= 3.5 \times 10^9 \text{ L mol}^{-1} \text{ s}^{-1}$$

which produces the carbon dioxide radical which reacts with oxygen

$$CO_2^- + O_2 \rightarrow CO_2^- + O_2^- \quad k= 2.4 \times 10^9 \text{ L mol}^{-1} \text{ s}^{-1} \text{ [2].}$$

Given that the formate concentration is 0.01 M and the rate constants are of the order of 10^9 L $mol^{-1}s^{-1}$ even at millimolar concentrations ,species which might compete with the formate ion for the primary radicals even at 1 mM could consume no more than 10% of the primary radical. This means that any interference that could occur would be in the reaction between the carbon dioxide radical and oxygen. This is not feasible in fresh water because the irradiated samples were saturated with oxygen (2.35×10^{-4} M) and as with the case for the formate ion there is no species present in solution at a high concentration to interfere with the reaction of the carbon dioxide radical.

In the case of sea water the chloride ion has a concentration of 0.55 M. The hydroxyl radical will react with the chloride ion

$$OH + Cl^- \rightarrow Cl^{\cdot} + OH^- \quad k=4.2\times10^9 \text{ L mol}^{-1} \text{ s}^{-1} \text{ at pH 2 [3]}$$

At higher pH the reaction is less favourable and it is difficult to deduce any rate constant in sea water. There is no interference between the chloride ion and the reaction of the carbon dioxide radical which is a strong reductant. Although there is a decrease in peak height of the superoxide radical from the gamma radiolysis of sea water solutions containing sodium formate compared to those made up in ultra pure solution. There is a similar decrease in signal in the blank solutions i.e unirradiated formate solutions made up in sea water and ultrapure water. This indicates that any reaction involving the chloride ion and the hydroxyl radical has a negligible effect on the generation of the superoxide radical, rather there is some interference in the oxidation chemistry of luminol. In view of the results for both fresh chemistry of the production of the superoxide radical in fresh and sea water there is unlikely to be any interference in the generation of the superoxide radical.

4.5 Luminol Interference

Another major issue in determining the response of the apparatus arises from the specificity of the detection technique. In the case of luminol as a chemiluminescent detection molecule for superoxide radical there are a number of other compounds which are capable of oxidising luminol, such as chlorine dioxide, permanganate and hydrogen peroxide [3]. These species can produce a false positive signal for the superoxide radical. Hydrogen peroxide is the most abundant of these possible

oxidants in natural water systems with a concentration range between 5x 10^{-8} M to 1x10^{-5} M [4]. However, the reaction of hydrogen peroxide with luminol is slow compared to the superoxide radical in the absence of a transition metal ion catalyst species such as Co^{2+} or Cu^{2+}.

4.6 Calibration in Milli-Q Water

An oxygenated 0.01 M sodium formate was prepared in ultra-pure water (Milli-Q) and irradiated. Under these conditions the superoxide radical concentration was monitored using the FIA apparatus described in Chapter 2. The calibration plot is shown for the oxygenated formate solution (pH 7.6) in Figure 4.1.

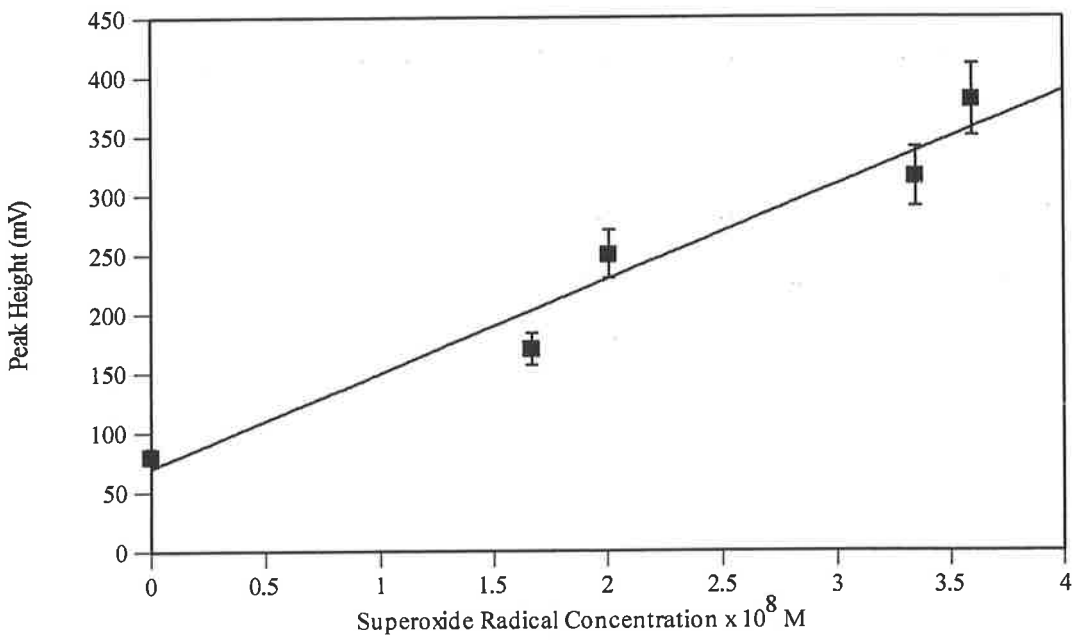

Figure 4.1 Calibration Plot for the radiolytically generated superoxide radical in Milli-Q water

4.6.1 Signal Response in Fresh Water

A fresh water sample obtained from the Mt Lofty Botanic Gardens was irradiated. The results are shown in Figure 4.2 and indicate that the signal produced by the irradiation of fresh water is 55% lower than that found in ultra-pure water. Price et al reported a similar reduction in signal response for the detection of hydrogen peroxide in fresh water using luminol. The decrease in signal in the case of hydrogen peroxide was thought to arise from the possible quenching behaviour that may be exhibited by dissolved organic matter in solution [4]. This is also the probable explanation for the decrease in signal seen in the case of the superoxide radical, although there could also be some reaction between the superoxide radical and organic or inorganic species present in the water sample.

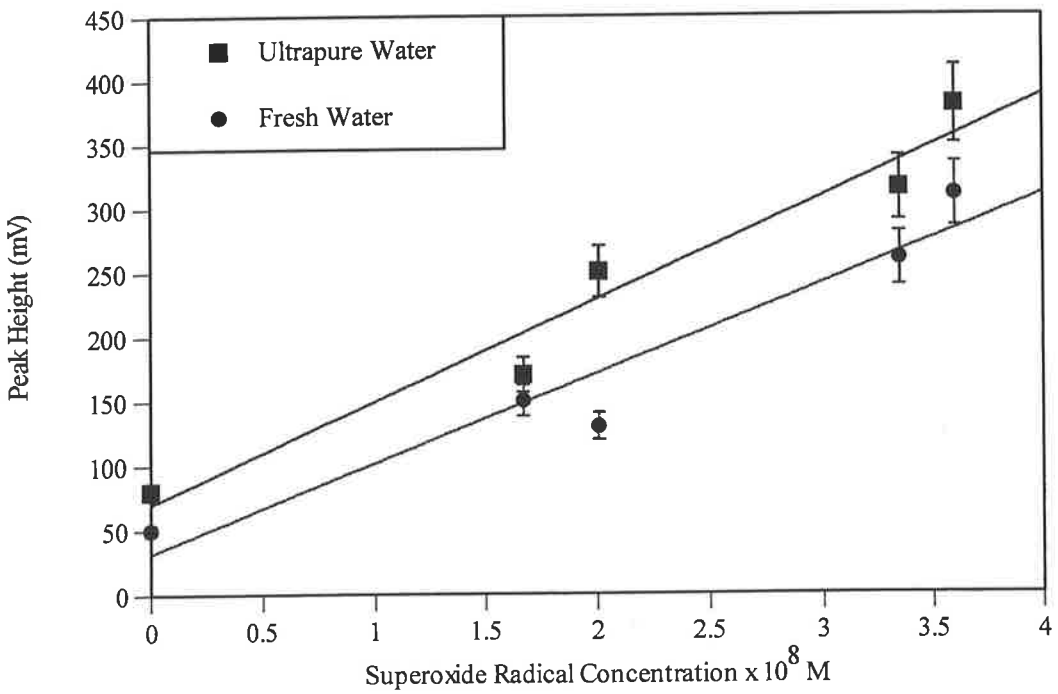

Figure 4.2 Response for Superoxide Radical in Ultra-Pure Water and Fresh Water

4.6.2 Seawater Calibration

The signal response to gamma irradiated formate solutions of seawater (Figure 4.3) indicates a 62% decrease in peak height compared to those made up in ultra-pure water. As discussed in 4.4 the rate of production of the superoxide radical is not likely to be responsible for this decrease in signal. The smaller signal may be due to interference with the oxidation of luminol or the decay rate of the superoxide radical. The fact that this reduction in signal occurs in the unirradiated samples as well as the irradiated samples indicates that this reduction is not a consequence of interference with the gamma radiolysis production method for generating the superoxide radical, i.e the reaction of hydroxyl radicals with chloride ions or changes in the decay rate of the superoxide radical. It suggests that there is some interference with the oxidation of luminol in the presence of the superoxide radical, which is also responsible for the decrease in the blank signal. This indicates that any effect is independent of the superoxide radical and is therefore most likely to be due to interference in the oxidation of luminol.

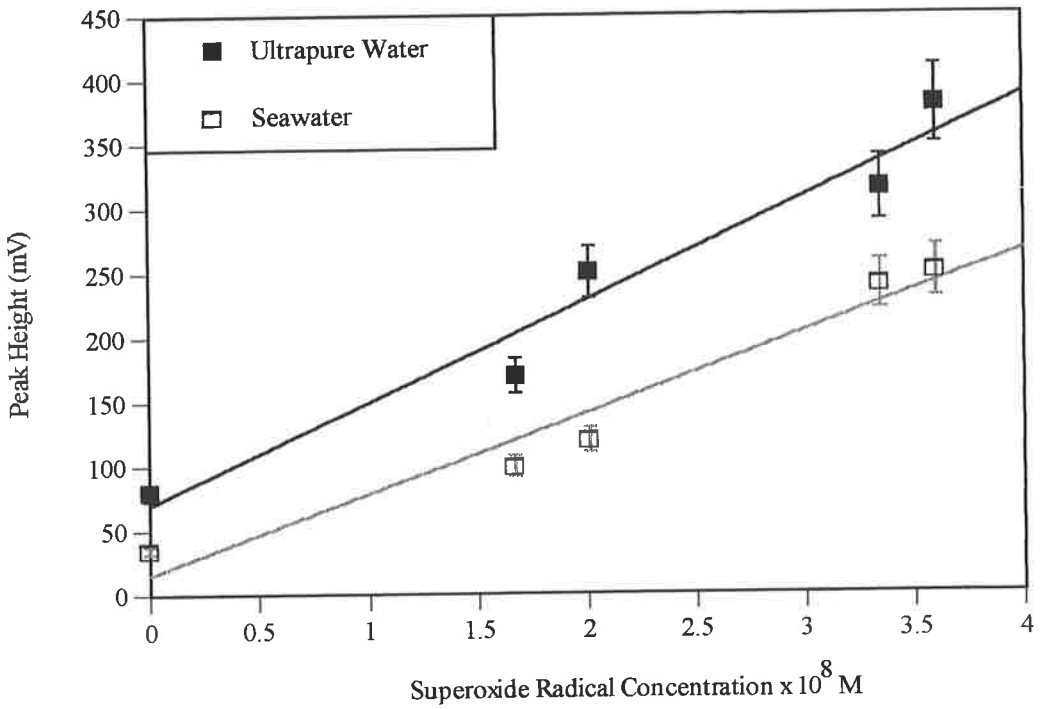

Figure 4.3 Signal Response for Superoxide Radical in Ultra-Pure Water and sea water

4.7 Hydrogen Peroxide Calibration

The hydrogen peroxide content of the natural water must be measured in order to establish whether or not the signal detected in natural water arises from the superoxide radical or from hydrogen peroxide. Both species are capable of oxidising luminol although in the absence of a catalyst the reaction with hydrogen peroxide is much slower than with the superoxide radical. However, the possibility of interference by hydrogen peroxide in detecting the superoxide requires the hydrogen peroxide concentration in natural water to be determined and any interference effects to be established. In order to determine the system response, a calibration plot was obtained for ultra pure water, while natural water samples were spiked with standard solutions of hydrogen peroxidein order to determine the response of the manifold .At hydrogen peroxide concentrations of less than 3.5×10^{-7} M no interference with

superoxide detection was observed (in the absence of a catalyst such as Co^{2+}). The measurement of hydrogen peroxide in water samples was undertaken using a cobalt (II) catalyst and luminol to measure its concentration.

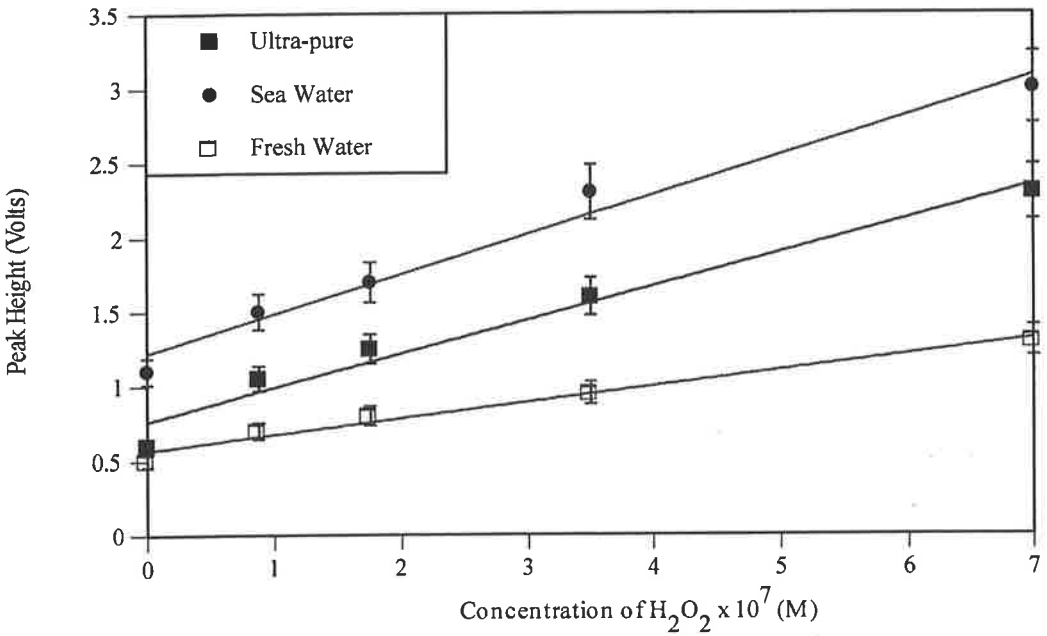

Figure 4.4 Response for hydrogen peroxide in ultrapure,fresh and seawater

Figure 4.4 shows the calibration for hydrogen peroxide in ultrapure water compared to that of the fresh and sea water samples. This calibration plot is in agreement with the literature where an increase in signal in sea water compared to that in ultra-pure water is seen and a decrease in fresh water is observed [4]. In order to determine the hydrogen peroxide content of sea water and fresh water samples, blank samples (i.e. non-irradiated samples) were examined. The concentration of hydrogen peroxide measured using cobalt catalyst was found to be 2.8×10^{-7} M in sea water and 3.1×10^{-7} M in fresh water. From an analytical perspective, these concentrations of hydrogen

peroxide are too low to interfere with the detection of the superoxide radical in the absence of transition metal catalysis.

4.7.1 Hydrogen Peroxide Interference

The interference effect of hydrogen peroxide depends not only on the concentration of hydrogen peroxide but also the concentration of transition metals which can catalyse the oxidation of luminol. In the absence of a transition metal catalyst the minimum detectable concentration of hydrogen peroxide is 3.5×10^{-7} M and the maximum measured concentrations (using a cobalt catalyst) in the samples of fresh water was 2.1×10^{-8} M and that in sea water was 3.1×10^{-7} M. In the absence of transition metal catalysts these concentrations would not cause any interference in the detection of the superoxide radical. The detection limits of the ICP-MS measurements for the fresh and sea water samples (maximum copper concentration 0.02 ppm and iron concentration 1 ppm) cannot rule out the effect of transition metals. However, the UV decay data (see Section 5.4) indicates that the apparatus is specific in the detection of the superoxide radical. When both the sea and fresh water samples are irradiated the decay data provides rate constant and reaction information which confirms that the disproportionation of the superoxide radical is being measured. This confirms the specificity of the apparatus to the detection of the superoxide radical and indicates that the concentration of transition metals and the amount of hydrogen peroxide present is too low to affect detection of the superoxide radical.

References

1. Fridovitch I, *Quantitative Aspects of the production of the superoxide radical by milk xanthine oxidase.* J.Biol. Chem, 1970. **245**: p. 4053.
2. Bielski B.H.J, Danielli C., Arudi R.L, Ross A.B,, *Reactivity of HO_2/O_2- radicals in aqueous solution.* J. Phys. Chem Ref. Data, 1985. **14**(4): p. 1041.
3. Jayson G.G, Parsons B.J, Swallow A.J., 1973. **69**: p.1597
4. Fridovitch I, Hodgson E.K., *The role of $O_2^{-\cdot}$ in the chemiluminesence of luminol.* Photochem. Photobiol., 1973. **18**: p. 451.
5. Price D, Worsfold P., Fauzi R, Mantoura C., *Determination of Hydrogen Peroxide in sea water by flow injection analysis with chemiluminesence detection.* Analytica.

5. Results and Discussion

There has been considerable debate as to the role of superoxide radical in natural water systems. Researchers [1] have accepted the hypothesis that superoxide is a source of hydrogen peroxide in aquatic systems based on indirect experimental evidence, but there has not been any direct experimental data to support the validity of this conclusion. The indirect evidence which supports the hypothesis that the superoxide radical is a major source of hydrogen peroxide is that superoxide dismutase increases the rate of hydrogen peroxide formation in natural water. (The dismutase enzyme catalyses the disproportionation of the superoxide radical and increases the rate of hydrogen peroxide formation [2]). This observation, because of its indirect experimental nature fails to provide the steady state concentration and kinetic data about the superoxide radical in natural water systems which is necessary to establish definitively the role of the superoxide radical in these systems.

The indirect experimental evidence that has been presented in support of the superoxide radical being a major source of hydrogen peroxide in natural water systems is not conclusive, as there are a number of biological factors which influence the rate of production of hydrogen peroxide and its steady state concentration. It is known that the marine coccolithophore, *Hymenomonas carterae* produces hydrogen peroxide extracellularly [1]. This generation pathway alone is capable of accounting for the 1 to 20x 10^{-8} M steady state concentration of hydrogen peroxide present in sea water. In light of this biological activity any conclusions based on the rate of

hydrogen peroxide production as an indicator of the role of the superoxide radical are unreliable.

5.1 Sampling of the Superoxide Radical in Natural Waters

In order to determine the effect of natural water composition on the superoxide radical concentration and behaviour, two sources of natural water were examined. Fresh water was sampled in-situ at two locations in the Mt Lofty Botanic Garden. Seawater analysis was undertaken at two sites in the Port River Estuary. At each of these sites the diurnal variation in steady state concentration of the superoxide radical was measured. In addition, the depth profile of the superoxide radical concentration was established. The variation in superoxide radical steady state concentration between sites also allowed an understanding of some of the factors that govern the steady state superoxide radical concentration. Samples were collected from each site and used in laboratory UV irradiation experiments to investigate the role of the superoxide radical in natural water systems.

5.2 Superoxide Radical Behaviour in Fresh Water

Site1

Main Lake Mt Lofty Botanic Garden

Sampling of sites in the Mt Lofty Botanic Garden (34°46/605S,138°46-371E) was limited to public access times between the hours of 9am and 5pm. All sampling was undertaken in the period 17/4/98 to 21/5/98. The hours of sunrise and sunset for this time of year are 0718 and 1713 respectively. Sampling of the main lake indicated the superoxide radical concentration varied diurnally between 18 and 72 nanomolar. The superoxide radical was sampled between 10am and 3pm when the solar UV intensity

is highest. The diurnal variation in superoxide radical steady state concentration in the main lake is shown in Figure 5.1. The variation in diurnal concentration is a function of the UV intensity. It can be seen that the variation of concentration follows the variation in UV intensity noted in Figure 5.1. The relationship between UV intensity and superoxide steady state concentration indicates that the radical is a transient photochemically generated species whose rate of formation is a function of UV intensity. Evening concentrations were not examined due to site restrictions although it is anticipated that the superoxide radical concentration would be negligible in the absence of sunlight. Due to the shallowness of the lake it was not possible to establish a depth profile of the superoxide radical concentration.

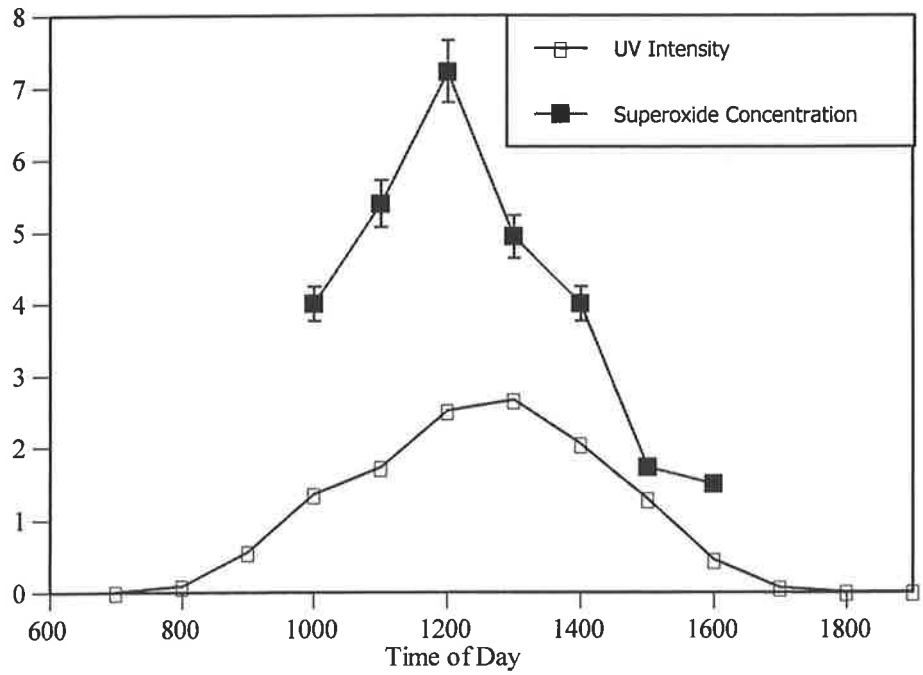

Figure 5.1 The diurnal variation of the Superoxide Radical Concentration (units $x10^8$ M) and UV intensity at Botanic Garden Site 1 on 14/5/98. The diurnal UV data is obtained from Skin-Cancer Foundation ($290nm<\lambda<350nm$) (The UV intensity data is the combination of UVA and UVB intensity with the intensity being measured as 1unit $=0.9mJ/cm^2$)

Site2

Spring Dam Mt Lofty Botanical Gardens

The second fresh water site examined was the Spring Dam. This dam is exposed to minimum sunlight. The dam is fed by natural run off as well as bore-water that has a high calcium carbonate composition that results in a dam pH of 8.6. The analyses from Spring dam were well outside the calibration range for the radiolytically generated superoxide radical making, it difficult to interpret the results in terms of a realistic superoxide radical concentration. The signal generated from the Spring Dam sample was 8 times larger than the signal obtained from the main lake sample. The sample data for both is presented in Figure 5.2.

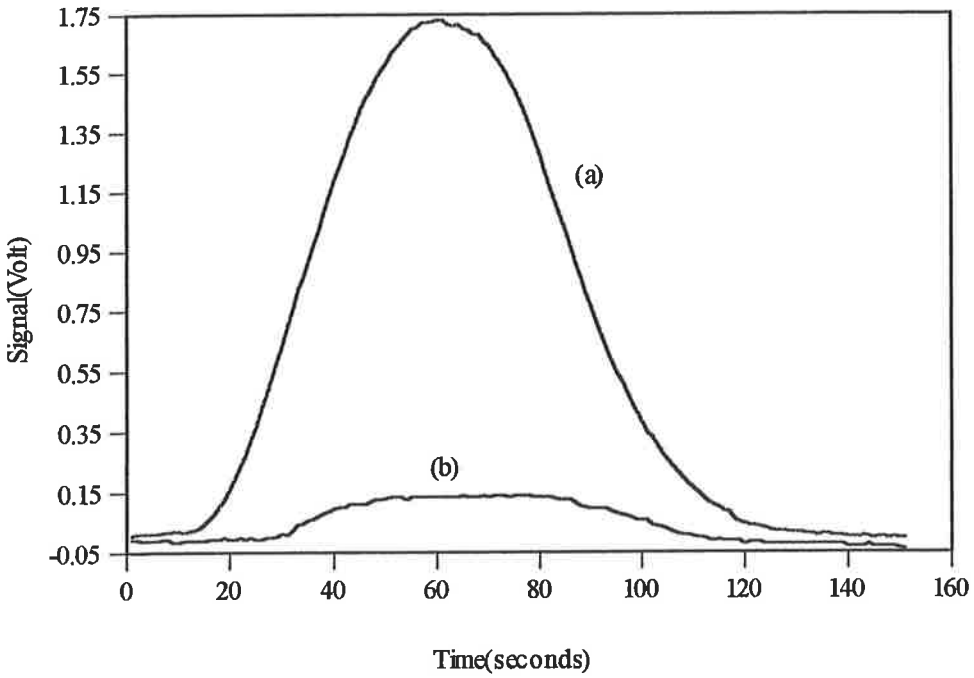

Figure 5.2 Signal Response for Spring Dam (a) compared with Main Lake (b)

The large difference in signal size between the two fresh water samples required investigation in order to determine whether the signal is due to the catalytic oxidation of luminol in the Spring dam. In order to investigate this possibility blank samples were examined in the laboratory to determine whether the signal was due to a transient or stable species in the water. This was necessary to establish whether catalytic oxidation of luminol was occurring in the presence of superoxide or hydrogen peroxide. If hydrogen peroxide was present, then catalytic oxidation normally requires the presence of a transition metal ion, and trace element analysis of the fresh water sample would be required to determine whether there was a difference in transition metal ion concentration between the samples.

When the blank samples from the Spring dam and Main lake were examined in the laboratory, it was found that there was no difference in signal between the blank samples (i.e samples examined in the absence of light). UV irradiation experiments in Section 5.4 indicate that the apparatus is monitoring superoxide radical disproportionation. This indicates that the large signal in the field must be due to the superoxide radical.

However, the fact that the signal is well beyond the calibrated limits for detection prevents any conclusion as to the steady state concentration of the superoxide radical in the Spring dam.

5.3 Superoxide Radical Behaviour in Sea Water

The studies of the superoxide radical at the Royal Yacht Squadron focused on the detection of the superoxide radical, and establishing its diurnal variation and depth dependency. Two sites in the Port River Estuary were examined (See Chapter 2 Site details). Analyses were undertaken at the maintenance berth and the centre of the estuary. The sample sites were approximately 150 m apart and were chosen because of the different levels of pollution that could affect the superoxide steady state concentration. The maintenance berth was likely to have a higher organic matter and microbial content whereas the centre of the estuary was closer to the mouth of the estuary and was regularly flushed by tidal flow and would have a lower organic content.

Site1

Maintenance Berth Royal Adelaide Yacht Squadron

Sampling of the maintenance berth indicated that the superoxide radical concentration varied diurnally between 1.2 and 47 nanomolar. The diurnal variation in superoxide radical steady state concentration at the maintenance berth is shown in Figure 5.3. It can be noted that the variation of concentration in Figure 5.3 corresponds with the variation in the solar UV intensity (Figure 5.4).

The variation in superoxide radical steady state concentration is similar to that found for the radical in freshwater and confirms the transient nature of the superoxide radical steady state concentration. The diurnal variations in concentration provide confirmation of earlier observations at the fresh water site that the superoxide radical is a photochemically generated transient species with a rate of formation dependent on the solar UV intensity. As is the case for fresh water superoxide radical concentrations it was be anticipated that the radical concentration would fall to negligible concentrations at night.

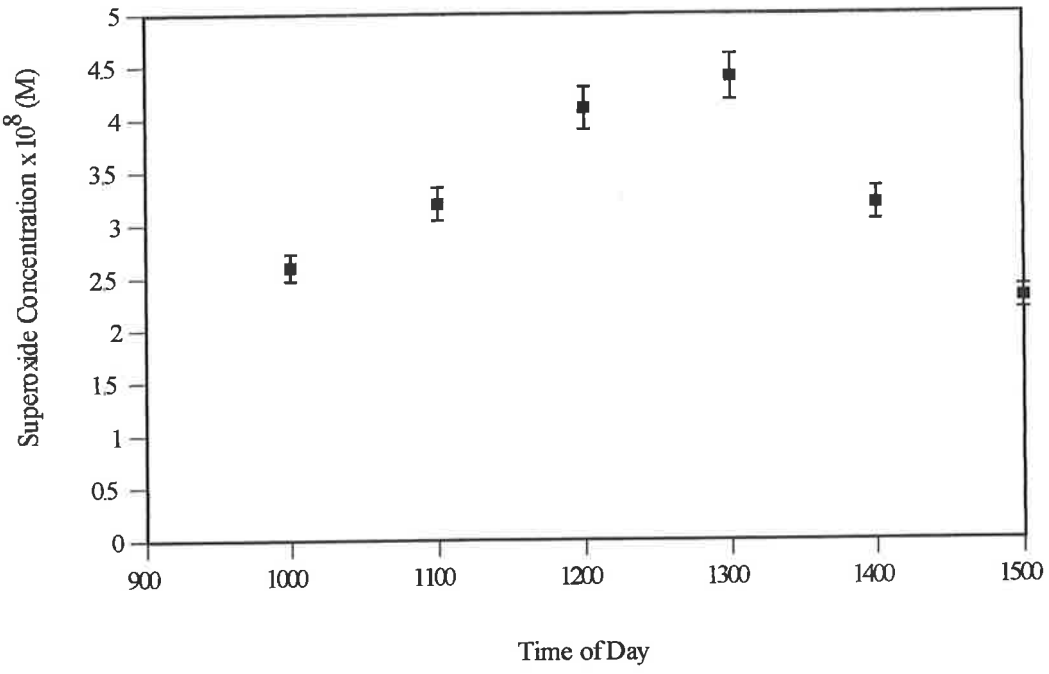

Figure 5.3 Diurnal Superoxide Radical Concentration at RSAYS Maintenance Berth

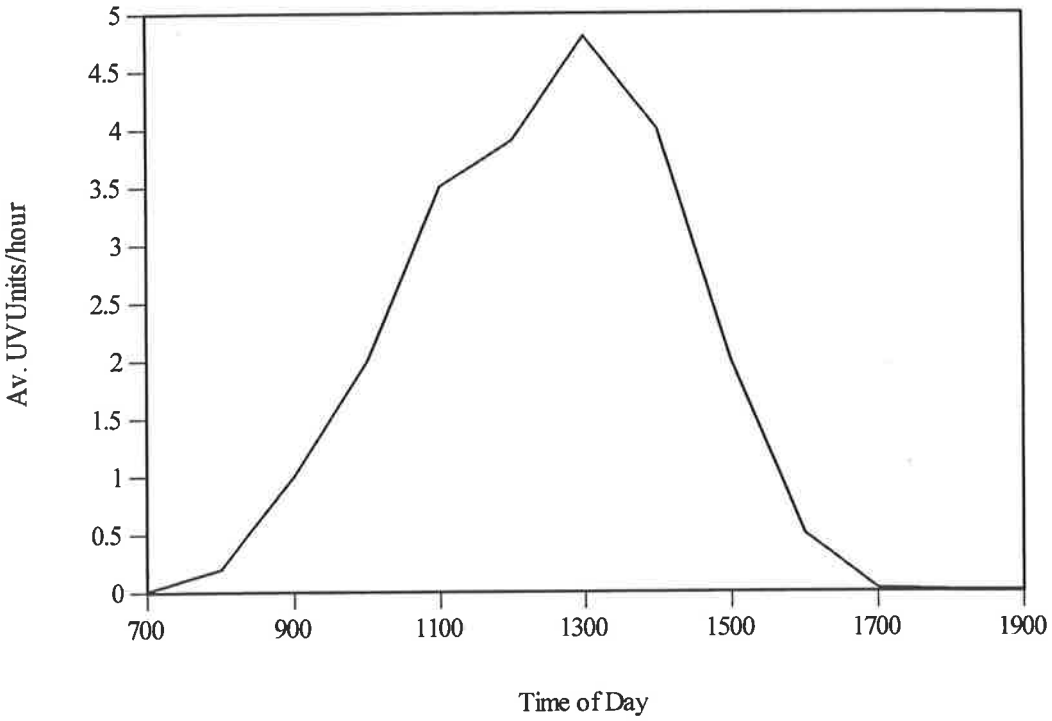

Figure 5.4 Diurnal UV Intensity on 23/4/98 The UV intensity data is provided by the Skin Cancer Research Foundation and measures UVA and UVB intensity with the intensity being measured as 1unit =0.9 mJ/cm^2

Another issue of interest in studying the superoxide radical is the variation of the superoxide radical steady state concentration with depth of water. This allows an understanding of the superoxide radical concentration distribution in surface waters where the radical will be at its highest. The superoxide radical concentration is a function of numerous parameters, such as the light attenuation coefficient of the water, and the amount of dissolved organic matter present. In the seawater studied it was found that the superoxide radical concentration decreased with depth. At the maximum depth examined the radical concentration was 25% less than that of surface water. However, there was only a 10% decrease in the radical concentration in the first 20cm of water. This study was intended only to provide an indication of the superoxide radical concentration at the surface. A comprehensive depth study would

require the redesign of the apparatus to permit under water operation or much more rapid sampling because the superoxide radical must be measured in-situ due to its decay through disproportionation. There are no comparative data for the superoxide radical in fresh water due to the difficulty in obtaining meaningful depth measurements in the accessible region of the lake where water depth did not fall below 15 cm.

The depth profile suggests that the superoxide radical is at its maximum concentration in the first 20 cm of depth and that as depth increases the radical concentration drops, and this indicates that significant chemical activity due to the superoxide radical will be restricted to the sea water surface.

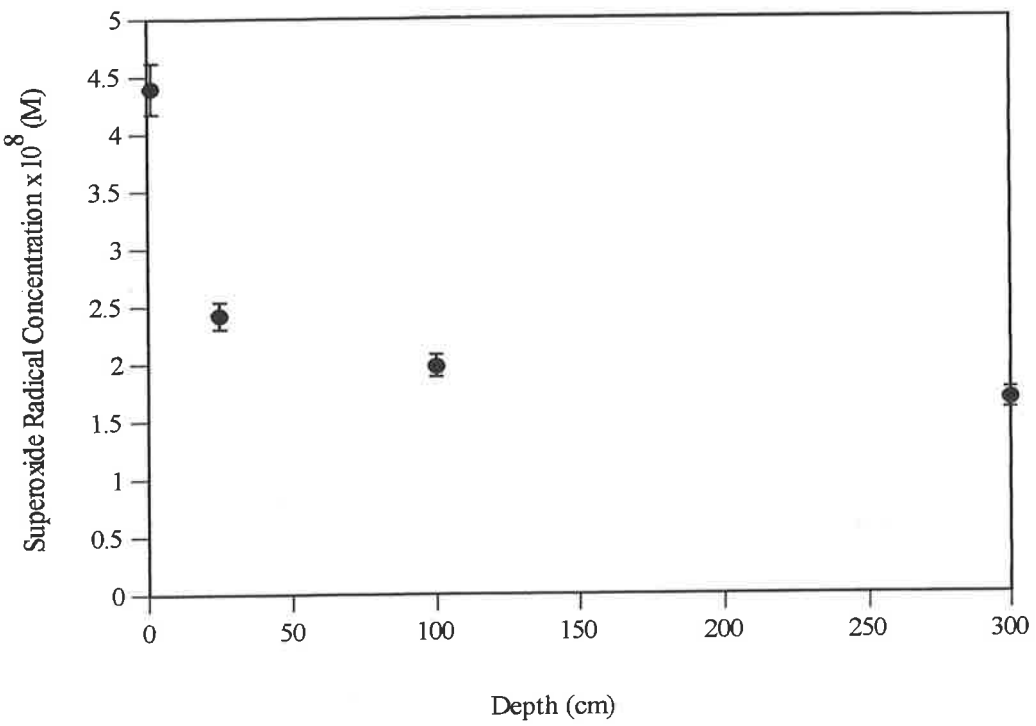

Figure 5.5 Superoxide Radical Depth Profile measured at the RAYS Maintenance Berth on 24/4/98

Site2

Estuary Royal Adelaide Yacht Squadron

Sampling of the maintenance berth indicated the superoxide radical concentration varied diurnally between 22 and 45 nanomolar. The diurnal variation in superoxide radical steady state concentration at the maintenance berth is shown in Figure 5.5. The variation in diurnal concentration is a function of the UV intensity. It can be seen that the variation of concentration in Figure 5.6 follows the variation in the UV intensity seen in Figure 5.7.

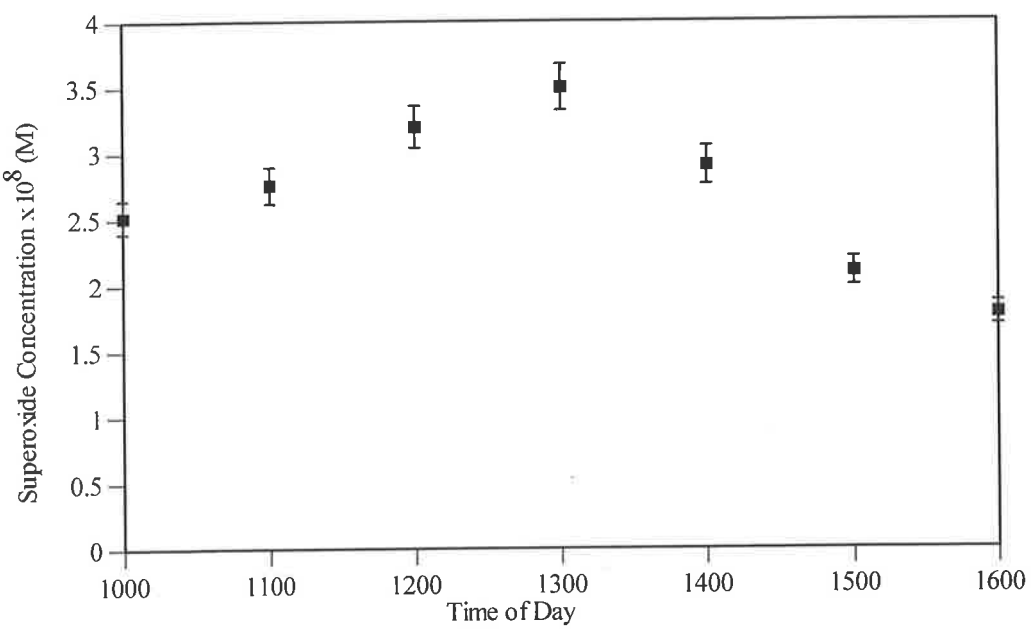

Figure 5.6 Diurnal Variation of the superoxide radical at the Port Estuary

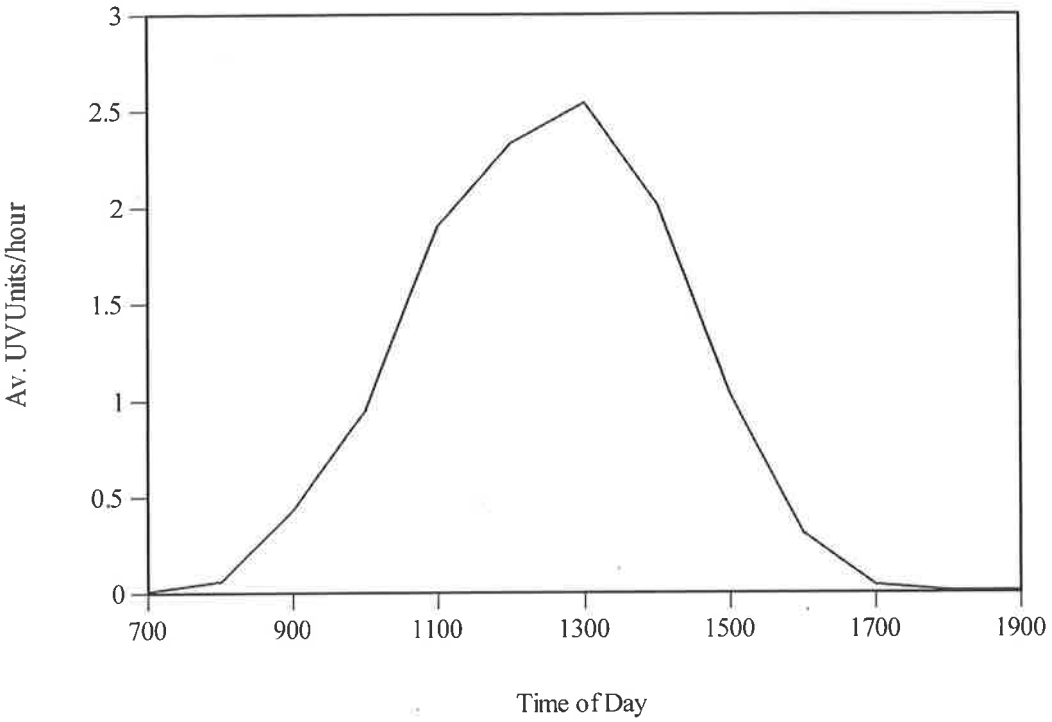

Figure 5.7 Diurnal UV Intensity on 27/5/98 The UV intensity data is provided by the Skin Cancer Research Foundation and measures UVA and UVB intensity with the intensity being measured as 1unit =0.9 mJ/cm^2

The major difference between the two sites examined is the difference in steady state concentrations. There is a 21% difference in steady state concentration between the main estuary and the maintenance berth, although there is a 200% increase in incident UV radiation (On different days). Given that the superoxide radical concentration is dependant on UV intensity as shown by the diurnal variation in superoxide radical concentration, the relatively small increase in superoxide concentration given a 200% increase in UV intensity suggests that there may be some removal mechanism in the maintenance berth water. Consequently this increases the rate of removal of the superoxide radical e.g. inorganic or organic pollutants. This conclusion is based on the observation that at the Maintenance Berth there was considerable amount of visible pollution such as oil slicks and dead marine life.

5.4 Pollution Effects on Superoxide Radical Steady State Concentration

The superoxide steady state concentration is a function not only of the rate of production of superoxide radical i.e. the UV intensity, but also because of the rate of removal of the superoxide radical. Possible removal pathways for the superoxide radical include: disproportionation to hydrogen peroxide, reaction with inorganic ions or organic molecules, or transition metal catalysed dismutation. The reaction of the superoxide radical with inorganic or organic species in natural water is governed by the nature of the species present, as the superoxide radical will react primarily through redox pathways. In the water samples examined, transition metal ion concentrations were measured, but organic species were not, due to the complexity of characterising organic species.

Steady state superoxide concentrations are listed in Table 5.1. The results indicate that there are only minor variations of superoxide radical concentration with each site, despite a 200% increase in UV intensity (measured on different days). Of particular interest is the variation in concentration between the marine sites, which would indicate that chemical or biological reactions might be affecting the steady state concentration.

Table 5.1 Maximum Steady State Superoxide Radical Concentration at Site

Site	Superoxide Steady State Concentration x 10^8 (M)	Maximimum Surface UV Intensity 1 unit = 0.9mJ/cm^2
Botanic Gardens- Main Lake	7.2	2.7
Botanic Gardens- Spring Dam	N/A	2.7
Port River Estuary	3.5	4.7
Maintenance Berth R.A.Y.S	4.5	2.4

5.4.1 Fresh Water

In the case of the fresh water sites examined there is an 8-fold increase in signal between the Spring Dam and Main Lake. UV decay data confirms that the signal from both sites is due to the superoxide radical. This difference between the sites in signal may be due to microbial activity producing the superoxide radical because both UV irradiated samples (see Section 5.5) produce rate constant data indicating that disproportionation is the only mechanism for the removal of the superoxide radical i.e there is no interference from transition metal catalysis.

5.4.2 Sea Water

The steady state superoxide concentrations measured in seawater indicated only a small increase in signal in the maintenance berth despite a 200% increase in incident UV. The small increase in signal despite a 200% increase in UV intensity suggests a metal catalysed removal of the superoxide radical. The ICP-MS data (Table 5.2) is inconclusive due to the ppm detection limits of this technique. However, UV irradiation data from 5.4 indicates that disproportionation is the only removal mechanism for the superoxide radical in the estuary, while some catalytic removal is taking place in the maintenance berth.

Table 5.2 Sea Water Metal Content

Site	Cu Concentration (ppm)	Fe Concentration (ppm)
Port River Estuary	<0.02	<1
Maintenance Berth R.S.A.Y.S	<0.02	<1

5.5 UV Irradiation Experiments

The diurnal variation of the superoxide radical steady state concentrations obtained in the marine and fresh water environments indicates that there is a correlation between the rate of formation of the superoxide radical and the solar UV intensity. The photochemical processes behind the generation of the superoxide radical cannot be replicated using the gamma radiolysis of sodium formate solution that has been used to generate standard solutions of the superoxide radical for calibration purposes. The use of UV irradiation allows an alternative method for generation of the superoxide radical and also permits an understanding of the superoxide radical's possible role in the environment by replicating to a certain extent its generation pathway.

A major consideration in using UV irradiation of natural water is that only 1.3 % of incident UVB radiation from sunlight is less than 304 nm. The time a sample is exposed to UV (304 nm) is important because exposure to high intensity UV light through long exposure times does not replicate natural conditions and may promote photochemical processes which are not significant or do not occur under natural sunlight.

5.5.1 Exposure Time

In order to investigate the effect of exposure time on the photochemical processes samples of fresh and sea water were exposed to varying amounts of UV light. Three exposure times were investigated, 5 minutes, 15 minutes, and one hour. It was found that 5minutes was not sufficient to generate steady state photochemical products. However, after 15 minutes steady state products were observed, which then decayed

when the UV light was turned off. The photochemical product in this case was shown to be the superoxide radical through its second order decay rate constant. The longer exposure time of one hour led to an extremely stable photochemical product, which did not decay even after 15 minutes from removal from irradiation. This product is almost certainly hydrogen peroxide, but its concentration is significantly higher than the steady state concentration of hydrogen peroxide in natural water systems. (Hydrogen peroxide does not interfere with superoxide measurements until its concentration exceeds 3.5×10^{-7} M)

5.5.2 Milli-Q Water

The first of the UV irradiation experiments was to confirm that ultra-pure Milli-Q water was essentially inert under UV irradiation conditions. Ultra pure water from a Milli-Q RX plant was irradiated for 15 minutes. There was a 25% increase in blank signal after this irradiation and the signal was found to be extremely stable after irradiation, which indicated a stable photochemical product capable of oxidising luminol, was formed. The most probable species is hydrogen peroxide. The change in peak height was negligible, compared to that found in natural water systems, where after 15 minutes irradiation the peak height in fresh water had increased by 800% (see Figure 5.9). The small increase in peak height in ultra-pure water compared to that of natural water indicates that the photochemically induced chemistry observed in natural water systems is not due to the photolysis of water. Rather photochemical reactions occurring between the UV light and chemical species present in the natural water, most probably DOM.

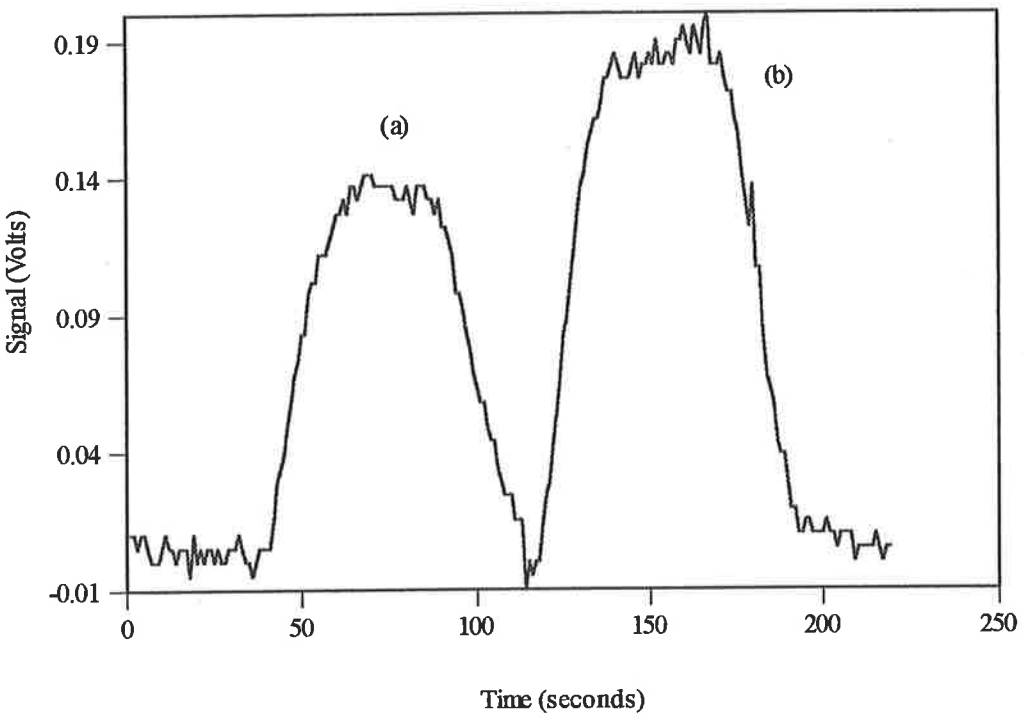

Figure 5.8 Milli-Q Water before(a) and after 15 minutes UVB Exposure (b)

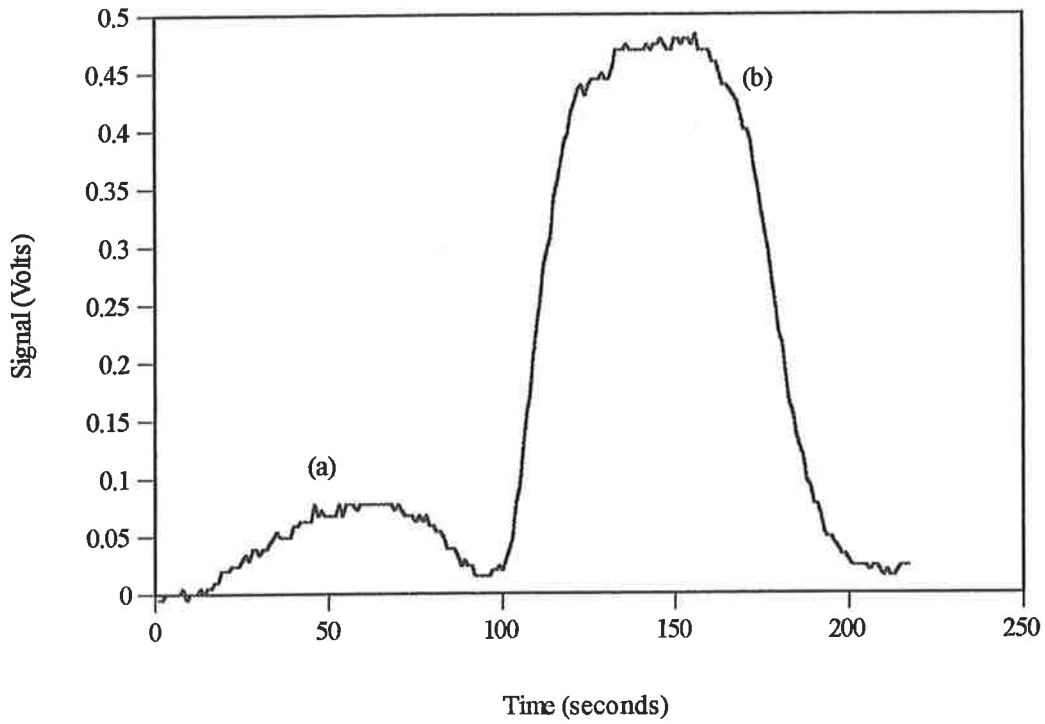

Figure 5.9 Fresh Water before (a) and after 15 minutes UVB Exposure (b)

5.5.3 Fresh Water UV Irradiation

Two fresh water samples from the Mt Lofty Botanical Gardens were irradiated with UV light (304 nm) in order to determine the photochemical products generated, in particular, the superoxide radical concentration and its decay pathway.

Main Lake

The field results indicated a diurnal variation in steady state concentration of the superoxide radical with a maximum measured concentration of 7.2×10^{-8} M which confirmed that the superoxide radical is a photochemically generated species in fresh water. Figure 5.10 shows the decay in the peak height with time of this photochemically generated species, the nature of the decay permits confirmation that it is the superoxide radical through both the rate constant and kinetic behaviour and the kinetics of the decay process.

The decay curve clearly shows a second order reaction. The second order kinetics suggests that the photochemically generated species detected is the superoxide anion. This is confirmed by the rate constant data for the decay curve is within experimental error of that obtained by Bielski [3] for the disproportionation of the superoxide radical in ultra-pure water at pH 7.9 (1.29×10^{4} $M^{-1}s^{-1}$ c.f. predicted value 9×10^{3} $M^{-1}s^{-1}$)(see Figure 5.11). The correlation between the rate constant values for fresh and ultra-pure water provides conclusive evidence that the major removal pathway for the superoxide radical anion is through disproportionation to hydrogen peroxide.

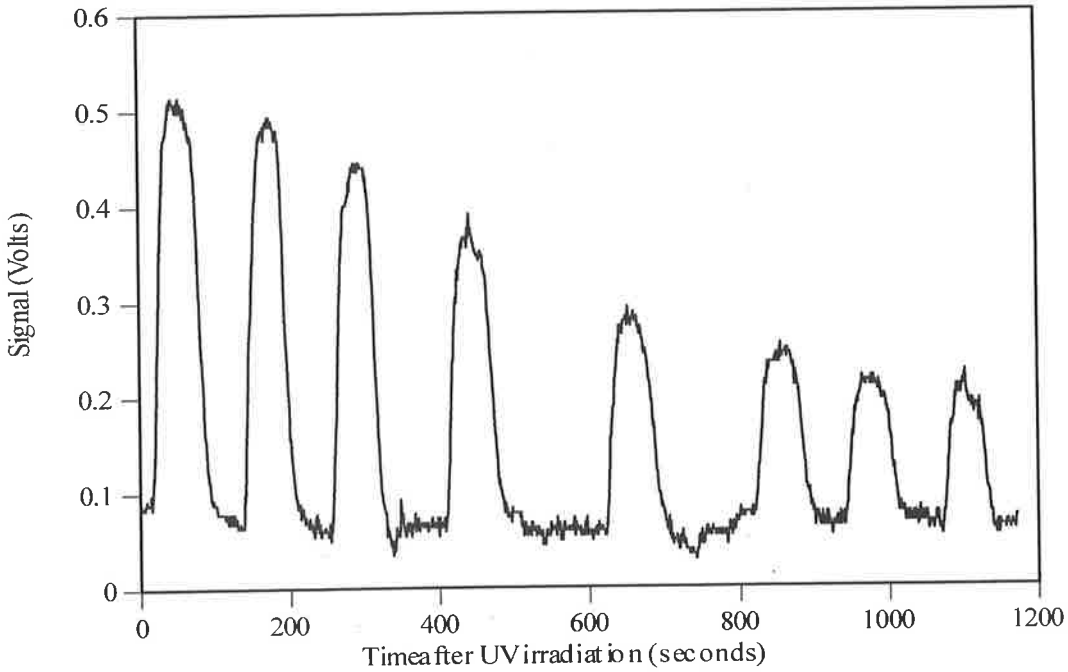

Figure 5.10 Decay Signal of UV Generated Superoxide Radical with Time (Botanic Gardens Main Lake)

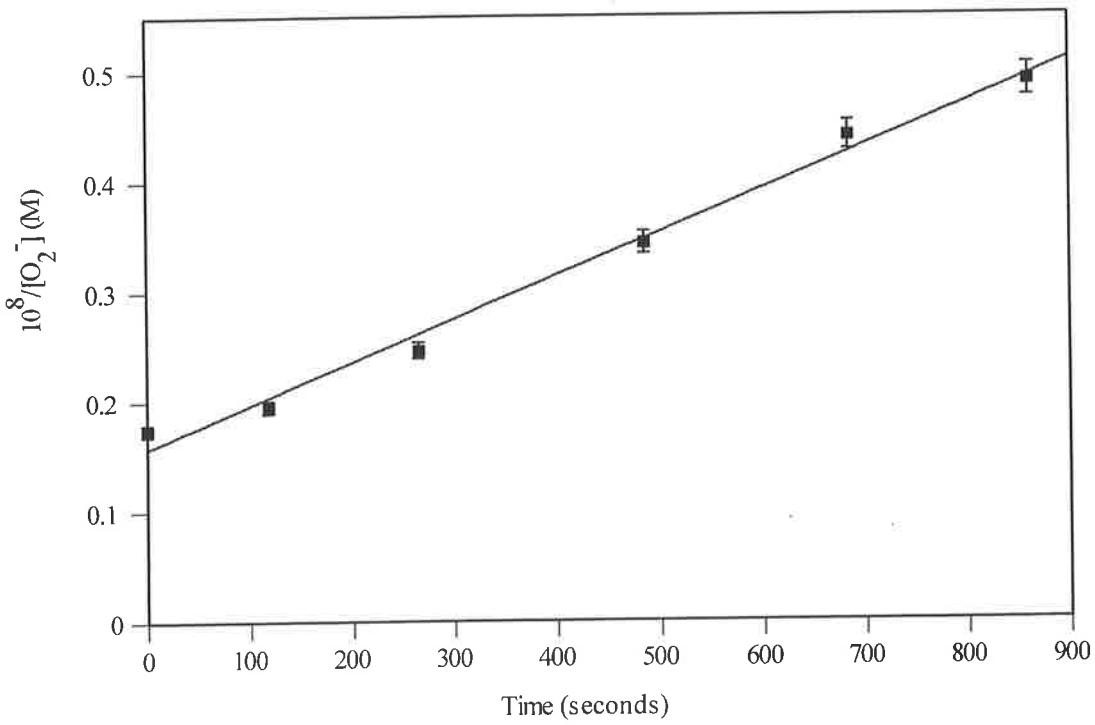

Figure 5.11 Second Order rate plot for UV Generated Superoxide in Main Lake (pH8.2) based on 5.10

Spring Dam

The reverse flow injection manifold response to the superoxide radical present in the Spring Lake was eight times that of the main lake although the blank signal was the same for both sites. This difference in signal was investigated using UVB irradiation of fresh water samples from both sites. On exposure to UV radiation, it was found that the water sample form Spring Dam had a decay constant of 1.29×10^4 $M^{-1}s^{-1}$ which increased to 3.4×10^4 $M^{-1}s^{-1}$ in the Main Lake.

The second order decay behaviour and the fact that the experimental rate constant is close to the predicted value of $9 \times 10^3 M^{-1}s^{-1}$ confirms that superoxide is being detected, and that its decay behaviour is similar to that found in the water sample taken from the Main Lake i.e. disproportionation to hydrogen peroxide. The correlation between the rate constant data and the values obtained in pure water and fresh water samples would suggest that the 800% difference in signal between the two sites examined indicates that the RFIA manifold is specific to the detection of the superoxide anion and that microbial activity may be responsible for the increased signal measured in the field. The UV results confirm that this is not due to transition metal ions because there is no evidence of the catalytic removal of the superoxide radical by transition metal ions, which are not affected by sample collection.

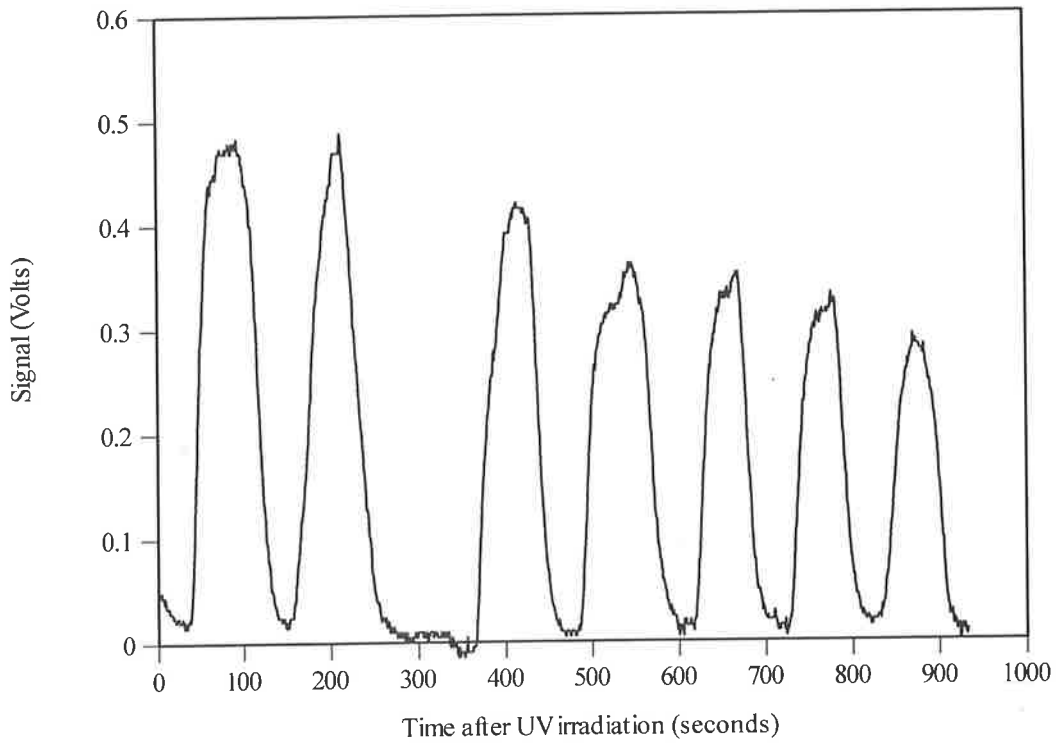

Figure 5.12 Decay of UV Generated Superoxide Radical with Time -Spring Dam (pH 8.6)

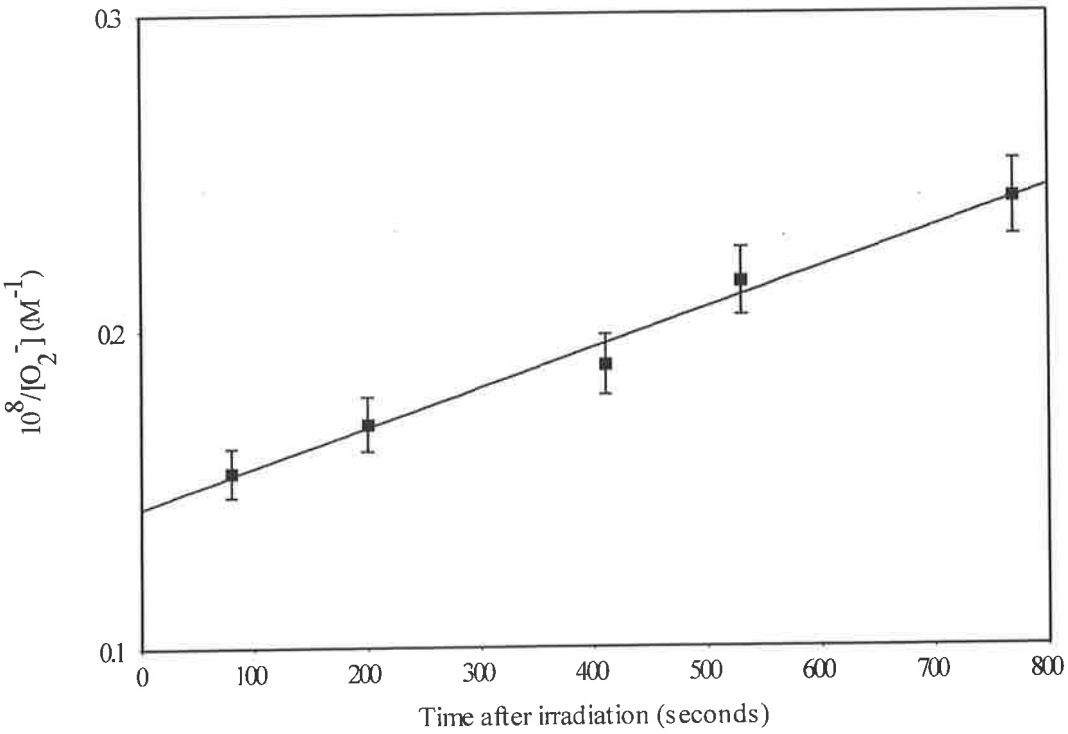

Figure 5.13 Second Order rate plot for UV Generated Superoxide in Spring Dam (pH8.6) based on 5.11

5.5.4 Sea Water UV Irradiation

Port River Estuary

The field results indicated a steady state superoxide radical concentration of 3.5 x 10^{-8} M. In order to study the radicals removal pathways as had been done for fresh water, a sea water sample was irradiated for 15 minutes until a photochemical product which reacts with luminol was generated at a steady state concentration. Figure 5.14 shows the decay in the peak height with time of this photochemically generated species.

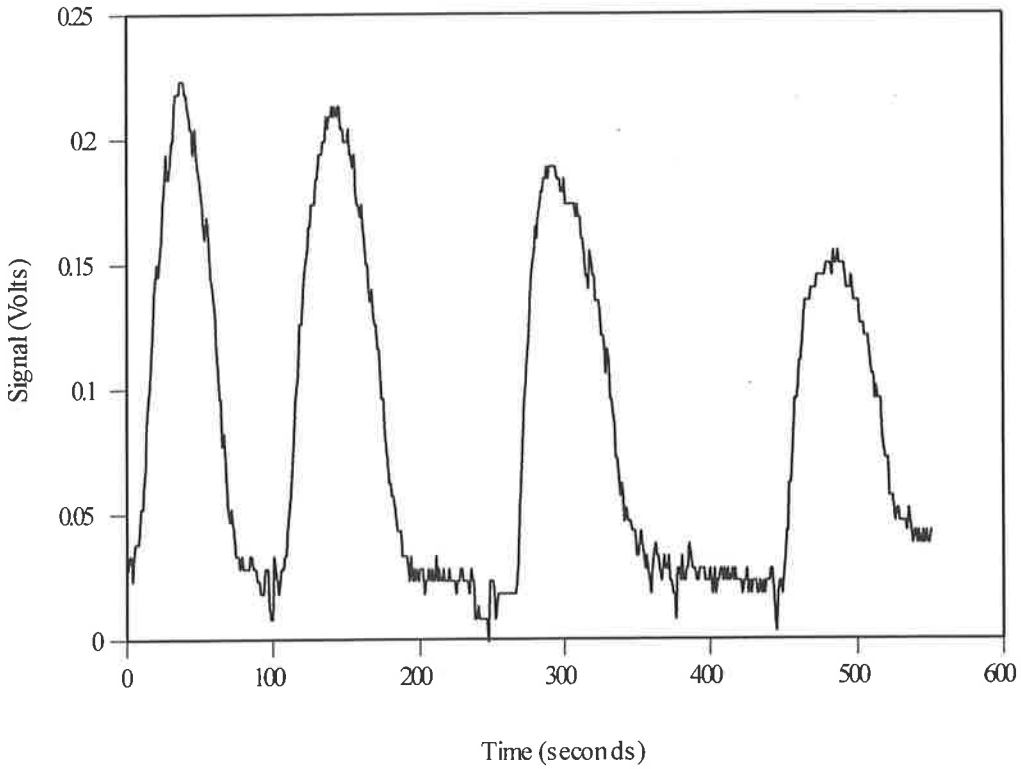

Figure 5.14 Decay of UV Generated Superoxide Radical with Time Port River Estuary (pH 8.1)

The decay behaviour of the superoxide radical concentration in the UV irradiated estuary water as shown in Figure 5.14 indicates that the decay process is second order with respect to time. This kinetic observation in addition to the rate constant obtained from this decay curve(5.5 x 10^4 $M^{-1}s^{-1}$) which is close to the expected value of 3 x 10^4 $M^{-1}s^{-1}$ for the superoxide radical at pH 8.2 provides confirmation that the

photochemically generated species being measured in sea water is the superoxide radical. In addition, the precise determination of the rate constant for the disproportionation of the superoxide radical and its correlation with the literature value confirms not only the presence of the superoxide radical, but also indicates that the primary removal pathway for the superoxide radical is through disproportionation to hydrogen peroxide.

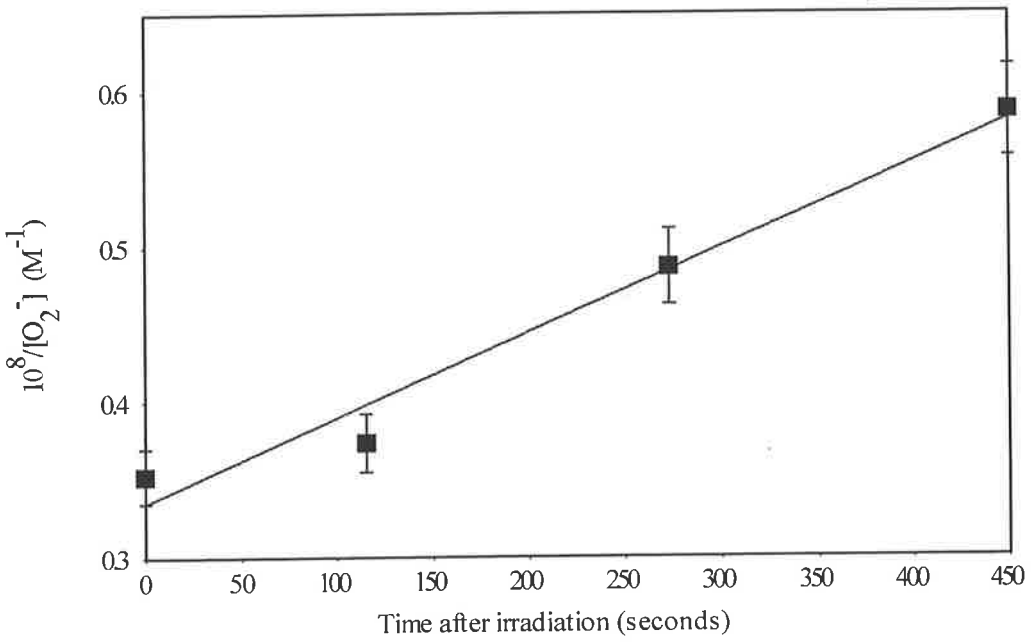

Figure 5.15 Decay of UV Generated Superoxide Radical with Time Port RAYS Maintenance Berth (pH 8.2)

Royal Yacht Squadron Maintenance Berth

The signal of UV irradiated sea water sampled from the maintenance berth provided an indication of the role of pollutants in the decrease of superoxide radical steady state concentration at the maintenance berth compared to that in the estuary. The absence of decay behaviour for the superoxide radical as shown in Figure 5.16 indicates that the photochemically generated product is most likely hydrogen peroxide. The formation of hydrogen peroxide is evidence that the superoxide radical

is being removed by a pathway other than disproportionation. This is most likely due to the dismutation of the superoxide radical in the presence of transition metals because it is not possible to obtain any rate constant data from the UV irradiated sample of water from the RSAYS maintenance berth which indicates disproportionation is a minor removal pathway. Similar dismutation behaviour in particular in the presence of copper and iron ions has been reported by Faust in oceanic water [4].

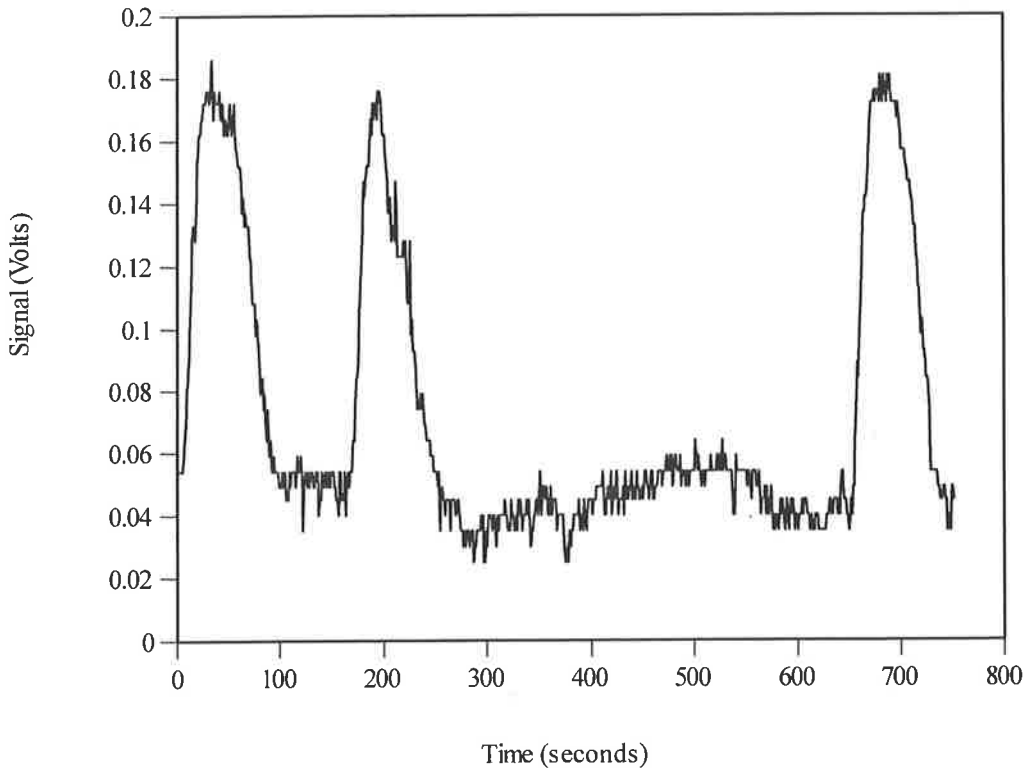

Figure 5.16 Photochemical Products of UV irradiated sample from RAYS Maintenance Berth

5.6 Implications

The decay signals obtained from the UV irradiation of natural water samples have established the major removal pathways of photochemically generated superoxide radicals in both fresh and seawater as distinguished from radiolytically generated

superoxide radical. The disproportionation rate constant and kinetic behaviour of the superoxide radical has been measured in natural water and is consistent with laboratory experiments in ultra-pure water. In-situ measurements of the superoxide radical indicate that it is a transient photochemically induced species whose photolytic rate of production and consequent steady state concentration varies diurnally. The steady state concentration data for the superoxide radical species enables some conclusions to be drawn on likely generation pathways for the superoxide radical.

5.6.1 Removal Pathways for the Superoxide Radical in Natural water.

In the UV (304 nm) irradiated seawater and fresh water samples a photochemically generated species have been detected. This species decays through a second order process which has a rate constant which agrees with that determined by Bielski for the disproportionation of the superoxide radical in Milli-Q solution. This agreement between the rate constant data not only confirms the detection of the superoxide radical i.e. second order decay with rate constants within 20-30% of the published rate constants in pure water, but also indicates that the major pathway for the removal of the superoxide radical is through disproportionation to produce hydrogen peroxide. Further support for this conclusion comes from experimental evidence, which links the addition of SOD with an increased rate of hydrogen peroxide formation.

The disproportionation behaviour of the superoxide radical is not surprising given its inability to react with organic compounds through pathways such as hydrogen abstraction, and addition, which are available to more reactive radicals such as the hydroxyl radical. In view of the superoxide radicals limited reactivity towards organic

compounds and the low concentration of transition metals in the water samples examined, the major pathway for removal of the superoxide radical (in the absence of a significant concentration of the transition metals) must be the production of hydrogen peroxide through disproportionation. This is confirmed by the UV irradiation data in Section 5.4

$$HO_2 + HO_2 \rightarrow H_2O_2 + O_2$$

$$HO_2 + O_2^- + H_2O \rightarrow H_2O_2 + O_2 + OH^-$$

5.6.2 Kinetic Data for Removal Pathway of the Superoxide Radical

The kinetic behaviour and empirical rate constants for the decay of the superoxide radical confirm that the photochemically generated species is the superoxide radical i.e. second order kinetics for decay and a rate constant within 20% of that determined in ultra-pure water. The empirically determined rate constants for the disproportionation of the superoxide radical compared to those obtained by Bielski for ultra pure water are shown below in Table 5.3.

Table 5.3 Empirical Rate Constant Data

Sample	Experimental Rate Constant ($M^{-1} s^{-1}$)	Predicted Rate Constant ($M^{-1} s^{-1}$)
Spring Dam (Fresh Water)	1.29×10^4	9×10^3
Main Lake (Fresh Water)	3.4×10^4	3.5×10^4
Port River Estuary (Sea Water)	5.5×10^4	3.5×10^4

5.6.3 Diurnal Variation of the Superoxide Radical

The diurnal variation of the superoxide concentration indicates not only the transient nature of the radical but provides a direct correlation between diurnal variations in incident UV intensity and the steady state concentrations of the superoxide radical (see Figure 5.17). The sea and fresh water superoxide radical concentration diurnal variations can be seen below together with, calculated and experimentally observed diurnal rates of photolysis of an organic pesticide (DMDE). The artificially calculated and measured diurnal variations in the rates of photolysis of DMDE [5] and the superoxide radical exhibit a similar variation. This result confirms that the superoxide radical is a transient species with its steady state concentration dependent on its photochemically generated rate of production, (its decay rate through disproportionation is the same throughout the day and is pH dependent only)

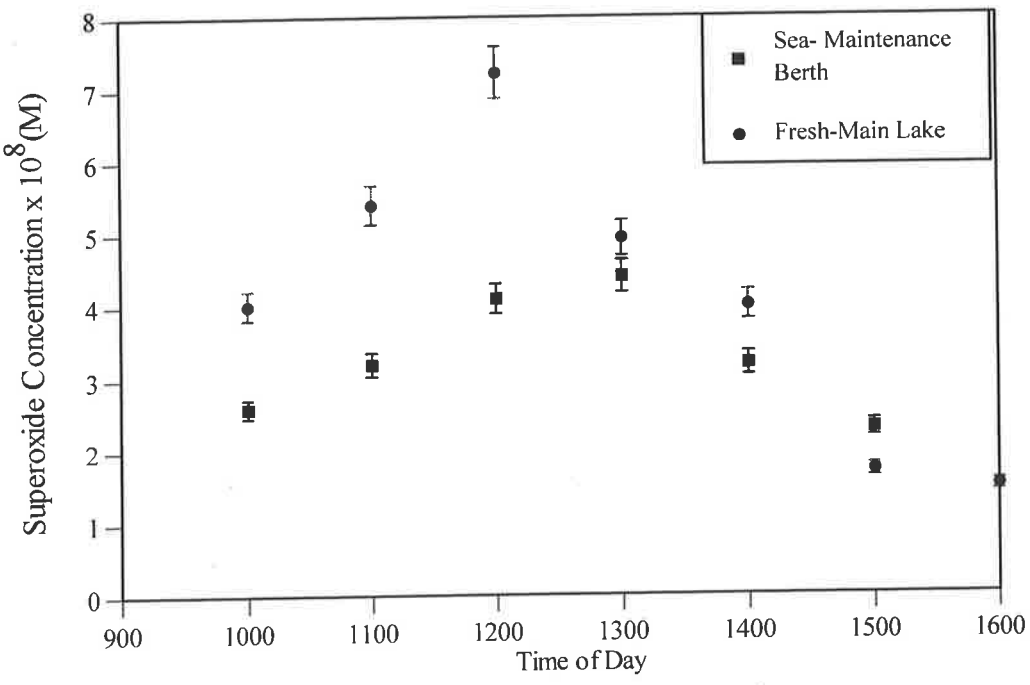

Figure 5.17 Diurnal Variation of Superoxide Radical Concentration in Fresh Water and Sea Water

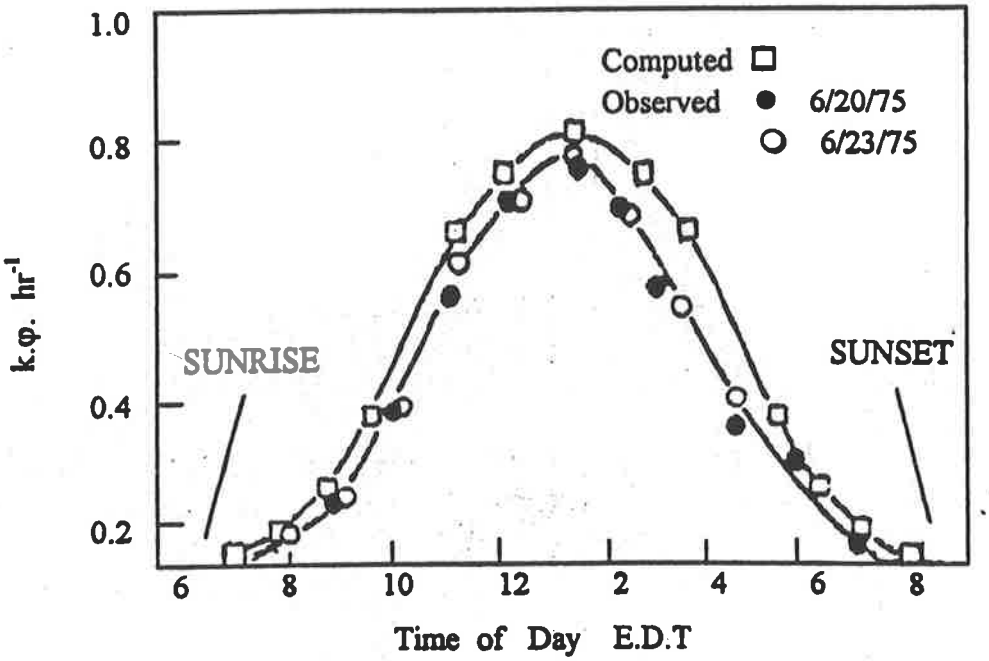

Figure 5.18 Diurnal Variation of computed and actual photolysis of the pesticide DMDE [5]

5.6.4 Generation Pathways

In addition to establishing the major decay pathway for superoxide in natural water, the steady state concentrations of the superoxide radical have been measured in both fresh water and seawater. The steady state concentrations were found to vary with UV radiation incident during the day, achieving a maximum concentration by 12.30pm during each day. Thi s maximal concentration is in agreement with the UVB measurements taken by the Skin Cancer Foundation of Adelaide which indicate maximum UVB occurs at approximately 1230-1330. Therefore, the generation pathway is photochemical and could follow one of three possible pathways, two involving DOM and the third the photolysis of hydrogen peroxide

1.Photo-electron Transfer

$DOM + hv \rightarrow DOM^{+} + e_{aq}$

$e_{aq} + O_2 \rightarrow O_2^{-}$

2. Charge Transfer within photoexcited sensitizer-O_2 complexes

$S + O_2 + hv \rightarrow [S.... O_2] \rightarrow Sox + O_2^{-}$

3. Hydrgogen Peroxide Photolysis

$HOOH + hv \rightarrow 2OH$

$OH + H_2O_2 \rightarrow HO_2 + H_2O$

The establishment of a steady state concentration of the superoxide radical means that it is possible to verify whether pathways such as the generation of superoxide radical through the photolysis of hydrogen peroxide are possible. We can estimate the rate of superoxide formation from the photolysis of hydrogen peroxide by sunlight.

If we consider a $5x10^{-8}$ M H_2O_2 concentration and path length of 1m, assuming that we are examining a segment of water 1m deep and $1cm^2$ Given that the absorption coefficient H_2O_2 is ($\varepsilon = 1\ M^{-1}cm^{-1}$) at $\lambda = 300$ nm [7]

Then

$$A = \varepsilon cl$$

$$\text{Then } A = 1x\ 5x10^{-8}\ M\ x\ 100$$

giving an absorbance of 0.00005

which in terms of light intensity from Beers law is 0.00116% of intensity absorbed.

In terms of light flux or photons incident on this column of water

Light Flux for (λ<300nm) is, say

2.7×10^{12} photons $cm^{-2}s^{-1}$

Therefore rate of [OH] production

$=0.000011 \times 2 \times 2.7 \times 10^{12}$ molecules / 100cc / s

$= 6.25 \times 10^{8}$ OH in 100cc water column per second

which in a water column of 1 metre i.e 100cc is 3.7×10^{-13} mol /L per hour. Therefore, assuming no decay of the superoxide radical through disproportionation to hydrogen peroxide or reaction with other chemical species present in natural water it would take 37.5 hours to achieve a steady state concentration of 5×10^{-8} M.

Given that the measured steady-state concentration if superoxide radical is at most 5.2×10^{-8} M it is possible to show that the photolysis of hydrogen peroxide is not a major source of the superoxide radical in the environment. The source must be through the interaction of DOM with incident UVB (reactions 1 and 2).

5.7 Conclusion

The experimental data obtained from UV experiments has shown that the superoxide radical can be generated photochemically in natural water and that its decay pathway is primarily through disproportionation. The correlation between kinetic behaviour and rate constant data obtained in natural water with that available for ultra-pure water would suggest that the major path for removal is through disproportionation to hydrogen peroxide which is the primary contribution of the superoxide radical to the natural water system.

References

1. Zafiriou O.C, Zepp R.G, Zika R.G, *Photochemistry of Natural Waters.* Environ. Sci & Tech., 1984. **18**(12): p. 358A.

2. Cooper W.J, Z.R., *Photochemical Formation of Hydrogen Peroxide in Surface and Ground Waters Exposed to Sunlight.* Science, 1983. **220**(May): p. 711.

3. Bielski BHJ, Danielli.C., Arudi R.L, Ross AB,, *Reactivity of HO_2/O_2- radicals in aqueous solution.* J. Phys. Chem Ref. Data, 1985. **14**(4): p. 1041.

4. Faust B.C. Aquatic Photochemical Reactions in Atmospheric,Surface, and Marine Waters. Influences on Oxidant Formation and Pollutant Degradation. Handb. Environ. Chem.,1999.**2**: p.100.

5. Fincher RC, G.J., Wolfe NL, Zepp RG, J. Agric . Food Chem, 1976. **24**: p. 727.

6. Cline D.M, Z.R., *Rates of Direct Photolysis in Aquatic Environment.* Environ. Sci. Technol., 1977. **11**: p. 798.

7. USACE, Advanced Oxidation Design Considerations. Eng.Tech.Ltrs, 1996. **1110**:p1-161

6.0 Conclusion

The reverse flow injection manifold constructed has proved capable of detecting and measuring the superoxide radical in natural waters. The detection limit for the superoxide radical using this manifold was 10 nanomolar. In the natural waters examined (both seawater and fresh water) the superoxide radical concentration ranged from 17 to 38 nanomolar.

UV irradiation of natural water was used to generate the superoxide radical without using gamma radiation, replicating the photochemistry of natural sunlight. This led to the formation of a photochemical product that was detected by the rfia apparatus. This photochemical product was identified because of its decay behaviour. The second order nature of the decay process, and the agreement between rate constant data with literature values for the disproportionation of the superoxide radical, confirmed that the superoxide radical is the species being generated by UV irradiation, and detected by the flow injection manifold.

The UV irradiation experiments indicate that the major pathway for the disappearance of the superoxide radical in natural water is via the formation of hydrogen peroxide through disproportionation. This conclusion is based on the decay behaviour of the UV generated superoxide radical. The steady state concentration measurements of the superoxide radical also indicate that the major formation pathways for the superoxide radical do not involve the photolysis of hydrogen peroxide, as it is most likely to be through the photochemical reaction of DOM.

On the basis of this experimental evidence from both UV and steady state measurements it appears that the superoxide radical is formed primarily through photochemical pathways i.e. photochemical reactions involving DOM. The radical's concentration varies diurnally from 0-60 nanomolar and would have seasonal variations with its highest concentration during summer months. The role of the superoxide radical in the degradation of organic species is uncertain. The UV experiments indicate that superoxide is removed from the environment via disproportionation to form hydrogen peroxide. Therefore it is unlikely to play a significant role in the degradation of organic species present in natural waters.

7.Introduction

7.1 Water Analysis

The experience of developing an analysis technique for the superoxide radical illustrated some of the major difficulties encountered in developing environmental analysis. Firstly a suitable chemical reaction must be found to permit the analysis of the analyte. Once a reaction has been identified suitable equipment must be either built or purchased. Finally, this apparatus has to be calibrated for each environmental system studied. In certain cases, for example, transient species such as the superoxide radical, it is necessary to construct analyte specific apparatus. However, there would significant advantages if a more broad-spectrum analysis technique could be developed. Existing water analysis techniques, which are multi-speciate such as ICP-MS, do not provide any structural information of analyte species such as oxidation state and are limited to inorganic species.

In terms of multi-speciate analysis, mass spectrometry is a technique that has the ability to detect a species on the basis of a single ion. However, access to mass spectrometry has been severely restricted for liquid phase analysis because common solvents such as water have a vapour pressure of 0.1Torr at 25°C. Early use of mass spectrometry was restricted to the evaporation of the water sample and then analysis of the residue, using techniques such as GC-MS. Only a few applications of MS/MS are available. Boon et al [1] used MS/MS with a pyrolysis ionisation source to study organic matter in European rivers. Surfactants in rivers have also been analysed by MS/MS [2]. The surfactants were extracted using chromatography and FAB MS was

used to obtain information on the surfactants. FAB was also used by Rivera et al [3] to study not only surfactants but also dyes present in municipal waters. Although MS/MS proved capable of identifying organic material present in the water samples, between 100 ng and 500 ng was required for unambiguous which provides a relatively poor sensitivity. Consequently mass spectrometry did not see widespread application in water analysis until the advent of electrospray [4] which allows liquid phase chemists greater access to mass spectrometry although there are still restrictions in the use of mass spectrometry.

7.2 Electrospray

The complications of high vacuum restrictions, and the freezing of liquid under vacuum have led to the development of a technique known as electrospray ionisation mass spectrometry. This technique allows solutions to be studied by avoiding the introduction of a bulk liquid sample directly into high vacuum The problems of introducing liquids into vacuum initially restricted studies to exotic solutions such as saturated lithium chloride solution. However, considerable effort was made to circumvent the difficulties of injecting liquids into vacuum by injecting gas phase ions though a thin capillary. Studies by Dole [5] focused on the injection of macroions into a vacuum through the use of primitive electrospray. His initial experiments involved the injection of a dilute solution of polymer into a nitrogen bath gas until the solvent evaporation increased the charge density on the liquid surface, on reaching the Rayleigh limit where coulombic repulsion exceeded the surface tension

the droplets would subdivide. If this process continued to a sufficient limit each droplet would contain only one ion. In fact Dole found that it was possible to detect macroions but the detection current was low (10^{-13} A) and the failure of macroions to emit secondary electrons meant that it was not possible to have the gains of 10^5 or 10^6 that multipliers would give.

Dole's experimental work, despite its limitations, did provide encouraging findings, which were followed up by Yamashita and Fenn [4]. These two researchers investigated the effect of applying high voltages (2-10 kV) to a small capillary and injecting the solution into a bath gas. The resulting gaseous dispersion of ions is then injected through a small capillary into the high vacuum region of a mass spectrometer. This technique is known as electrospray and the basis of present day apparatus. Figure 7.1 is a schematic of the electrospray set up. The ions are generated by passing the liquid containing the analyte through a thin capillary to which a high potential is applied (2-10 kV). The ions are generated and leave as a spray of charged droplets. The ions are then ejected from the droplets through a coulomb explosion mechanism; these ions then pass into the high vacuum region of the mass spectrometer via a thin capillary.

Electrospray has become a commercialised technique with widespread application in both the biological and chemical fields. It is used extensively in biochemistry to allow mass spectra to be obtained for large molecules such as proteins and myoglobin [6,

7]. In chemistry it has found application in numerous areas such as organometallic and inorganic chemistry [8].

The electrospray technique although a significant advance in the analysis of ionic species, has some disadvantages. Firstly, not all ionic species can be detected using electrospray. Many ions do not enter the mass spectrometer itself because of the lengthy path from ionisation source to the entrance of the mass spectrometer, i.e. through a bath gas and then through a capillary into the mass spectrometer itself. In fact in the early stages of electrospray these problems, in particular the collisionally activated decomposition of solvated metal ions, prevented the detection of simple inorganic ions in water. These problems have been overcome to an extent by varying the carrier solvent for the analyte solution and it is possible to obtain bare divalent metal ions from methanol and aqueous solutions. However, it is not possible to detect trivalent metal ions using electrospray. Another disadvantage of this technique is the need to pre-process analyte solutions by adding suitable electrolytes which can lead to masking of analyte species.

The major complication with using electrospray mass spectrometry is the difficult pathway that exists between the ion generation electrode and entry to the mass spectrometer. This project has focussed on the possibility of improving the overall sensitivity of the electrospray technique by investigating the possibility of ion generation inside the mass spectrometer with the aim of increasing the sensitivity of the detection apparatus.

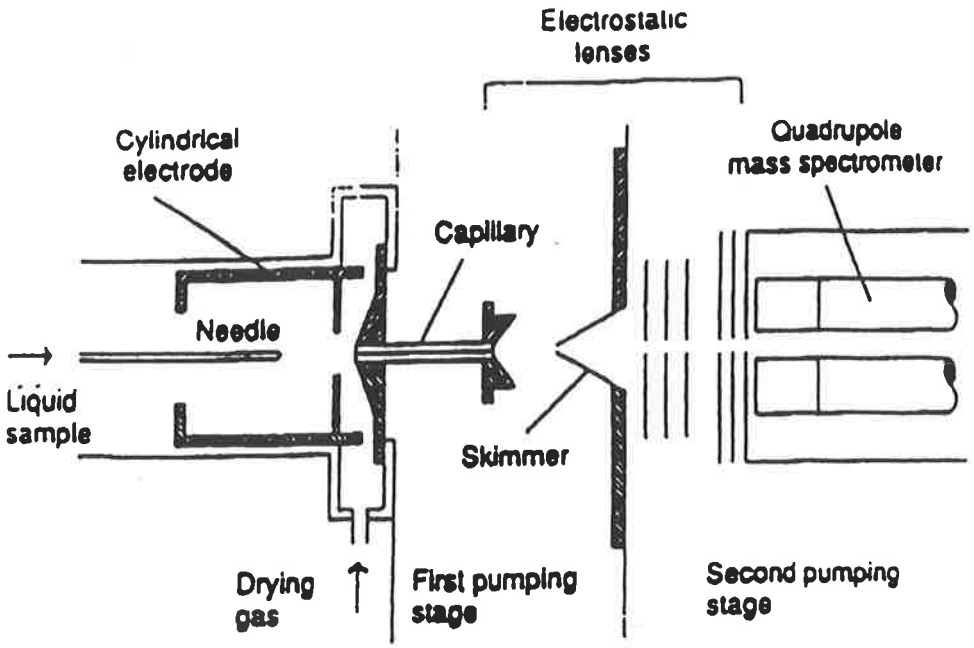

Figure 7.1 Electrospray Schematic [4]

7.3 Coulomb Explosion

An essential aspect of mass spectrometry is the formation of ions, which is critical to the development of the electrospray technique. As this technique involves liquids, the mechanism of ion generation is significantly different from the gas phase, and involves the ejection of ions from the liquid phase. The mechanism used to explain the ejection of ions from the solvent sphere into vacuum from the bulk liquid is known as a Coulombic Explosion. This concept is essential to an understanding of the ejection of ions from the surrounding solvent sphere into vacuum. As can be seen in figure 7.2, the steadily shrinking droplet diameter resulting from the evaporation of solvent molecules increases the electrostatic repulsion between like charges. This repulsion increases until the electrostatic repulsion exceeds the energy of solvation of

the ion, leading to the ejection of the ion into the surrounds. This is the mechanism for ion formation and ejection for analysis in electrospray and also the mechanism proposed by Kondow [9] for the appearance of various solvated species in his paper.

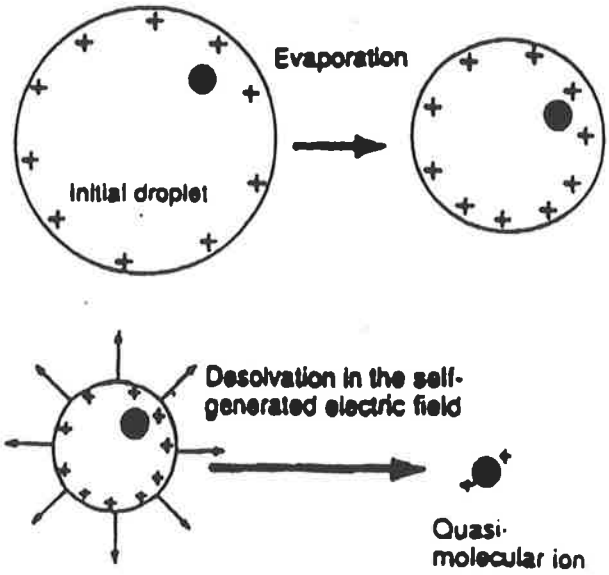

Figure 7.2 Coulomb Explosion Mechanism

7.4 Liquid Microjets

Recent work in Germany by Faubel[10] has led to the development of liquid microjets as a technique for introducing liquid into high vacuum. The technique involves the production of high velocity liquid jets (5-50 μm) by forcing liquid through electron microscope apertures in order to produce high velocity liquid jets. Investigations by Faubel on jet freezing phenomena confirms that the jet remains as a liquid for at least the first 3-5 millimetres as it enters into a vacuum. This technique is the first to successfully introduce pure solvent into vacuum and maintain a liquid

under high vacuum conditions. Previous attempts required the use of saturated solutions to reduce the vapour pressure of the liquid to enable high vacuum conditions to be maintained. The microjet technique developed by Faubel allows the liquid to remain in a liquid state under high vacuum for extended periods of 2-3 hours. The high vacuum conditions can be maintained due to the fact that the liquid jet diameter is small which reduces the amount of liquid in the vacuum chamber. In addition, there are extensive cold surfaces available to trap the vapour from the jet and maintain high vacuum properties. Furthermore, not only can the liquid surface be maintained but it is a "clean" surface [11], i.e. there is no vapour cloud which will reduce the collisionally activated decomposition of solvated metal ions evident in early electrospray techniques.

From a chemical perspective, and in particular from the practical view point of developing a machine capable of multi-speciate analysis, the work of Kondow and fellow researchers is of considerable importance [9]. Kondow and fellow researchers have investigated solvation effects of aniline ions in ethanol by ejecting solvated aniline ions through laser irradiation of liquid microjets. The studies of Kondow involved coupling an ion-generation and ejection technique with mass spectrometry.

7.5 Liquid Microjet Applications

The coupling of mass spectrometry with ion ejection from liquid microjets by Kondow indicates that it is possible to construct an apparatus that could identify liquid contents for both organic and inorganic ions simultaneously and simplify the equipment requirements to carry out such analysis. However, for field analysis a laser

is not a suitable ionisation source due to its fragility. A further problem with the use of a laser is the high unit cost, which would make the overall cost of a liquid micro-jet prohibitive, compared to existing systems for water analysis. It is these limitations in terms of an ionisation source, which have prompted the study of electrokinetic charging effects produced by liquid micro-jets. This study was undertaken in order to understand the charging effect and to examine its use as a potential ionisation source in a liquid micro-jet mass spectrometer.

The interest in this project in static electrification arises from the early work done on the electrokinetic charging of liquid microjets by Faubel [12]. The studies of jet electrification indicated that the extent of jet charging led to a charge concentration of 10^{-8} A at the surface. In particular, the work of Faubel indicated an irregular pH dependence (see Figure 6.3) which warranted further investigation in order to gain a better understanding of the mechanism and factors affecting micro-jet charging.

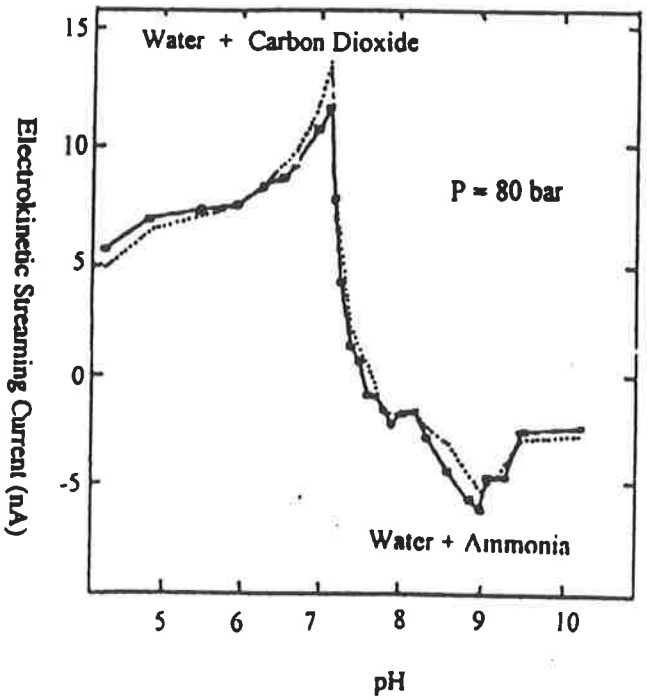

Figure 7.3 Streaming current as a function of pH, with a dependent charging of 10 μm PtIr nozzle and pressure of 80Bar. pH of high purity water is changed by the addition of small amounts of CO_2 or NH3 gas respectively (adapted from Faubel and Steiner)

References

1. Boon J.J, G.W., Van der Valk F, Dallinga J, Koernig S.A. *Abstracts of Papers*. in *189th National Meeting of the American Chemical Society*. 1985. Miami Beach FL.
2. Rivera J, Ventura F, Figueras A, Dessalces G,, Adv. Mass. Spectrom, 1986. **10**: p. 1453.
3. Rivera J, Ventura F, Figueras A, Fraisse D, Blondot V,. . in *35th Annual Conference on Mass Spectrometry and Allied Topics*. 1987. Denver CO.
4. Fenn J, Yamashita M., *Electrospray ion source.* J. Phys. Chem, 1984. **88**: p. 4451.
5. Dole M, Hines R.L, Mobley R.C, Ferguson L.D, Alice MB,, J. Chem. Phys, 1968. **49**: p. 2250.
6. Whitehouse C.M, Dreyer R.N, Yamashita M, Anal. Chem, 1985. **57**: p. 675
7. Smith R.D, Ogorzalek-Zoo R.R, Barinaga C, Anal. Chem, 1990. **62**: p. 882
8. Colton R, Traeger J.C, *Electrospray Mass Spectrometry Applied to Inorganic and Organometallic Chemistry.* Mass. Spectrom. Rev., 1996. **14**: p. 79.
9. Kondow T, Mafune .J., *Ion-Molecule Reaction between Ionised Photochemical Intermediates of Acetophenone and Alcohol Following Multiphoton Excitation in a Liquid Beam.* J.Am Chem.Soc, 1994. **116**: p. 9801-9803.
10. Faubel M, Steiner .S., Toennies J.P, *A molecular beam study of the evaporation of water from a liquid jet.* Z.Phys, 1988. **269**: p. 751.
11. Siegbahn H, *Electron Spectroscopy for Chemical Analysis of Liquids and Solutions.* J.Phys.Chem, 1984. **89**: p. 897.
12. Faubel M, Steiner .B., *Strong bipolar electrokinetic charging of thin liquid jets emerging from 10um Pt-Ir nozzles.* Ber. Bunsenges. Phys. Chem, 1992. **96**: p. 1167.

8. Construction

8.1 Theoretical Background

The pioneering work by Faubel on the physical characteristics of liquid micro-jets [1] introduced the concept of the liquid microjet as a technique for maintaining liquid surfaces under vacuum conditions. This breakthrough in terms of the introduction of liquid into a vacuum was made possible due to the use of microtechnology. Faubel combined electron microscope apertures with a high-pressure solvent delivery system to generate high velocity liquid microjets (10-50 um) in diameter.

The development of liquid microjets has permitted researchers to gain a better understanding of solvent-solute interactions by combining the technology with the highly sensitive technique of mass spectrometry. Both Faubel [2]and Kondow [3] have studied solvent-solute interactions using liquid microjet technology. Faubel extended his research not only to examine solute -solvent interactions, but also the physical characteristics of the liquid microjet. These studies were undertaken using mass spectrometry as the primary method of analysis. In the course of this work, Faubel discovered that relatively large streaming currents are generated as the liquid passes through the aperture [4].

Faubel's preliminary studies of streaming current behaviour are of particular interest because of the unusual pH dependent behaviour which prompted this investigation of the factors affecting the electrokinetic streaming current behaviour of liquid micro-jets. In order to undertake such an investigation it was necessary to construct a liquid micro-jet apparatus.

8.2 Design Objectives

- To design and construct an apparatus capable of generating liquid microjets
- To examine the factors affecting electrokinetic streaming currents

8.3 Design Parameters

The laboratory prototype was constructed using design criteria from both Faubel's research and preliminary experimental work in the laboratory. The key components identified in the construction of a liquid beam mass spectrometer were:

- A source for the generation of the microjet
- A condensation chamber for removal of vapour in vacuum

8.3.1 Source Design

The most critical component of the liquid microjet injection technique is the construction of the liquid jet source. The source provides a means of connecting the aperture to the solvent delivery system. The design parameters that needed to be satisfied in order to build a liquid jet source were:

- The design of a suitable aperture to generate a liquid micro-jet
- Simplicity of construction to enable access for cleaning and for removing the aperture.
- Source does not leak at the high operating pressures needed to generate a microjet
- Source needs to be constructed of material suitable for vacuum use
- Corrosion resistant construction material.

Suitable Aperture to generate liquid micro jet

To generate the microjet, it is necessary to use a suitable aperture that can be connected to a solvent delivery system. Both Faubel and Kondow used electron microscope apertures as these are available with drilled holes as small as 5um. Other possible methods for generating microjets are gas chromatography capillaries or specialised flat disk apertures of a much larger cross section than electron microscope apertures. These flat disk apertures were selected for use in the optimised prototype design.

Simplicity of construction

From the design viewpoint, it is essential that the source construction be rugged but simple enough to enable frequent servicing to be undertaken. The apertures are subjected to both high velocity and high pressure flows and become worn and must be removed and replaced. In addition, the source has to be removed periodically and disassembled for cleaning. The solution to this requirement was the use of compression fittings as the means of securing the aperture in the initial design, but later experiments indicated a more permanent method of attaching the aperture was essential.

- ***Source Design does not leak*** at ***high operating pressures***

One of the major problems with designing a source for the generation of a liquid microjet is the high-pressure drop required to push the solvent through the aperture and produce a micro-jet. This pressure, as large as 2000psi, placed strain on the fitting holding the aperture and resulted in compression fittings leaking under general operating conditions. It was therefore important to design fittings that could withstand high pressure without leaking.

• ***Source must be constructed of material suitable for vacuum use***

The source must be constructed of materials that allow it to operate under vacuum conditions without outgassing. Although much of the vapour in the chamber is due to solvent molecules evaporating from the liquid jet, the materials selected for the construction of the jet should be stable in the vacuum environment and not be oxidisable or outgas.

• ***Source must be constructed of corrosion resistant material***

The source must be constructed of corrosive resistant materials because salts are used extensively in electrokinetic measurement studies and the source is in contact with these corrosive liquids. The material of the aperture itself is also critical because it is continuously exposed to corrosive environments which, can corrode and distort the aperture hole.

8.3.2 Condensation Chamber

The condensation chamber is the component that reduces the operating pressure of the main vacuum chamber by cryogenically trapping the vapour from the liquid being injected into the vacuum. In the absence of this chamber, it would be impossible to operate even a roughing vacuum as the amount of vapour generated from evaporation of a liquid micro-jet is far greater than that of any traditional gas-phase experiment There are a number of design parameters which needed to be satisfied in designing the condensation chamber. These include:

- Maximising the available surface area for trapping vapour from the liquid microjet
- Ease of access for removal of trapped liquid vapour
- Corrosion resistant construction material for the chamber

• ***Surface Area Maximisation***

A key consideration in designing the condensation chamber is to maximise the surface area for trapping vapour from the liquid microjet and therefore providing the most efficient trapping system but with the minimum volume. This involved the evaluation of a number of possible configurations in order to obtain the most efficient design. The following factors needed to be considered in determining the design of the condensation chamber area: alignment of the jet, maximum volume of a trap due to size constriction; and the possibility of choking diffusion pumps.

• ***Ease of access for removal of trapped vapour***

A consideration in the design of the condensation chamber is that the surfaces that are available to trap the vapour in the chamber should be easily accessible, and no solid material should remain in the chamber upon removal of the trapping surfaces. These design criteria meant that evaluation of numerous designs was necessary in order to achieve one in which frozen vapour from the liquid microjet could be easily removed.

• ***Construction Material***

The possibility of the trapped vapour being corrosive meant that careful selection of the material used to construct the condensation chamber was essential. The external chamber was constructed of stainless steel. Stainless steel was selected despite of its poor thermal conductivity because of its corrosion resistance compared to metals such as copper

8.4 Construction of a Liquid Microjet Injection System

8.4.1 Liquid Microjet Source

A key component identified in the design stage of the project is the construction of a suitable source for the liquid microjet. In order to generate a liquid jet with a beam diameter of 5-50μm it is necessary to obtain a suitable aperture that could be coupled to a solvent delivery system. Both Faubel and Kondow used electron microscope apertures as these can be obtained with drilled holes as small as 5μm.

Initially electron microscope apertures were used. However, when using the latter, early electrokinetic streaming current studies undertaken indicated that the streaming current data was only reproducible for a short operating time. After only one or two hours of operation, the beam deviated in both the horizontal and vertical positions and the electrokinetic streaming current data became irreproducible. The deviation of the microjet indicates either debris obstructing the aperture hole or serious deformation of the hole in the aperture.

Further investigations revealed that at the typical microjet operating pressures i.e. between 50 and 250 psia, the aperture is subjected to considerable force. This force is a consequence of the driving pressure necessary to force the solvent through the aperture. At these operating pressures, the rim surrounding the holes in the electron microscope apertures was being distorted. This was a consequence of the combination of high operating pressure, and the fact that the channel depth in the electron microscope apertures is between 5 and 10 microns. This

thin layer of metal was easily distorted at the jet operating pressures and led to irreproducible electrokinetic streaming current data when electron microscope apertures were used.

The erosion of the electron microscope apertures forced a design change. In order to solve this problem, it was necessary to obtain apertures which had a larger channel depth and which were constructed of a harder material than platinum e.g. stainless steel. An American company, Lennox Laser produces specialised apertures in a variety of materials, and it was decided to use #304 stainless steel apertures with a 50μm channel depth because of the accuracy of the drilled holes in stainless steel (+-5% for hole diameter > 5μm) [5]. The corrosion and wear resistance of the stainless steel was also an important factor, as electrokinetic studies involved the use of strong electrolytes such as sodium chloride, and sodium hydroxide, which would accelerate the corrosion of aperture materials. Another advantage of the stainless steel apertures was that the channel depth of the aperture was 50 μm, 10 times the channel depth of electron microscope apertures.

The selection of the stainless steel apertures raised another design issue: the method of attaching the aperture to the solvent delivery system. Two methods of securing the aperture have been reported in the literature. The first method is that used by Faubel which uses a compression fit to secure the aperture on to a PTFE surface which allowing easy access to the aperture for both cleaning and removal. The second approach is that preferred by Kondow, who used a permanent technique-the aperture is soft soldered onto a stainless steel tube and insulated by a PEEK fitting.

3mm O.D platinum Aperture Channel Depth 7μm

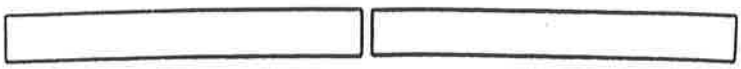

16.5mm O.D Stainless Steel Aperture Channel Depth 50μm

Figure 8.1 Cross Section of Electron Microscope and Laser Drilled Apertures

Both the designs reported in the literature have a number of intrinsic advantages and disadvantages. Faubel's compression fit design offered easy access to replace the aperture should it become blocked or worn, although it is difficult to maintain a water tight seal given the high operating pressures of the liquid microjet (50-250 psia). Conversely, the soldered attachment of the aperture to a surface means that although the seal is watertight, it is not possible to remove a worn aperture easily, and the difficulty of cleaning the microjet source should any material block the aperture also arises.

Initially, a soldered source was constructed. This design was chosen because a soldered source was far simpler to manufacture than a compression fit source as it only required the attachment of the aperture to a length of tubing and none of the machining required for a

compression fit design. However, this source design had a number of problems that eventually resulted in the rejection of this design. Firstly, the heating and cooling process for soft soldering (solder mp 220 °C) subjected the aperture to heat stress which had the potential to distort the aperture. It was also found that at the melting point of the solder, it was difficult to control the flow of melted solder which, flowed into the aperture hole and blocked the aperture permanently. A prototype source was constructed using 9/16 inch diameter tube and a Lennox Laser drilled disk. However, the hole in the aperture was found to be distorted and when this hole became blocked, the obstruction could not be removed. Consequently, the use of soft solder to attach an aperture to tubing was abandoned.

A redesign of the source was necessary to overcome the problems associated with the soldered liquid microjet source. An alternative approach to soldered source design was Faubel's compression fit design, which used a compression fitting to attach the aperture onto a surface and allowed the liquid to pass through the hole in the aperture.

In order to construct a successful design using a compression fit to attach the aperture to the pumping system, it was necessary to develop a compression fitting that would allow the aperture to be easily removed for cleaning and replacement and yet would not leak solvent at high pressure. A prototype using stainless steel compression fittings that compressed the aperture onto a PTFE support was constructed (see Figure 8.2). This design was initially successful, but it was found that after extended use, the PTFE surrounding the aperture compression fit became elongated and under high velocity and pressure flow conditions, small fragments of the Teflon around the edge support separated and blocked the aperture. In order to replace the aperture, when it became blocked or after cleaning, the PTFE surface had

to be re-machined because the PTFE had been compressed and would not retain a watertight seal unless remachined. This process was impractical as remachining resulted in a thin source that was incapable of supporting the aperture.

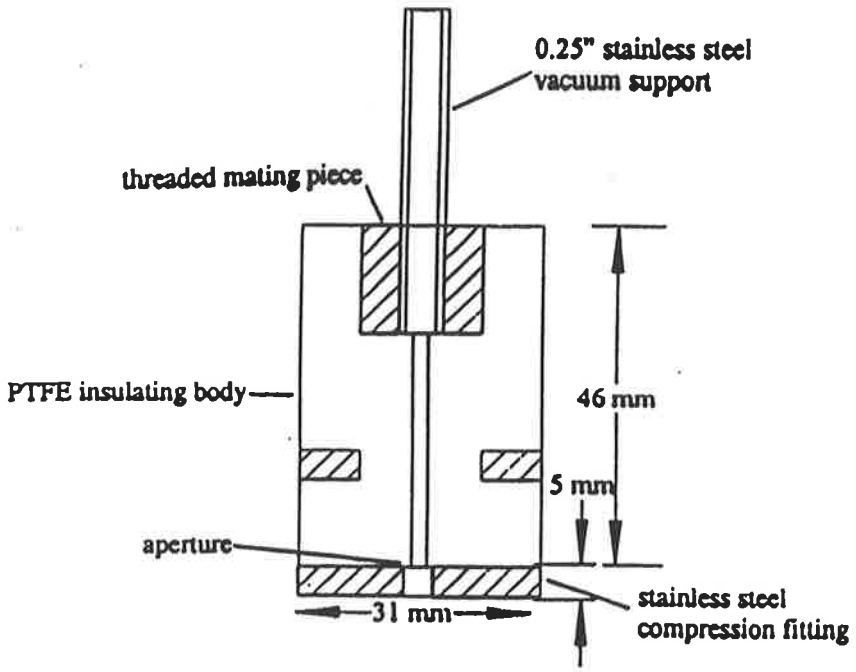

Figure 8.2 Early Source Design based on Compression Fitting

The problems associated with the two early liquid jet prototypes required a major rethink of the microjet source design and considerable effort was involved in the redesign of the source in an attempt to rectify existing problems. The design criteria for mounting the aperture was twofold- firstly the aperture had to be electrically insulated to permit electrokinetic studies, and secondly it had to be readily accessible for cleaning if it become blocked and worn. In order to achieve these design criteria, it was decided to avoid the difficulty of maintaining compression fittings which had been shown to be ineffective at high pressure. The numerous problems encountered with the soldered design, principally through heat distortion of the

aperture also led to the rejection of that design

An alternative method adopted for mounting the aperture involved the use of a bonding agent to attach the aperture directly to a metal support. Such a technique allowed the aperture to be removed chemically from the support rather than mechanically preventing mechanical damage to the aperture and, in particular, the distortion of the aperture through bending. The adhesive used had to be stable under vacuum i.e. not to outgas, and also to be electrically insulating. These requirements led to the selection of the silicate epoxy resin adhesive Torr Seal™. Torr Seal is an epoxy resin with low vapour pressure and is also chemically inert to the solutions that were to be studied as part of the electrokinetic studies. Torr-Seal's adhesive properties were found to be of sufficient strength to maintain a watertight seal between the aperture and the steel support. Torr-Seal could also be removed chemically through immersion in glacial acetic acid, which minimised the risk of mechanical damage when removing it from its support. In addition, being an electrical insulator, Torr-Seal fulfilled the requirement of electrically insulating aperture from the rest of the solvent delivery system. Another benefit of Torr-Seal was its ability to bond to both ceramic and stainless steel surfaces, allowing these materials to be evaluated as aperture supports.

The choice of support for mounting the aperture was important as it linked the aperture to the 1/16" stainless steel HPLC tubing that delivered solvent from the solvent reservoir via HPLC pump. A commercial Swagelok fitting was used to secure the support to the HPLC tubing. The support had to possess the mechanical strength to withstand Swagelok compression seals and also be chemically inert. Two types of support were investigated, a ceramic support and a 1/8", #316 stainless steel smooth bore HPLC tubing.

A ceramic support (alumina) was examined because it was both chemically inert and an electrical insulator. However, the brittle nature of the alumina surface caused problems during cleaning. This problem arose as the cleaning protocol involved the immersion of the support in an ultrasonic bath. When the alumina support was placed in this bath, small particles of alumina dislodged, blocking the aperture.

An alternative support, a 1/8" stainless steel tube, proved to be the most suitable, because it could be cleaned easily in an ultrasonic bath. The only concern with the use of stainless steel was the fact that salt solutions used in the electrokinetic studies could cause corrosion of the support. However, at the salt concentrations (10^{-8}M) used in this project there was no evidence of corrosion of the support when examined under microscope after use with salt solutions.

8.4.2 Construction of Condensation Chamber

The introduction of a liquid micro-jet into the vacuum chamber poses considerable problems from the viewpoint of maintaining high vacuum. If an untrapped liquid jet was operated under roughing vacuum alone, the minimum pressure sustainable in the chamber is 450 micron. In view of the fact that diffusion pumps can only be operated if the chamber pressure is less than 50 micron, an efficient trapping system had to be constructed to reduce the chamber pressure to below 50 micron in the presence of the micro-jet. The method used to

reduce the vacuum pressure in all previous experimental work has been to cryogenically pump the vapour.

Although cryogenic traps are routine in vacuum chambers, the difference with liquid microjets is the extent of the pumping required to maintain high vacuum. This difference in pumping requirements arises from the concept of a liquid jet which is effectively a long filament in the chamber, (up to 20 cm long), from which the liquid molecules are evaporating. Consequently, the amount of vapour being introduced into the chamber is much larger than any of the traditional gas phase experiments. To reduce the amount of vapour in the chamber, a customised trapping arrangement of a size not used in gas phase experiments had to be constructed. The design of this trapping arrangement depended on the alignments of the liquid jet, which could be either horizontal or vertical.

Initially, it was decided to introduce the liquid jet vertically and to trap the jet in a liquid nitrogen cooled copper cup positioned 15cm below the source. This design proved unsatisfactory because the liquid jet froze and there was a build up of ice around the source, damaging the aperture. Furthermore, size restrictions in mounting a cup in the throat of a diffusion pump meant that the surface area of the cup was too small to effectively trap the jet. Consequently, the minimum pressure obtained with this design was 120 micron, which was too high to permit the operation of a diffusion pump.

The failure of the cup as an effective trap indicated the need to dramatically increase the cold surface area in the chamber to trap the vapour and reduce the vacuum chamber pressure to the level at which diffusion pumps could operate. Size constraints in the vertical direction

limited the amount of available area for cryogenic pumping. This constraint prompted the realignment of the jet on a horizontal axis, which it would make it possible to arrange a series of cryogenic traps along the path of the liquid beam in order to increase the available surface area. The advantage of this design was to trap the liquid away from the main chamber, enabling the chamber pressure to be reduced to a level at which diffusion pumps could be used.

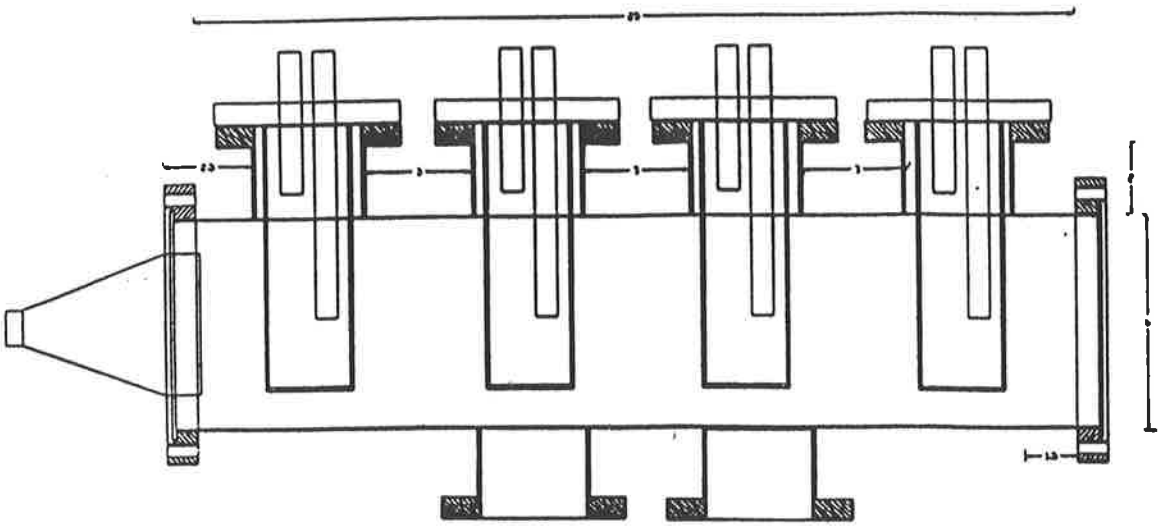

Figure 8.3 Cross Section of Condensation Chamber

The use of a horizontal injection axis simplified the removal of the trapped vapour as the cold traps (see Figure 8.3) unbolted easily to allow the condensed vapour to be removed. The cold surfaces used to trap the liquid jet in the horizontal direction are shown in Figure 7.3. These were manufactured from stainless steel and TIG welded. The two feeds into each trap enable it to be continuously refilled with liquid nitrogen allowing the nitrogen vapour to escape. In order to obtain the most effective trap, it was necessary to fill the traps 10 minutes before jet operation. When the liquid jet was operating, the traps had to be refilled with liquid nitrogen every 5-10 minutes, and under these conditions, the chamber was capable of trapping vapour and maintaining a vacuum of $5x10^{-4}$ microns for a period of one hour.

In addition to the three traps in series, the condensation chamber was designed to act as a differential pumping chamber, which would assist in the reduction of the main chamber

pressure. This was achieved by welding a conical reducer to the chamber providing a one-inch hole to the condensation chamber. This created a differential pumping situation between the main chamber and condensation chamber. Despite these measures, the pressure in the main chamber was 40-70 micron depending on the amount of liquid injected, which was too high for diffusion pumps to be operated. A further reduction in main chamber pressure could only be achieved by creating additional cold surfaces to trap the vapour. It was apparent that in the absence of any cold surfaces in the main chamber there was too much untrapped vapour, which prevented the operation of the diffusion pumps. The copper cup previously used in earlier trials with a vertical jet was reintroduced into the main chamber. The cup, when cooled to liquid nitrogen temperature, reduced the pressure in the main chamber to less than 10microtorr. At this pressure, it was possible to open all the diffusion pumps on the apparatus and reduce the main chamber pressure to 1.5×10^{-4} Torr when injecting a liquid microjet of a 20μm diameter with flow rates between 0.2 and 0.5ml/min.

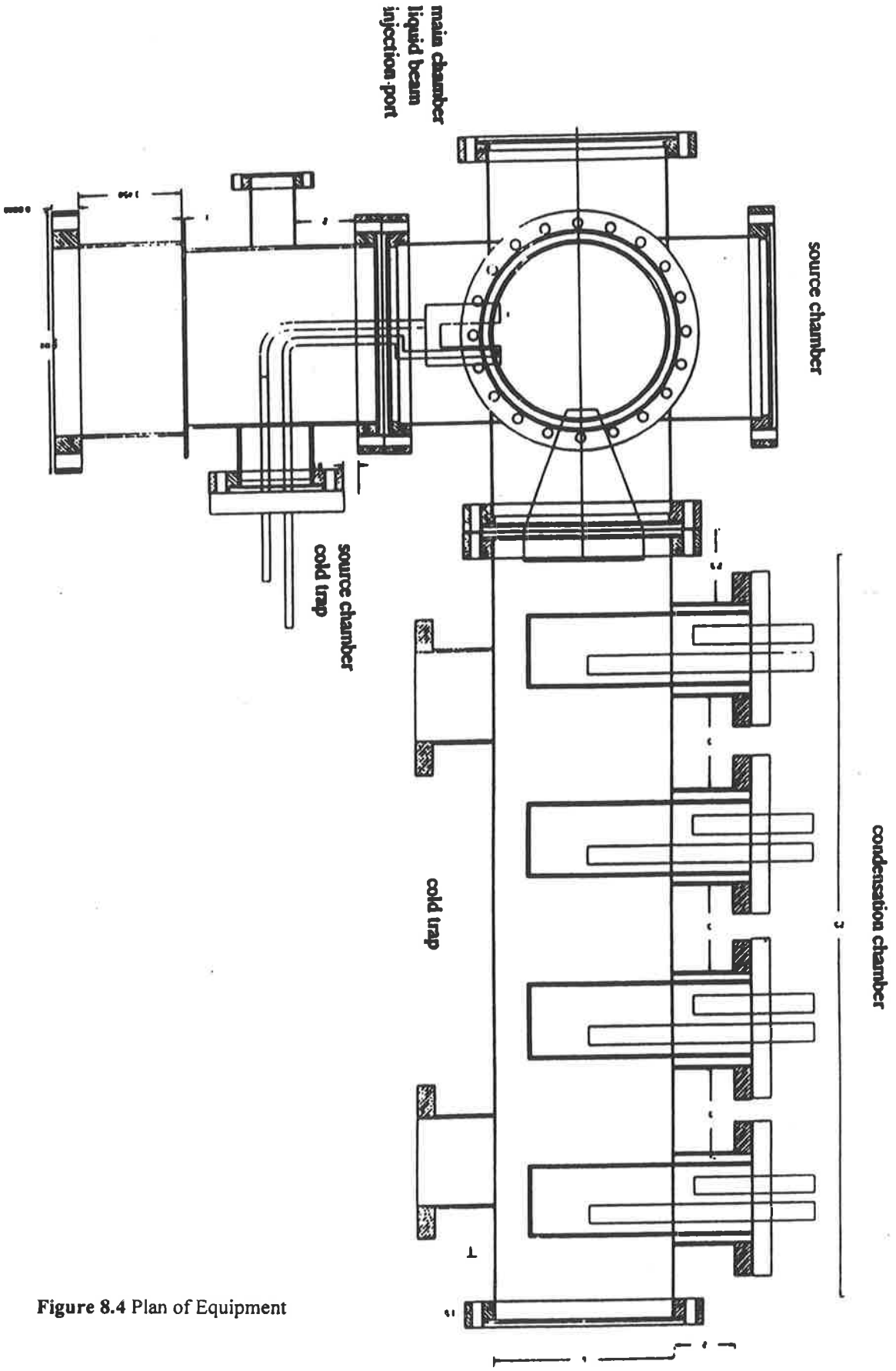

Figure 8.4 Plan of Equipment

8.4.3 Pumping Equipment

The injection of liquid microjets into vacuum introduces a very high vapour load into the chamber. In order to reduce this chamber pressure to high vacuum conditions there must be both effective trapping surfaces described in Section 8.3.1 for the removal of vapour, and also a roughing pump and diffusion pump arrangement with large pumping capacities. The roughing pumps used were a Welch 1375 to reduce the main chamber pressure to roughing vacuum and two Welch model 1401 pumps to produce a roughing vacuum in the condensation chamber. The larger model 1375 was used to pump out the main chamber because of its large pumping capacity where it was essential to reduce the chamber pressure as much as possible. The role of the condensation chamber is to trap the vapour and prevent trapped vapour from re entering the main chamber. Therefore, the pumping capacity of this chamber need not be as large as that of the main chamber. The diffusion pump arrangements used were Edwards Diffstak 7 to pump the main chamber and two smaller Edwards E03 diffusion pumps to pump out the condensation chamber. The reasons for using a large pump in the main chamber and two smaller ones for the condensation chamber were the same as for the roughing pump combination, i.e. it is critical to reduce the main chamber pressure as much as possible, but maintain the condensation chamber at a sufficiently low pressure to retain the trapped vapour.

Table 8.1 Diffusion Pumps Technical Specifications

Pump Type/Model	**Pump Capacity(lpm)**	**Ultimate Vacuum(Torr)**
Welch 1375	1000	$1x10^{-4}$
Welch 1401	160	$1x10^{-3}$

Table 8.2 Diffusion Pumps Technical Specifications

Pump Type/Model	**Pump Capacity(ls^{-1})** **1 Air 2 H2**	**Ultimate Vacuum(Torr)**
Edwards Diffstak 8	1700, 3000	$2x10^{-8}$
Edwards E03	250, 290	$5x10^{-8}$

8.5 Solution Preparation

In order to undertake electrokinetic studies, three solvents were examined- water, methanol and hexane. A number of salts and organic bases were added to these solvents in order to gain a more comprehensive understanding of the factors influencing the charging behaviour of the liquid microjets. Of the solvents examined, water and methanol are polar solvents. The electrokinetic charging effects of water were studied because of its widespread use as a solvent. The water used was ultra pure water obtained from a Milli-Q plant. Methanol was studied because it has a lower polarity than water and was the simplest polar organic solvent that is a liquid at room temperature. The methanol used was redistilled from bulk grade methanol and stored in bottles.

An important aspect of the electrokinetic charging effects in polar and non-polar liquids was the investigation of the effects of strong and weak electrolytes additives such as dissolved salts and organic compounds in the pure solvents. The salts studied as part of the strong electrolyte system were alkali metal chlorides- (caesium chloride and sodium chloride) and sodium hydroxide. These salts allowed a comparison of the effects of changing the cation and anion hydrodynamic diameter on the electrokinetic charging mechanism.

The effect of pH on the electrokinetic charging behaviour of the microjets was examined. Faubel has shown that pH affected the magnitude and polarity of the streaming current in polar solvents. Initially, it was thought that to acidify the solvents, the addition of carbon dioxide gas would decrease the pH, and ammonia gas would increase the pH. However, these solutions outgassed as they were being drawn into the HPLC pump. An alternative method that would permit both the study effect of the addition of strong and weak

electrolytes, and pH changes, and avoid the problem of outgassing and the consequent change of pH, was to add acids and bases which could not be removed by the filtration system of the HPLC pump. Acetic acid was selected as a weak electrolyte acid. Tri-ethyl amine was chosen as a weak electrolyte base. Hexane, a non-polar solvent, was studied to provide a comparison of the electrokinetic charging mechanism in polar and non-polar solvents. Hexane was selected as the non-polar solvent because it is the simplest non-branched alkane that is a liquid at room temperature.

8.6 Solvent Delivery

A key component of liquid jet generation is a reliable solvent delivery system that is capable of delivering the solvent at an accurate flow rate at the high pressures required to generate a liquid micro-jet. Due to the small hole diameter ($d<50$ μm), the pressure required to drive the liquid through the hole is between 50-250 psia, and is dependent on the flow rate through the hole and the viscosity of the solvent. In order to pump solvent at high pressures, a number of pressurising systems can be used. Faubel used a helium pressurised system to drive the solvent.

An alternative method of solvent delivery is the use of an HPLC pump that can deliver a very accurate flow rate at the pressures required to generate a liquid jet. This solvent delivery system has a number of advantages over a pressurised gas propulsion system. In the present experimental configuration, a programmable Waters 590 HPLC pump was used. This pump generates a liquid flow rate that can be controlled in microliter/minute flow rate intervals from 0.001 ml/min to 20 ml/min. The pump has programmable functions, allowing pressure

limits to be set that protect the aperture from pressure surges, which may occur if the aperture becomes blocked. The pump is able to operate at constant pressure providing a constant flow rate function. A further advantage of this model is the double piston-pumping configuration that enables the production of a very smooth solvent flow profile. The pump outflow also passes through flow dampeners to further reduce any flow perturbations. This condition was found to be extremely important in electrokinetic current studies. Early electrokinetic studies used a model 580 (a single piston pump with flow dampener highlighted the importance of uniform flow rates). However, it was found that the variation of electrokinetic current from its mean value was as large as 15% in a single pump system, whereas with the double piston pump incorporating flow dampening, the variation is less than 5%.

The solvent which is used in the microjet is prefiltered from the solvent reservoir using an aqueous In-line Filter Device (Whatman Aqueous IFD™) [6] containing a 0.2 μm nylon membrane in a sealed polypropylene housing. This filter not only protected the aperture and pump from particles that could damage them, but also degassed the solvent, using the bubble point principle. This last function is important because it allows the role of dissolved gases in solution to be discounted when examining electrokinetic charging effects. A bubble point is the pressure at which gases will pass through the wet membrane. If pressure is maintained below the bubble point, the gas will not pass through the membrane, and all the gas in the solvent will be trapped by the IFD.

All solvent passes through 304 stainless steel tubing and on the outlet from the pump, a stainless steel in-line filter (0.2 μm) filters the pump out-flow. The wetted parts in this system

are made from 304 stainless steel with the exception of the sapphire pump plunger heads. By using these materials, corrosion is reduced to a minimum. This was important because corroded ferric materials could block the aperture as has been found to be the case when mild steel is used as tubing.

8.7 Measuring Equipment

The detection of the small currents generated through electrokinetic effects requires a number of special experimental conditions to be satisfied. The sensitivity of the picoammeter is such that human movement and general RF noise can create small changes in current that interfere with the measurement of the electrokinetic currents generated by the microjet. This means that it is not possible to undertake benchtop experiments without extensive shielding around both the microjet and the picoammeters. In order to shield the microjet from external interference, a Faraday cage must be constructed to shield the apparatus. The simplest method is to use the metal vacuum chamber as the Faraday cage. The shielding of the microjet source by placing the source in the vacuum chamber was found to be sufficient to prevent interference from external sources.

Once the interference effects of external sources had been removed, it was necessary to determine the optimal technique for measuring the current generated at the aperture. The small magnitude of the current, (10^{-8} A), required extensive shielding for the electrical connection between the aperture to the picoammeter to prevent interference effects. A stainless steel wire was physically attached to the aperture surface to provide an electrical

connection. This wire was then connected to a vacuum electrical feedthrough that was connected directly to the picoammeter through a shielded cable.

An additional requirement in the experimental set-up for the measurement of electrokinetic streaming currents was the detection of the current. As the jet disintegrated the electrokinetic current was measured at a copper plate which was placed in the entrance to the condensation chamber. The currents at both the aperture and the copper plate were measured by two Keithley Model 410 picoammeters connected to the electrical feed-throughs. The voltage output from these picoammeters was then passed through a LaB PC+ board) an analogue to digital conversion device and recorded by computer).

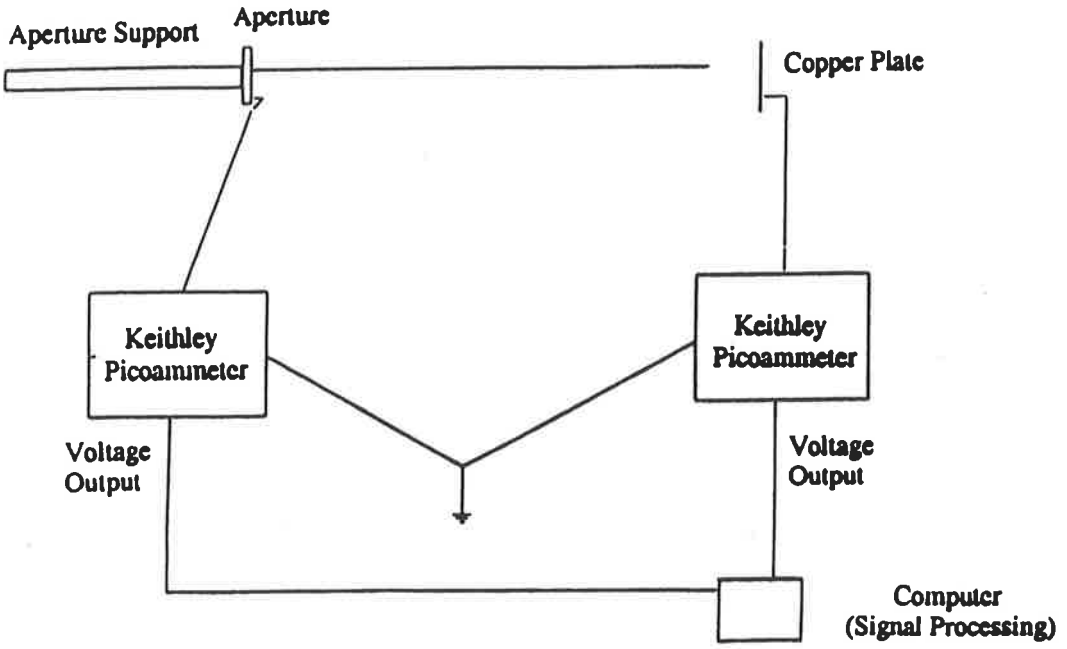

Figure 8.5 A simplified diagram showing the electrical connections for electrokinetic current measurements

8.8 Experimental Protocol

The flow rate used for the liquid jet is governed by the size of the aperture. Typical flow rates are between 0.2 and 0.8 ml/min. The liquid jet was generated on the bench prior to running it under vacuum, to verify that the jet was functioning correctly. As the jet was being prepared, the vacuum chamber was filled with continuously flowing nitrogen gas to prevent any moisture from entering the chamber. When a positive flow of nitrogen was established, the stainless steel traps were filled with liquid nitrogen until they reached cryogenic temperatures.

When the traps had cooled to liquid nitrogen temperature, the source, which was mounted on a vacuum feed-through flange, was introduced into the vacuum chamber at atmospheric pressure. The liquid micro-jet was operational as the source was being introduced into the chamber at atmospheric pressure. The nitrogen gas was then turned off and the valve separating the vacuum chamber from the roughing pumps opened, and the chamber pumped down to 30-40 micron. When this chamber pressure was reached, the copper cup was cooled with liquid nitrogen and the chamber pressure reduced to l0 micron. On completion of this pump down procedure, the butterfly valves separating the chamber from the diffusion pumps were opened, allowing the chamber to be evacuated.

It was found that it is necessary to start the liquid jet before pumping down the chamber because any liquid present on the aperture surface before the operational jet was exposed to vacuum would freeze and form a plug in the aperture. Under these circumstances there was a risk of damage to both the aperture and pump because the pump will create extremely high backpressures. In order to prevent blockages, due to frozen solvent, the jet had to be operating before the chamber is pumped down.

8.9 Recording Results

All data processing from the electrokinetic streaming current studies was undertaken using a PC as a data collection station. The Microsoft Windows© based Labview© visual graphics program allowed a PC to be configured to accept voltage output from the picoammeters. The program converts the analogue voltage output to a digital format that was stored in a data file prior to processing.

References

1. Faubel M, Schmidt .S., Toennies J.P, *A molecular beam study of the evaporation of water from a liquid jet.* Z.Phys, 1988. **269**: p. 751.
2. Faubel M, Kirsters.T., *Non Equilibrium Molecular Evaporation of Carboxylic Acid Diamers.* Nature, 1989. **339**: p. 527.
3. Kondow T, Mafune.J., *Ion-Molecule Reaction between Ionised Photochemical Intermediates of Acetophenone and Alcohol Following Multiphoton Excitation in a Liquid Beam.* J.Am Chem.Soc, 1994. **116**: p. 9801.
4. Faubel M, Steiner.B., *Strong bipolar electrokinetic charging of thin liquid jets emerging from 10um Pt-Ir nozzles.* Ber. Bunsenges. Phys. Chem, 1992. **96**: p. 1167.
5. Laser, Lennox., *Material Data Sheet*, 1996
6 Whatman, *IFD Data Sheet*, 1995.

9 Micro-jet Charging Behavior

9.1 Experimental Background

9.1.1 Generation of charge in Fluid

Numerous researchers have undertaken investigations into various aspects of electrokinetic charging of fluids [1-3]. These studies have concentrated on the charging behavior of non-polar solvents, and have established a number of factors that affect the electrokinetic charging of non-polar fluids. Conduit material, type of non-polar solvent, solvent viscosity, flow regime, and the role of additives, are all factors that have been identified when investigating electrokinetic charging of non-polar fluids. Preliminary studies by Faubel [4]have indicated that electrokinetic currents were also generated by liquid micro-jets. Faubel's studies also established that the pH of the microjet affected the polarity and magnitude of the current. In this investigation, the effects of a range of chemical impurities on the generation of electrokinetic streaming current has been studied to gain a better understanding of the pH dependent micro-jet charging behavior as reported by Faubel.

9.1.2 Electrostatic Charging of Fluids- Simple Model

The movement of fluid though a conduit generates an electric current. The charge generation responsible for this current occurs in a small layer of fluid at the conduit wall in which a Helmholtz layer is developed. The electrokinetic streaming current arises from the preferential diffusion of ions in the Helmholtz layer to the wall. The

ion mobility and charge determine the sign and magnitude of the current. At the conduit wall, the charge generation is diffusion controlled with a minimal convective contribution. The diffusion controlled nature of the electrokinetic charge generated at the wall implies that any chemical impurities added to the solvent could affect charge generation in the Helmholtz layer. The majority of the studies into electrokinetic charging have concentrated on non-polar fluids and remain relevant because the charge generation mechanism is identical in both non-polar and polar fluids. This is due to the presence of polar solvents in non-polar liquids. However, in non-polar solvents, the concentration of polar species (present as impurities) is significantly lower. Consequently, the electrokinetic current produced by non-polar solvents will be less than that of polar solvents.

9.2 Physical Factors Affecting Electrokinetic Current Generation

Before any study of the chemical factors affecting electrokinetic charging of liquid microjets could be undertaken it was necessary to determine the physical operating parameters of the liquid microjets. These parameters included the volumetric flow rate, linear velocity and operating pressure of the vacuum chamber. The volumetric flow rate is determined by the aperture size. The latter also determines the linear velocity of the liquid microjet. A series of experiments were conducted to determine the effect of the aperture size on the volumetric flow rate and the effect volumetric flow rate had on the chamber operating pressure.

9.2.1 The Effect of Aperture Size on Flow Rate

The small diameter of a liquid jet has important implications for jet operation. Flow rates required to generate the liquid jet must be sufficiently low for the jet to operate under vacuum but not so low as to introduce too much vapour into the vacuum chamber. Consequently, the jet diameter and flow rate are important factors in restricting the amount of liquid injected into the vacuum and to maintain high vacuum conditions. The effect of varying both the flow rate and jet diameter on the chamber operating pressure had to be determined experimentally.

To determine the flow rate at which the microjets could be operated, methanol was pumped through various sized apertures (5-50 μm). The minimum flow rate necessary to generate a liquid jet and the maximum possible flow rate for each aperture was established. The minimum flow rate is the rate at which the liquid microjet is stable. Lower flow rates will cause fluid to appear on the aperture surface but fail to generate a liquid microjet. The maximum flow rate is determined by the backpressure on the HPLC pump. The backpressure was limited to less than 500 psi. The key consideration in selecting the aperture diameter was the rate of solvent delivery needed to sustain a liquid micro-jet. As the solvent is introduced into a vacuum chamber, the pressure of the chamber increases. Therefore, in order to minimise the increase in chamber pressure associated with the introduction of a liquid micro-jet, there must be a reduction in the amount of solvent used. Kondow and Faubel have successfully used 10 μm apertures to produce liquid microjets[5, 6]. A summary of the results of these experiments is shown in Table 9.1.

Table 9.1 The Effect of Aperture Size on Flow Rate [1]

Aperture Size (microns)	Flow Rate (ml/min)
5	< 0.1
10	0.1-0.3
20	0.3-1.1
40	0.9-1.8

[1]Backpressure <500psi

The results in Table 9.1 indicate that the optimal jet size necessary to inject liquid into high vacuum is a 5μm diameter liquid jet. However, 5μm and 10μm apertures were unsatisfactory because they blocked easily. A 40 μm aperture does not have the problem of blockage, but the high volumetric flow rate required to generate a liquid micro-jet with this size aperture prevents vacuum from being obtained. Given the data in Table 9.1 it was decided to select a 20 μm aperture, as it was unlikely to become blocked, and it also had the advantage of operating at a low volumetric flow rate.

9.2.2 The Effect of Flow Rate on Chamber Operating Pressure

The size of the aperture used to generate the liquid micro-jet determined the flow rate of solvent into the vacuum. The operating pressure of the vacuum chamber is a function of the amount of solvent injected by the micro-jet. At solvent flow rates

above 0.5 ml/min the chamber pressure was above 50 microtorr, and this prevented the use of diffusion pumps. However, the use of the smaller apertures of 5-20 micron, permitted smaller solvent flow rates to be obtained and high vacuum conditions maintained.

A series of experiments were undertaken to determine the flow rate required for the optimum chamber pressure. Two aperture sizes were investigated using the minimum flow rate for a methanol microjet. The apertures were used to monitor the effect of solvent flow rate on the chamber pressure. During each experiment the solvent flow rate was changed and the pressure of the chamber measured. The results in Table 9.2 indicate that the pressure in the main chamber was a function of the solvent flow rate when diffusion pumps were used.

Table 9.2 Operating Pressure Characteristics

Flow Rate (ml/min)	**Aperture Size (microns)**	**Pressure (Torr)**
0.35	10	3.2×10^{-4}
0.5	10	6×10^{-4}
0.35	20	8×10^{-4}
0.5	20	1×10^{-3}

The above figures established that the use of a smaller jet diameter with the same flow rate as a larger jet diameter results in a lower chamber pressure. It was also found that for the main chamber pressure to be less than 50 microtorr and diffusion pumps used, the liquid jet diameter could not be larger than 20 μm. A 10 μm diameter jet would provide the optimum operating pressure. Table 9.2 does not include data for the 40μm aperture because it was not possible to operate this size microjet in conjunction with the diffusion pumps.

The smaller diameter micro-jet has the advantage of both minimising the chamber pressure by allowing the use of low solvent flow rates, and also preventing the jet from freezing under vacuum conditions. Although the jet cooled extremely rapidly and sections of the jet froze; the high velocity of the jet prevented it from freezing completely. For the most effective operation, it was established that the jet velocity must be between 20 and 40 ms^{-1} as microjet velocities below 20 ms^{-1} caused the jet to freeze.

9.3 Flow Characteristics

All models of electrokinetic current indicate that the flow regime, irrespective of whether it is laminar or turbulent, is an important characteristic in determining the relationship between linear flow velocity and the magnitude of the streaming current generated. Gibbings [7] presents a mathematical model that predicts a direct relationship between linear flow velocity and magnitude of electrokinetic current in a laminar flow regime. In a turbulent flow regime, the empirical models of Schon [8] and Gibson [9] predict a velocity dependent exponent value of 2.4 and 1.8 - 2.0

respectively. Klinkenburg [10] also proved mathematically that the velocity dependent exponent is 1.85 for a turbulent flow regime.

A Reynolds number calculation was used to determine the flow characteristics inside the aperture conduit. (The Reynolds number (N_{RE}) is a dimensionless number which provides an indication of the flow regime of a fluid in a conduit). A Reynolds Number less than 2400 indicates a fully developed laminar flow regime

$$N_{RE} = \frac{DVp}{u}$$

where D = Jet diameter (m) = 2×10^{-5}

V = Flow Velocity (ms^{-1}) = Q/A which for a 0.4ml/min flow rate through a 20*u*m hole is $22ms^{-1}$

p = Fluid density (water) (Kgm^{-3}) = 1000

u = absolute viscosity (Poise) = 0.001

yields $N_{RE} = \frac{2 \times 10^{-5} \times 22 \times 1\,000}{0.001}$

$N_{RE} = 440$

The low Reynolds number indicates that the flow regime in the liquid microjet is laminar. The laminar flow regime is in agreement with the electrokinetic current data obtained for non-polar and polar solvent microjets. Figure 9.1 shows the linear relationship between electrokinetic current and linear flow velocity of the microjet. This linear relationship confirms the result of the Reynolds number calculation i.e. the flow regime is laminar.

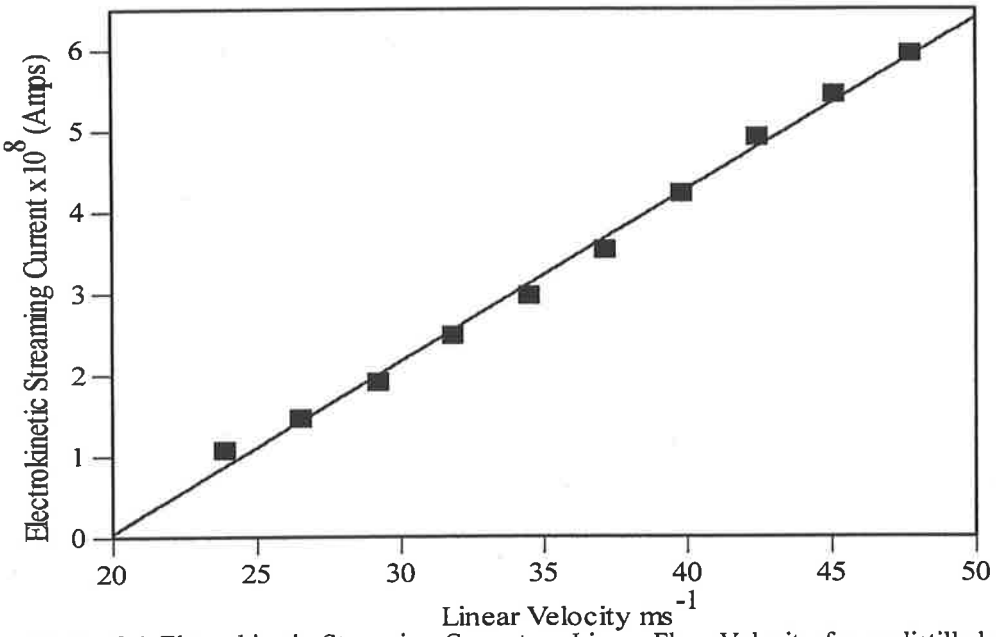

Figure 9.1 Electrokinetic Streaming Current vs Linear Flow Velocity for re-distilled methanol (K= 0.86 μScm^{-1})

9.4 Electrokinetic Measurements

In order to provide a reference for the electrokinetic charging current studies, the electrokinetic current was measured for three pure solvents, methanol, hexane and water (Figures 9.1-9.3). These measurements provide a background measure and also a comparison between the electrokinetic charging behavior of polar fluids and non-polar fluids.

The largest magnitude electrokinetic current was generated by methanol ($5.9x10^{-8}$ A). The magnitude of the electrokinetic current was double that of water. However, the linear relationship between flow velocity and current magnitude was found to be similar for both water and methanol.

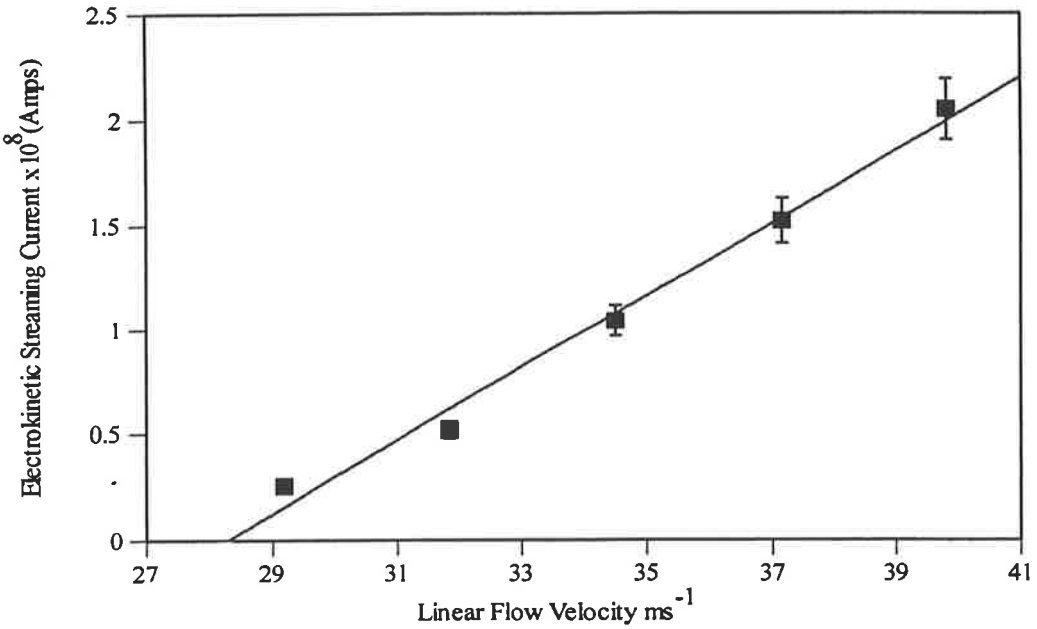

Figure 9.2 Electrokinetic Streaming Current vs Linear Flow Velocity for ultra-pure water (K= 2.19 μScm^{-1})

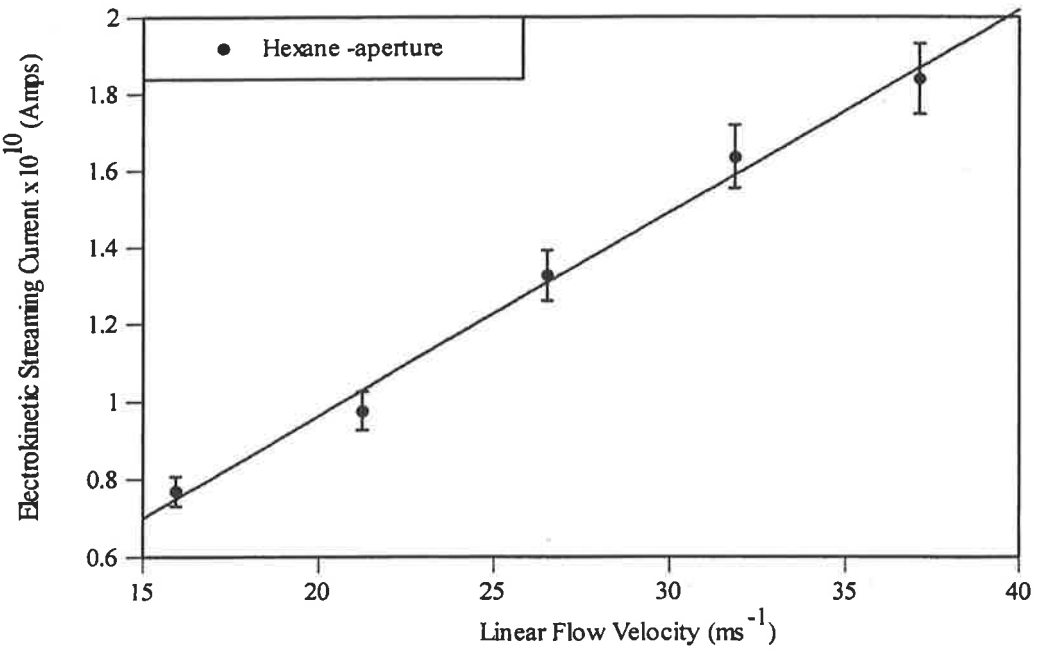

Figure 9.3 Electrokinetic Streaming Current vs Linear Flow Velocity for re-distilled hexane

Figure 9.3 shows the electrokinetic current as a function of linear flow velocity for the non-polar solvent, hexane. In the non-polar micro-jet, the magnitude of the current has decreased by two orders of magnitude compared with that in the polar solvent liquid micro-jets. The decrease in current in the non-polar solvent is due to the reduction in concentration of polar solvent present in the microjet. The current generated by the non-polar solvent is due to the presence of polar solvent impurities such as water or methanol. The charging mechanism in the non-polar solvent is no different from that found in water or methanol. This can be explained by the fact that trace amounts of these polar solvents are responsible for the generation of the electrokinetic current. It should be noted that in ultra pure non-polar solvents, i.e. in the absence of polar impurities there would be no electrokinetic charging

9.5 Conductivity Studies

The objective of this study of the charging behavior of liquid micro-jets was to identify the major factors affecting current generation. In studies of non-polar fluids, solvent viscosity, solution conductivity and dielectric constant have been identified as important [3]. In this investigation the amount of additive added to pure solvent is insufficient to modify the viscosity or dielectric constant of the solvent. Consequently, the objective of this study was to identify the importance of conductivity in the modifying the charging behavior of liquid micro-jets. This bulk fluid property was used as a comparative reference in electrokinetic current studies because the solution conductivity allows comparison of fluids with different chemical properties. The chemical effect of various types of ions on electrokinetic current

generation was also of interest in order to establish whether the type of ion could affect the current polarity or magnitude. Such an effect was anticipated because ions of different hydrodynamic diameter could affect the diffusion controlled electrokinetic current generation. Researchers[1, 11] have reported that the addition of polar solvents to non-polar solvents influenced the polarity of the streaming current and this change was due to the type of polar solvent added to solution. This suggested that the addition of ions to polar solvents might affect the current magnitude and polarity.

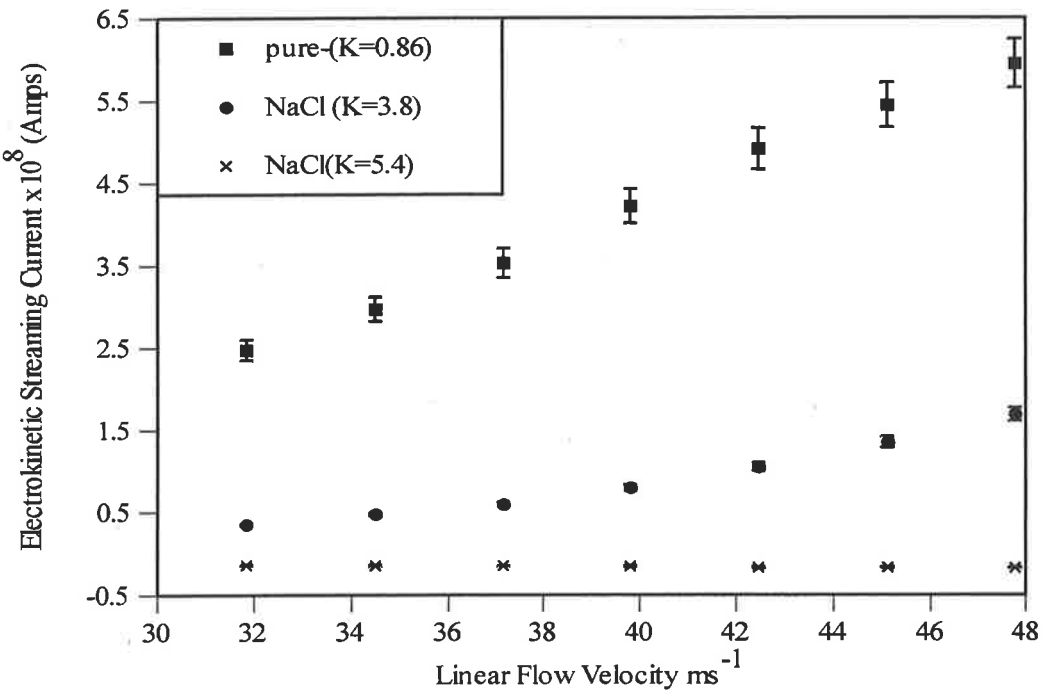

Figure 9.4 Electrokinetic Streaming Current vs Linear Flow Velocity for re-distilled methanol (K= 0.86 μScm^{-1}) and methanol containing NaCl (K= 3.8μScm^{-1} and 5.4μScm^{-1})

In order to investigate the role of such additives to pure solvent, a preliminary study of the chemical effects on micro-jet charging was undertaken by adding sodium chloride to methanol. Two different sodium chloride solution conductivities were examined (K =3.8 uScm^{-1}, 5.4 uScm^{-1}). The results are shown in Figure 9.4. The electrokinetic data indicated that the magnitude of the electrokinetic current fell to 28% of that of pure methanol when the solution conductivity increased from 0.86 μScm^{-1} to 3.8 μScm^{-1}. Similarly, the electrokinetic current magnitude fell to 2% of that of the pure methanol solution when the methanol conductivity was increased to 5.4 μScm^{-1}.

These results are contradictory to a diffusion model for current generation because an increase in ions present in solution should lead to a greater number of ions diffusing to the conduit wall and an increase in the electrokinetic current. The results for sodium chloride solution are also contradictory to the data obtained by researchers for non-polar solvents [2, 3, 12]. Their results indicated that current magnitude increased with conductivity to a maximum, and then decreases slightly for non-polar solvents, independent of the additive. The differences in conductivity dependence between aqueous and non-aqueous solutions indicated that further investigation of the effect of conductivity on the electrokinetic charging behavior of aqueous solutions was warranted. It should be noted that the conductivity ranges studied for polar solvents

(0.85-5.8 μScm^{-1}) are significantly higher than that of non-polar solvents (0.01-0.001 μScm^{-1})

It was important to determine the effect of ions on the generation of electrokinetic current. If the current is diffusion controlled with a positive polarity, the addition of ions of a small hydrodynamic diameter and high ionic mobility should enhance the generation of current if they are cationic and decrease the current if they are anionic. In order to test this hypothesis, a number of ions were selected for addition to water and methanol, based on their charge and ionic hydrodynamic diameter The cations chosen were sodium and cesium, while the anions selected were chloride, hydroxide and tri-ethyl amine.

In order to establish whether the decrease in electrokinetic current when sodium chloride was added to methanol (see Figure 9.4) was an ionic effect or pH related phenomenon as postulated in the literature, sodium hydroxide and tri-ethyl amine were added to both methanol and water solutions. This allowed a comparison between the effect of adding an ionic or non-electrolyte base to the solution. The data is presented in Figure 9.5 and indicates that in both water and methanol the magnitude of the electrokinetic current fell significantly to 61 % and 82 % in methanol and water respectively. It was evident that the nature of the base had a minimal effect on charging behavior.

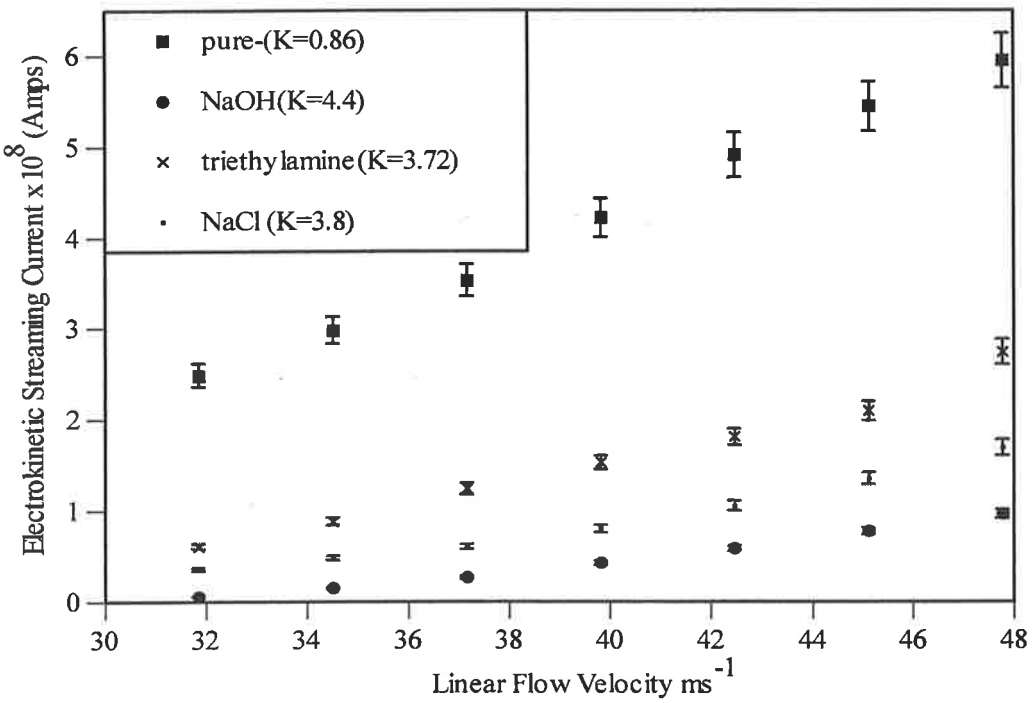

Figure 9.5 Electrokinetic Streaming Current vs Linear Flow Velocity for re-distilled methanol (K = 0.86 μScm^{-1}) and methanol containing NaCl (K = 3.8μScm^{-1}), NaOH (K =5.4μScm^{-1}) and tri-ethyl amine (K = 3.72μScm^{-1})

To establish that the decrease in electrokinetic current was a conductivity related phenomenon, salt solutions with different cation hydrodiameters were prepared. The anions were kept the same in order to eliminate anionic effect. Cesium chloride and sodium chloride were added due to their different ionic mobility. However, in both solutions there was a significant drop in electrokinetic current (30% for cesium chloride and 72% for sodium chloride) as shown in Figure 7.6. This result is contrary to an argument based on the chemical effect of ions because both cations reduced the electrokinetic streaming current. This was not the anticipated result given that the positive streaming current should be enhanced by the presence of more cations in

solution if the generation of streaming current is dependent on the chemical species present in solution.

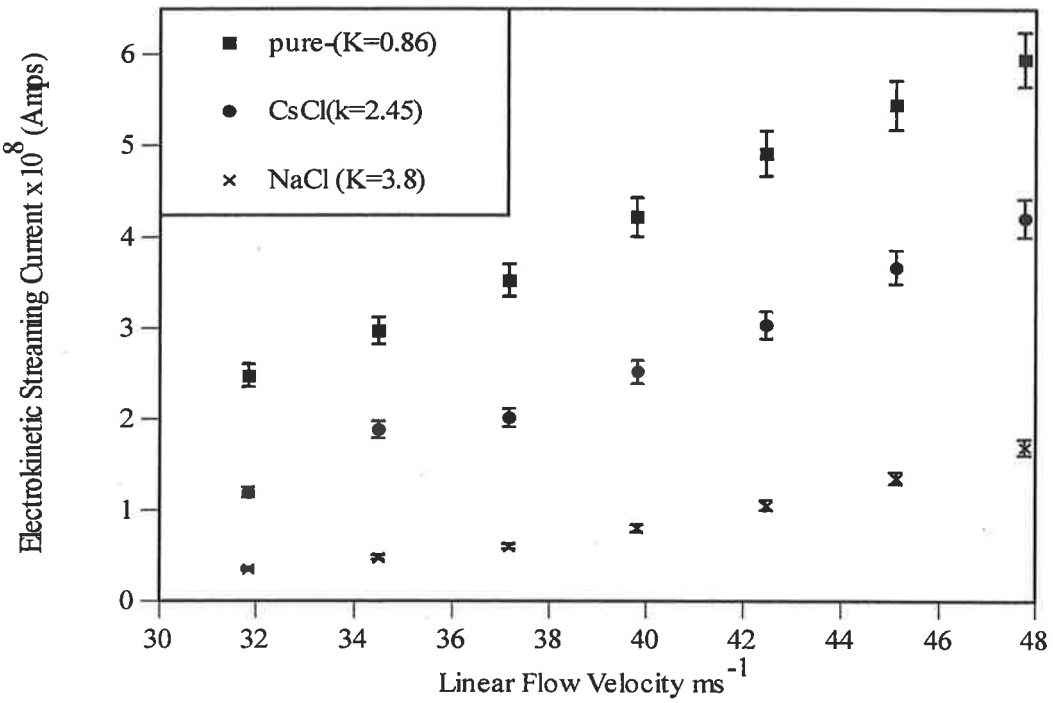

Figure 9.6 Electrokinetic Streaming Current vs Linear Flow Velocity for re-distilled methanol (K = 0.86 μScm^{-1}) and methanol containing NaCl (K = 3.8μScm^{-1}), and CsCl (K = 3.72μScm^{-1})

The data from the conductivity studies in methanol indicated that the solution conductivity, rather than chemical effects, was responsible for changes in the magnitude of the electrokinetic streaming currents. Figures 9.7 and 9.8 show the data obtained for all methanol and water solutions studied. The data demonstrates that the magnitude of the electrokinetic current decreases as solution conductivity increases. It is evident in both plots that the introduction of ions into the pure solvent, irrespective of whether it is methanol or water, results in the magnitude of the streaming current

falling below that of the pure solvent, regardless of the type of ions. Moreover, the current magnitude decreases as the solution conductivity increases.

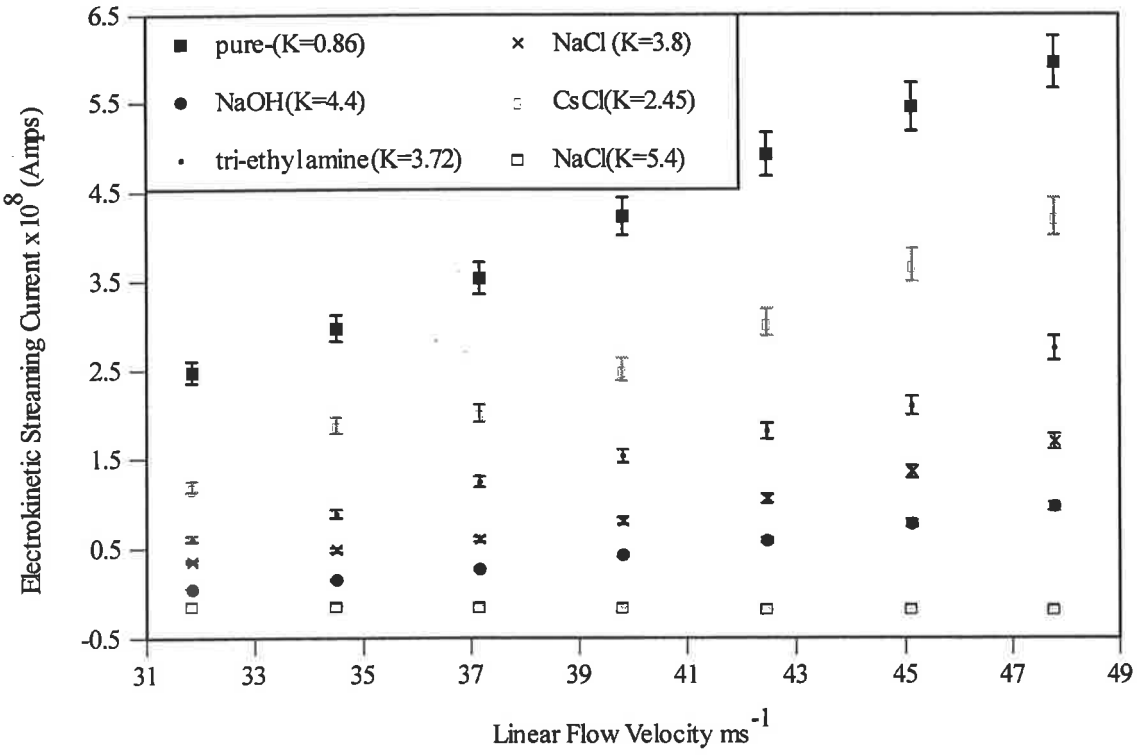

Figure 9.7 Electrokinetic Streaming Current vs Linear Flow Velocity for all solutions of re-distilled methanol studied.

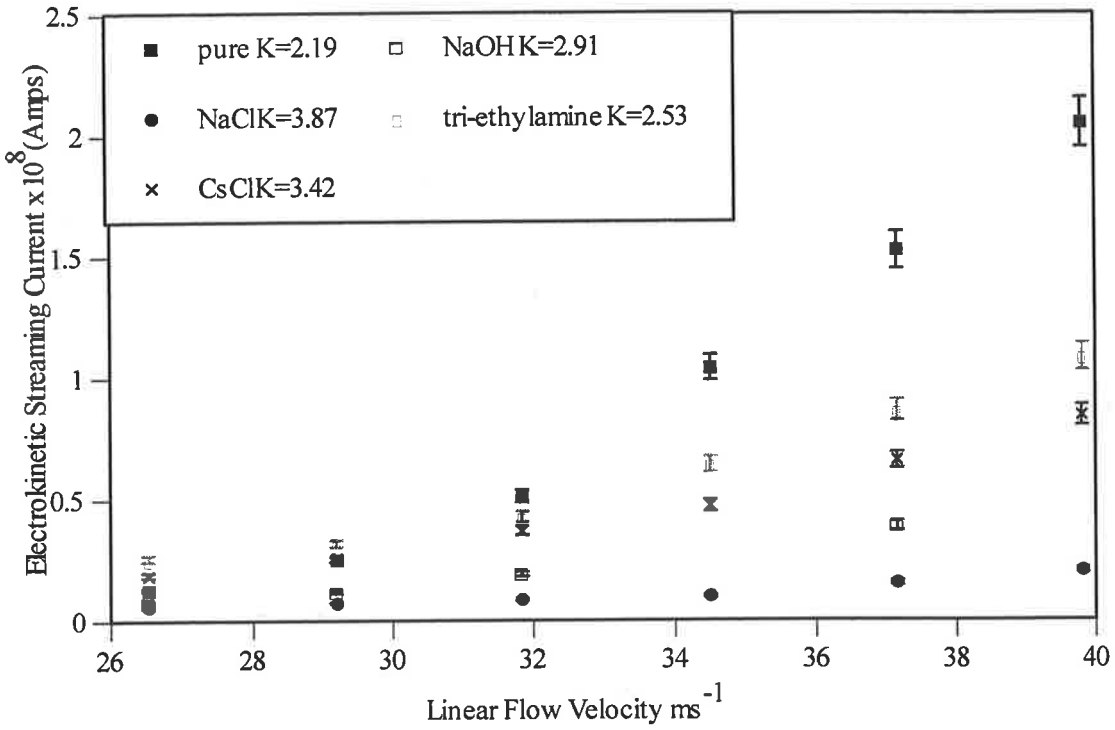

Figure 9.8 Electrokinetic Streaming Current vs Linear Flow Velocity for all aqueous solutions studied.

9.6 Conductivity Dependence

The dominant factor in electrokinetic current generation is the diffusion of ions to the conduit wall. Figures 9.9 and 9.10 show the streaming current –conductance dependence for both methanol and water. The data suggests that there is an inverse relationship between electrokinetic current magnitude and conductance. The nature of this relationship requires further investigation in order to establish the numerical dependence. However, this effect is independent of the ionic species in solution which indicates that the decrease in electrokinetic magnitude is a physical, not chemical phenomena.

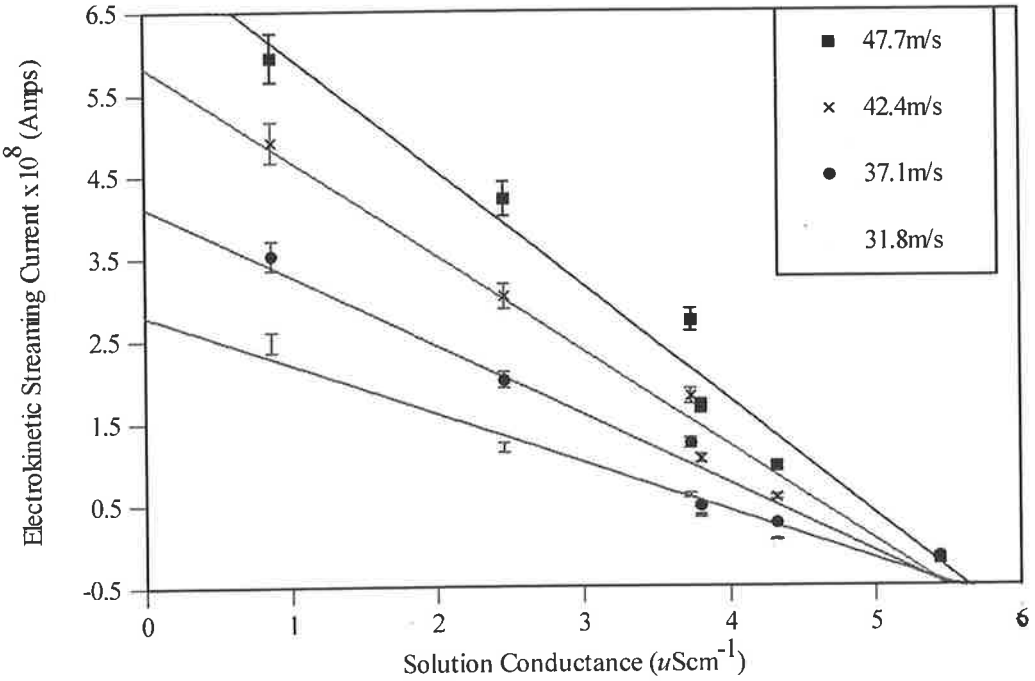

Figure 9.9 Electrokinetic streaming current as a function of conductance for all methanol solutions studied.

Figure 9.10 illustrates the function of conductance for all the solutions studied. However, very low flow velocities are not shown because at low flow velocities ice formed on the electrical connections in the vacuum producing irregular results seen at flow velocities less than 26.5m/s. Despite this problem the relationship between electrokinetic current and conductance is similar to that found in the studies using methanol.

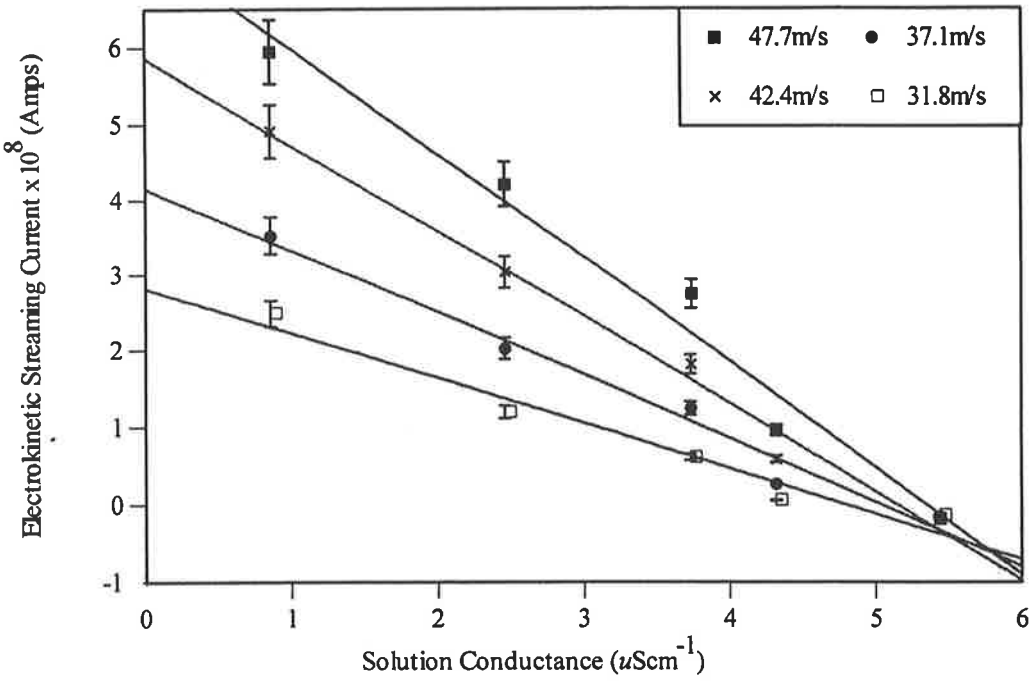

Figure 9.10 Electrokinetic streaming current as a function of conductance for all aqueous solutions

The conductance dependence exhibited by the charging behavior suggests that the diffusion-controlled generation of the electrokinetic current is due to the hydronium ion. The mobility and concentration of this ion in both water and methanol, is the most likely explanation for the positive charge detected at the aperture wall.

The conductivity effects observed in the microjets do not correlate directly with the results of hydrocarbon studies. This discrepancy can be explained in terms of the difference between the conductivity ranges examined. Some of the factors identified in the study such as conductivity dependence are similar to those found in non-polar fluids. The results of this investigation show that the conductivity dependence of polar solvents varies significantly from the behavior observed in non-polar solvents.

In the latter an increase in conductivity results in an increase in streaming current. This observation is contrary to the results obtained in polar solvents. However, it was found that impurities although altering electrokinetic current magnitude, failed to exhibit any chemical dependence on the species present in the solution. The conductivity studies have confirmed the important role of conductivity in electrokinetic charging behavior and the fact that conductivity dominates the magnitude of the electrokinetic current generated. The independence of any conductivity effect from chemical species suggests, that this is a physical rather than a chemical effect. This conclusion is in agreement with studies of non-polar charging behavior. Although the conductance dependence seen in polar solvent liquid micro-jets is different from that of non-polar solvents, the investigations of Gavis [11], Leonard [12] and Goodman [1] all support the conclusion that it is the solution conductivity which determines the magnitude of the electrokinetic current.

9.7 Implications

The objective of this research has been to examine the possibility of using the electrokinetic current as a mechanism for generating ions *in vacuo*. It has been found that the magnitude of the streaming current generated when water and methanol microjets are produced is 10^{-8} A. The magnitude of the electrokinetic current is such that it is only one order of magnitude below that required to achieve a coulomb explosion. A coulomb explosion is the technique currently used by electrospray to generate ions for analysis in a mass spectrometer. In a liquid microjet the generation of the streaming current through kinetic motion of the solvent indicated that a

considerable number of ions are being generated in solution (see below) and it may be possible to extract these ions from the microjet using a self generating coulomb explosion. A simple calculation to determine the number of electrons flowing into the liquid microjet is shown below for a $1x10^{-8}$ Amp streaming current.

10^{-8} Amp = 10^{-8} C/s = $7x10^{10}$ electrons per second

Charge on electron is 1.6×10^{-19} C

This number of ionisation events occurring in a 20 μm diameter liquid jet is important because mass spectrometry requires the detection of one ion only to be effective.

The investigation of the streaming current behaviour of liquid microjets has also established that the microjet is electrically charged on leaving the aperture. This can be demonstrated by placing a copper trap in the path of the disintegrating jet. At the disintegration point of the microjet the shower of droplets fell onto the copper plate. The current is measured at both the aperture and the plate. To illustrate the electrically charged nature of the microjet, the magnitude of the current at both the plate and the aperture have been plotted in Figure 9.11 using a pure methanol sample. Both currents have similar magnitude although the streaming current magnitude is slightly lower at the plate than the aperture. This difference is attributed to the

evaporation of charged solvent or a small amount of solvent not impacting on the plate. The polarity of the aperture current is positive whereas that of the plate is negative indicating that charge is being removed from the microjet as it passes through the aperture.

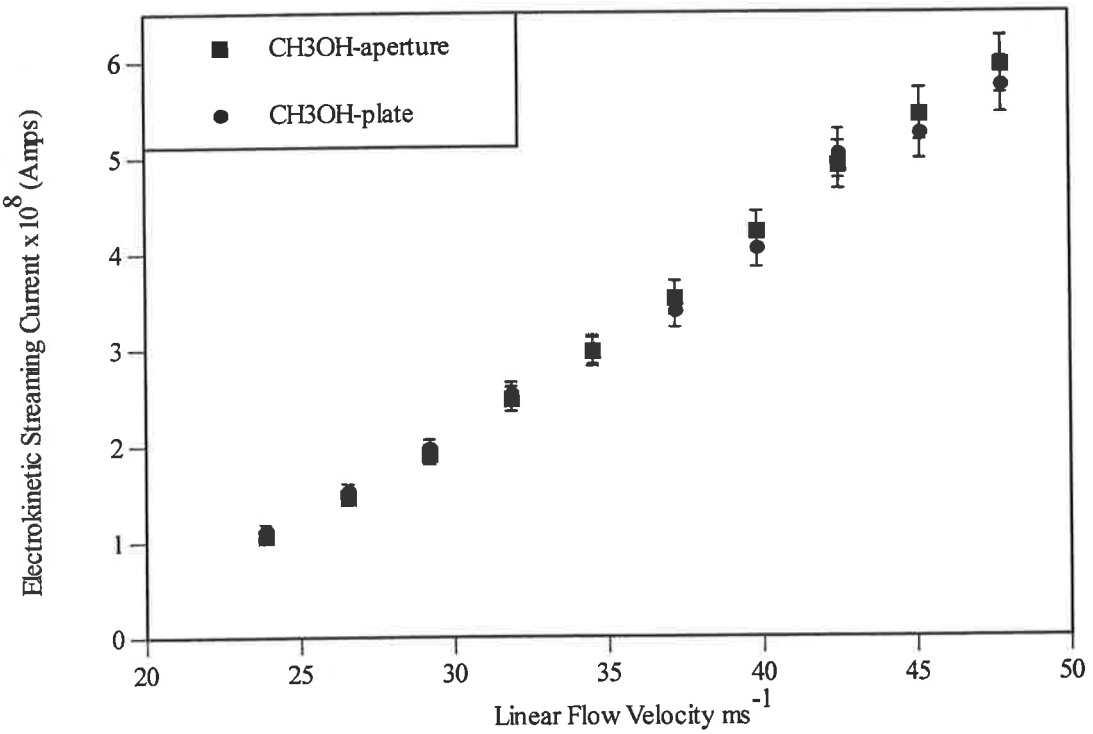

Figure 9.11 Electrokinetic streaming current as a function of linear flow velocity for all re-distilled methanol at the plate and aperture.

The fact that the magnitude of the current at the aperture and plate has the same value confirms that the jet droplets are charged. The presence of charged droplets is a condition for a coulomb explosion to occur which will result in the ejection of ions *in vacuo*. The research to date has established that it is not possible to generate ions *in*

vacuo from electrokinetic charging of the micro-jet. This is due to the fact that the currents generated remain one order of magnitude below that required for a coulomb explosion to occur.

In this chapter it has been shown that the addition of impurities to pure solvents increases the solvent conductivity and reduces the streaming current magnitude. This observation means that electrokinetic streaming currents alone cannot be used to generate ions *in vacuo*, and that although micro-jets are suitable for injecting liquid into vacuum there needs to be a supplementary ionisation source. However, the research presented has identified the factors that affect the electrification of liquid microjets in addition to establishing numerous correlations with existing models for non-polar solvents with respect to the factors affecting electrification.

References

1. Goodman HD, Goodfellow.W., *Electrostatic charging current characteristics for different fluid systems.* Chemical Engineering Science, 1968. **23**: p. 1267-1281.
2. Gibson N, *Static in Fluids.* Static Electrification, 1971. **Paper 9**.
3. Gavis J, Koszman.I., *Development of charge in low-conductivity liquids flowing past surfaces.* Chem.Eng.Sci, 1962. **17**: p. 1013-1022.
4. Faubel M, Steiner.B., *Strong bipolar electrokinetic charging of thin liquid jets emerging from 10um Pt-Ir nozzles.* Ber. Bunsenges. Phys. Chem, 1992. **96**: p. 1167.

5. Faubel M, Schmidt.S., Toennies J.P, *A molecular beam study of the evaporation of water from a liquid jet.* Z.Phys, 1988. **269**: p. 751.

6. Kondow T, Mafune.J., *Ion-Molecule Reaction between Ionised Photochemical Intermediates of Acetophenone and Alcohol Following Multiphoton Excitation in a Liquid Beam.* J.Am Chem.Soc, 1994. **116**: p. 9801.

7. Gibbings J.C, Henderson E., *Electrostatic Streaming Current developed in the turbulent flow through a pipe.* J. Electroanalytical Chemistry, 1968. **16**: p. 239.

8. Schon G, *Handbuch fur Raumexplosionen*, ed. H.H. Freytag. Vol. 196. 1965: Verlag Chemie.

9. Gibson N, Chem. Engng. Sci, 1970. **25**: p. 87.

10. Klinkenberg A, Chem. Eng.Sci, 1970. **25**: p. 223.

11. Gavis J, *The effect of ion dissociation and recombination on the relaxation of charge in low dielectric constant fluids.* Chem. Eng Sci, 1968. **23**: p. 451.

12. Leonard J, Carthart.H., *US Naval Research Laboratory Report 6952*, . 1968, US Naval Research Laboratory.

10. LBMS Conclusions

The study of the electrokinetic charging currents generated by liquid micro-jets has established a relationship between electrokinetic current and solution conductivity, flow velocity and flow conditions. The relationship between streaming current and flow velocity agree with predicted behaviour for laminar flow regimes for non-polar solvents.

In addition, the conductivity dependent charging behaviour of liquid m
micro-jets has been correlated with existing theories for fluid flows in much larger diameter pipes, although direct comparisons cannot be made due to the different conductivity ranges studied. The relationship between conductivity and streaming current magnitude has been found to be independent of chemical effects which is also in agreement with the literature.

In terms of use of the electrokinetic streaming current as an ionisation technique for environmental analysis it has been found that pure solvents produce the maximum current magnitude. The largest current magnitude is ~ which is an order of magnitude below that required for the ejection of ions from the liquid surface using a coulomb explosion.

The addition of salts and weak electrolytes decreased the charging current compared to the pure solvent. The electrokinetic charging data confirms that self ionisation through electrokinetic charging of liquid micro-jets is not feasible. However, it may be possible to enhance the charging effect by applying an electrical potential across the aperture to using increase the charging of the micro-jet. It is known that ions can be generated and detected using a micro-jet apparatus in conjunction with a mass spectrometer using laser irradiation.

The application of an electrical potential across a needle is used to generate charged droplets in the electrospray technique and may well be applicable for use with liquid micro-jets.